ABSTRACT

Title of Document: THE REGULATION OF CRITICAL PERIOD FOR OCULAR DOMINANCE PLASTICITY

Yu Gu, Doctor of Philosophy, 2014

Directed By: Associate Professor, Elizabeth Quinlan, NACS / Department of Biology, University of Maryland

The experience dependent plasticity of stimulus selectivity, including ocular dominance plasticity, is highest during a postnatal critical period. The developmental constraint on this plasticity is thought to underlie the inability to recover from amblyopia in adults, which has generated interest in understanding the mechanisms for the initiation and termination of the critical period. Previously, it had been shown dark exposure initiated in adulthood (P90) reactivates robust ocular dominance plasticity in the visual cortex. In this thesis, I showed dark exposure initiated earlier (P45-55) in postnatal development does not facilitate rapid ocular dominance plasticity, demonstrating the presence of a refractory period for the regulation of synaptic plasticity by visual deprivation.

Using an anesthetic other than barbiturate revealed that ocular dominance plasticity persists much later in postnatal development (up to ~ P55), which can be inhibited by diazepam, a positive allosteric modulator of ligand bound $GABA_A$Rs, suggesting a

regulatory mechanism that is upstream of inhibitory synaptic transmission. To test this, I used NARP and NRG1-ErbB4 to manipulate excitation onto FS (PV) INs, a major subtype of inhibitory neurons which exert powerful perisomatic inhibition onto principal neurons in the visual cortex. NARP is an activity dependent pentraxin which has been shown to accumulate AMPARs onto FS (PV) INs. Transgenic deletion of NARP decreases the number of excitatory synaptic inputs onto FS (PV) INs and reduces net excitatory synaptic drive onto FS (PV) INs. Accordingly, the visual cortex of NARP $^{-/-}$ mice is hyperexcitable and unable to express ocular dominance plasticity, although many aspects of visual function are normal. NRG1 is an activity dependent neutrophic factor which is proposed to promote excitability and excitatory synaptogenesis onto FS (PV) INs. Pharmacological manipulation of the NRG1-ErbB4 pathway can regulates the excitability of FS and RS neurons in visual cortex, and promotes or inhibits the expression of ocular dominance plasticity, depending on the state of maturation of cortical circuitry. Importantly, manipulations of the excitability of FS and RS neurons into the permissive range can enable the expression of ocular dominance plasticity, at any age, which holds promise to future treatment of clinical disorders such as amblyopia.

THE REGULATION OF CRITICAL PERIOD FOR OCULAR DOMINANCE PLASTICITY

By

Yu Gu

Dissertation submitted to the Faculty of the Graduate School of the
University of Maryland, College Park, in partial fulfillment
of the requirements for the degree of
Doctor of Philosophy
2014

Advisory Committee:
Dr. Elizabeth Quinlan, Chair
Dr. Matthew Roesch
Dr. Alfredo Kirkwood
Dr. Patrick Kanold
Dr. Ricardo Araneda

Dedication

To my mom, dad.

Acknowledgements

First of all, I would like to thank my advisor Dr. Elizabeth Quinlan, who opened my mind in the world of science and guided me through step by step during these years. She is a great scientist and also incredible mentor, whenever I have difficulties or confusions about my research, she is always there, helps me, supports me and encourages me. I am very grateful to her and really enjoy working with her.

I also would like to thank all my committee members who always showed their support and gave me valuable suggestions on my research. In addition, I want to thank all the other NACS faculty and staff, who helped me in every aspect of my study and research.

I want to thank my colleagues in Quinlan Lab. They made the work environment very positive, and working with them was very comfortable. I really learned a lot from them.

At last, and very important, I want to thank my family, especially my parents. I could not have finished my study and thesis without their precious love and support.

Table of Contents

Dedication……..ii

Acknowledgements……iii

Table of Contents……iv

List of Figures……vii

Chapter 1: Introduction……1
1.1 The critical period for ocular dominance plasticity……1
1.2 Ocular dominance plasticity and amblyopia……3
1.3 Regulation and reactivation of the critical period ……...4
1.4 The role that FS (PV) INs plays in the regulation of ocular dominance plasticity and orientation tuning ……6

Chapter 2: A refractory period for rejuvenating GABAergic synaptic transmission and ocular dominance plasticity with visual deprivation ……...……10
2.1 Introduction……10
2.2 Materials and methods……...12
2.2.1 Animals……...12
2.2.2 Slice electrophysiology……...12
2.2.3 Monocular deprivation……13
2.2.4 Visually evoked potentials……..……14
2.2.5 Drug solutions……..……...14
2.3 Results……15
2.3.1 A refractory period for the rejuvenation of GABAergic transmission……...15
2.3.2 A refractory period for the reactivation of ocular dominance plasticity……20
2.3.3 Endocannabinoid-mediated regulation of inhibitory synapse maturation and ocular dominance plasticity……..22
2.4 Discussion……..26
2.4.1 The rejuvenation of inhibitory synaptic transmission……27
2.4.2 The role of inhibition in the developmental constraint of ocular dominance plasticity…….……....28

Chapter 3: Obligatory role for the immediate early gene NARP in critical period plasticity ……...30
3.1 Introduction……30
3.2 Materials and methods……...32
3.2.1 Animals……...…32

3.2.2 In vitro electrophysiology……...33
3.2.3 In vivo electrophysiology……...34
3.2.4 Drugs ……..……36
3.3 Results……36
3.3.1 Reduced excitatory drive onto FS (PV) INs in NARP $^{-/-}$ mice……...36
3.3.2 Hyper-excitable visual cortex in NARP $^{-/-}$ mice……43
3.3.3 Normal vision in NARP$^{-/-}$ mice……..……46
3.3.4 Absence of ocular dominance plasticity in NARP $^{-/-}$ mice ……..…….52
3.3.5 Differential response of NARP $^{-/-}$ mice to low frequency versus high frequency visual stimulation ……..……...55
3.4 Discussion……..58
3.4.1 Role of NARP in initiation of the critical period……59
3.4.2 Absence of critical period plasticity in NARP $^{-/-}$ mice……..……..59
3.4.3 Visual function and pre-critical period plasticity are normal in NARP $^{-/-}$ mice…….60
3.4.4 Unique phenotype of NARP $^{-/-}$ mouse ……..……..……62

Chapter 4: Regulation of cortical excitability and ocular dominance plasticity via NRG1-ErbB4 signaling ……..……...64
4.1 Introduction……64
4.2 Materials and methods……...68
4.2.1 Animals……...68
4.2.2 In vivo electrophysiology……...69
4.2.3 Drug solutions……70
4.3 Results……70
4.3.1 Regulation of neuronal excitability and inhibition of ocular dominance plasticity during the critical period with NRG1……71
4.3.2 Regulation of neuronal excitability and ocular dominance plasticity in NARP $^{-/-}$ mice and dark exposed wild type adult mice with NRG1……..75
4.3.3 Regulation of neuronal excitability and rescue of ocular dominance plasticity in adults with ErbB4 inhibition……..……..81
4.3.4 Regulation of cortical excitability and recovery from chronic monocular deprivation in amblyopic adults following inhibition of ErbB4 ……..84
4.4 Discussion……..87
4.4.1 The locus for the regulation of ocular dominance plasticity……...89
4.4.2 Mechanisms of NARP and NRG1 – ErbB4 pathway to enhance excitation onto FS (PV) INs……91

Chapter 5: Conclusions and future directions……... ..94
5.1 The recruitment of inhibition in vivo……....94
5.2 The regulation of refractory period……96
5.3 A direct rescue of the NARP $^{-/-}$ phenotype ……...……98
5.4 The possible application of FS (PV) INs excitation in the clinical research for amblyopia……...99

Abbrevations……………………………………………………………………………101
Bibliography……………………………………………………………………………102

List of Figures

Figure 2-1. 10d DE cannot reactivate iLTD at P35 and the iLTD reactivated by dark exposure at P90 is endocannabinoid-dependent……...……..16

Figure 2-2. A refractory period for the rejuvenation of inhibition in the visual cortex by 10 days of dark exposure..…….……...18

Figure 2-3. Increase in CB1R mRNA in the visual cortex following dark exposure at P90……...…19

Figure 2-4. Refractory period for the reduction of maximal IPSC amplitude in the visual cortex by 10 days of dark exposure…….……..20

Figure 2-5. Refractory period for the reactivation of ocular dominance plasticity by 10 days of dark exposure ……..21

Figure 2-6. Systemic administration of the CB1R agonist WIN (open circles) but not vehicle (filled circles) reverses the effect of adult dark exposure……..…….23

Figure 2-7. Parallel regulation of adult ocular dominance plasticity by the CB1R agonist WIN and diazepam revealed by layer IV and surface VEPs……..……25

Figure 3-1. Altered Connectivity between Layer II/III Pyramidal Neurons and FS (PV) INs in the Visual Cortex of NARP$^{-/-}$ Mice…….……38

Figure 3-2. NARP Deletion Reduces the Number of Release Sites and Increases the Release Probability at Pyr to FS (PV) IN Connections……...……40

Figure 3-3. Validation of the mean variance analysis for determination of unitary EPSC synaptic parameters……..……..41

Figure 3-4. Normal Inhibitory Input onto Pyramidal Cells but Reduced Excitatory Input onto FS (PV) INs in NARP$^{-/-}$ Mice…….…43

Figure 3-5. Enhanced Neuronal Excitability in Layer II/III of NARP$^{-/-}$ Visual Cortex……...…..45

Figure 3-6. Enhanced neuronal excitability in layer IV of NARP$^{-/-}$ visual cortex……...46

Figure 3-7. Normal Vision in NARP$^{-/-}$ Mice……...……...47

Figure 3-8. Normal ocularity and retinotopy in NARP$^{-/-}$ mice……...……49

Figure 3-9. Normal orientation selectivity and orientation tuning in NARP$^{-/-}$ mice……50

Figure 3-10. Normal experience-dependent regulation of VEP contralateral bias in NARP$^{-/-}$ mice……..51

Figure 3-11. Absence of Ocular Dominance Plasticity in Juvenile NARP$^{-/-}$ Mice…….53

Figure 3-12. Absence of Ocular Dominance Plasticity in Adult NARP$^{-/-}$ Mice…….54

Figure 3-13. Differential Response of NARP$^{-/-}$ Mice to Low- versus High-Frequency Visual Stimulation……...57

Figure 4-1. Regulation of spiking output and inhibition of ocular dominance plasticity in juvenile (P30) wild type mice with NRG1……..73

Figure 4-2. Orientation tuning of RS and FS are not affected by PD 158780 and NRG1 administration……...74

Figure 4-3. Regulation of spiking output by knocking out NARP……..…...……...75

Figure 4-4. Rescue of ocular dominance plasticity in NARP $^{-/-}$ and reversal of DE effects in adult WT with NRG1……...78

Figure 4-5. DE effects are occluded in NARP $^{-/-}$ mice…….……80

Figure 4-6. Acute effects in RS evoked spiking of PD 158780 in P90 WT mice……81

Figure 4-7. Regulation of spiking output and reactivation of ocular dominance plasticity in adult (P90) wild type mice with PD 158780 …….....83

Figure 4-8. Regulation of spiking output and recovery of ocular dominance in chronic MDed adult wild type mice with PD 158780 ……..……86

Chapter 1: Introduction

1.1 The critical period for ocular dominance plasticity

Humans, together with other animals such as non-human primates, cats and rodents, have binocular vision, in which an object in central visual space is processed by both eyes together. With binocular vision, images perceived by two eyes can generate precise depth perception. However, the size of the binocular visual field is determined by the position of the eyes. Humans, with the two eyes positioned at the front of their heads, have approximate 190 degrees of horizontal visual field, in which about 120 degrees is binocular. Rodents, in contrast, with their two eyes positioned laterally, have a broader horizontal visual field but only the central 30 degrees is binocular (Gordon and Stryker, 1996).

Although binocular neurons receive inputs from both eyes, most binocular neurons have a preference for stimulation from one eye. The pioneering work of Hubel and Wiesel demonstrated binocular neurons in the cat visual cortex prefer stimulation from the contralateral eye, and this ocular preference is experience-dependent (Hubel and Wiesel, 1962). For example, monocular deprivation of the contralateral, dominant eye for 3 months from eye opening, shifts the preference of the majority of the principal neurons in the primary visual cortex towards the ipsilateral eye (Hubel and Wiesel, 1963). As ocular preference of principal neurons in the layer IV of feline and primate binocular visual cortex are grouped into eye-specific columns, early monocular deprivation also shrinks the area of the ocular dominance columns receiving input from the deprived eye (Shatz and Stryker, 1978; Hubel et al., 1977). Importantly, the physiological and anatomical response to monocular deprivation is the strongest during a postnatal critical period.

Thus, the plasticity of ocular dominance provides a sensitive assay of the level of plasticity available to circuitry in the binocular region of primary visual cortex.

Ocular dominance plasticity has been examined in many species including ferrets (Issa et al., 1999), rodents (Gordon and Stryker, 1996), non-human primates (Hubel et al., 1977) and humans (Braddick & Atkinson, 2011). Recently a lot of researchers have focused their attention onto rodent visual cortex, because of the similarities in the visual system organization between rodents and other mammals. For example, the spatial organization of the receptive field of simple cells in rodent visual cortex are identical to cats and monkeys, indicating the mechanisms for development and plasticity at single cell level are similar (Niell and Stryker, 2008). In rodents, 90% of the retinal ganglion cell axons decussate at optic chiasm and innervate the contralateral dLGN, and 10% project to the binocular core of the ipsilateral dLGN, whose projection neurons innervate layer IV neurons in binocular visual cortex (V1b). The preference for contralateral eye stimulation in binocular neurons in rodents is high (CBI=0.69, Gordon and Stryker, 1996), due in part to two fold greater contralateral eye inputs than ipsilateral inputs from dLGN to cortex (Coleman et al., 2009).

In juvenile rodents (P21-35), a brief monocular deprivation (3 day MD) induces a rapid depression of the strength of the pathway serving the deprived eye, which shares many characteristics with homosynaptic LTD (long term depression, Yoon et al., 2009). Prolongation of the MD to 5 days reveals a slow potentiation of the strength of the pathway serving the nondeprived eye (>= 5 days, Frenkel & Bear, 2004), which has been proposed to be mediated by

either homosynaptic LTP (long term potentiation, Cho et al., 2009) and/or homeostatic synaptic scaling (Kaneko et al., 2008). In adult rodents (~P90), a brief MD is insufficient to induce ocular dominance shift (Sawtell et al., 2003), one of many demonstrations of the existence of critical period for ocular dominance plasticity in the rodent.

1.2 Ocular dominance plasticity and amblyopia

The restriction of synaptic plasticity over development has important implications for the treatment of amblyopia in the clinic. Amblyopia has been estimated to affect 1-5% in population (Webber and Wood, 2005) and results from unequal visual input across the two eyes. Strabismic amblyopia is caused by the misalignment of the two eyes, which can be treated by patching the strong eye to encourage the use of the amblyopic eye. Anisometropic amblyopia is caused by unequal refractive error across the two eyes, which can be treated with a refractory correction of the abnormal eye. Deprivation amblyopia is caused by an obstruction of vision in one eye, such as that caused by a congenital cataract, which can be treated with an early removal of the cataract. However, the chances of success are greatly reduced if the cataract is removed after ~ 6 months of age (Mitchell and MacKinnon, 2002), which suggests there is a critical period for the treatment of amblyopia. One line of reasoning is that the developmental constraint on receptive field plasticity constrains the ability to recover from amblyopia with age.

Nonetheless, some methods for treating amblyopia in adults or older children have had modest success. For example, visual perceptual learning (VPL), repetitive performance of a visual

recognition/discrimination task can improve visual recognition (Polat et al., 2004). Playing virtual reality computer games that requires the combined processes of different images perceived by each eye simultaneously can also improve the binocularity in the amblyopic patient (Waddingham et al., 2006). Repetitive transcranial magnetic stimulation (TMS) may temporarily improve contrast sensitivity and spatial resolution in the affected eye of amblyopic adults (Benjamin et al., 2008). However, visual improvements may be temporary following TMS or are restricted to familiar visual stimuli for VPL.

1.3 Regulation and reactivation of the critical period

Perisomatic inhibition exerts powerful spatial and temporal control of the postsynaptic spiking of principal neurons, which promotes Hebbian mechanisms of synaptic plasticity (Pouille and Scanziani, 2001; Goldberg et al., 2008). Therefore, the regulation of the critical period for ocular dominance plasticity is likely to be sensitive to maturation of inhibitory circuitry over development (Fagiolini and Hensch, 2000). For example, knocking out GAD65, the synaptic isoform of the GABA synthetic enzyme glutamic acid decarboxylase (GAD), prolongs the duration of evoked neuronal spiking trains, and prevents the initiation of the critical period, unless inhibitory output is enhanced with the allosteric $GABA_AR$ modulator diazepam (Hensch et al., 1998).

Similarly, manipulation of inhibitory output can reopen the critical period in adults. Direct reduction of GABAergic transmission with the GAD inhibitor 3-mercaptopropionic acid (MPA), restored ocular dominance plasticity in adult rodents (Harazouv et al., 2010). The reduction of extracellular GABA concentration and GAD65 expression observed following food restriction in

adult rodents is correlated with enhanced ocular dominance plasticity (Spolidoro et al., 2011). Similarly, genetic deletion of Lynx1, an endogenous prototoxin that binds to nAchRs and co-localizes with parvalbumin positive GABAergic interneurons enhances rapid ocular dominance plasticity which can be suppressed with diazepam (Morishita et al., 2010). Finally, we have previously demonstrated 10 days of dark exposure in adults decreases the ratio of the main ionotropic inhibitory receptor to excitatory receptor ($GABA_AR$ / GluR2) ratio, and restores the developmental changes in specific subunits of the NMDA subtype of glutamate receptor NR2B to NR2A (Quinlan et al., 1999), and reactivates ocular dominance plasticity (He et al., 2006). Together this suggests that manipulation of inhibitory output can reopen the critical period in adult visual cortex. However, we will present an alternative to this model in Chapter 3.

The regulation of extracellular matrix (ECM), a complex of proteoglycans (including heparan sulfate PG and chondroitin sulfate PG) and fibrous proteins (including collagen and elastin) formed in the interstitial space (Haylock-Jacobs et al., 2011), has also been implicated as a key component in the regulation of the critical period for ocular dominance plasticity. ECM molecules form a condensed perineuronal net (PNN) around the soma and proximal dendrites of neurons, which build up over development, and reach adult level around P70 in the rat visual cortex (Pizzorusso et al., 2002). PNNs are particularly dense around parvalbumin interneurons (Balmer et al., 2009), and the maturation and distribution of PNNs, as well as the developmental constraint on ocular dominance plasticity, are attenuated by dark rearing rats from birth (Pizzorusso et al., 2002; Gianfranceschi et al., 2003). The mature ECM may limit plasticity by inhibiting axonal sprouting and regeneration after injury (Mckeon et al., 1995). ECM can also modulate synaptic plasticity by limiting lateral diffusion of cell surface molecules (such as AMPAR, Frischknecht et

al., 2009). Indeed, MMP9, an ECM-digesting protease, regulates lateral diffusion of NMDAR and synaptic potentiation (Michaluk et al., 2009; Wang et al., 2008). Importantly, pharmacological blockade of MMP activity does not affect the depression of deprived eye responses following long-term MD, but inhibits non-deprived eye potentiation (Spolidoro et al., 2012).

In addition, the first success in the reactivation of ocular dominance plasticity in adult rodent (>P100) was achieved by degradation of ECM by chondroitinase (Pizzurosso et al., 2002). Environmental enrichment (rodents are reared in a more stimulating environment with ladders, tunnels and running wheels), which restores ocular dominance plasticity in adults, is accompanied by ECM degradation and reversed with enhancing inhibitory output by diazepam (Sale et al., 2007). Transgenic reversal of a developmental change in the prevalence of two different types of chondroitin sulfate proteoglycans (4S/6S CSPGs) in adult visual cortex reduces PNN density, prevents the maturation of membrane potential and spiking width of fast-spiking neurons, resulting in an increase of the cortical excitability and retention of robust ocular dominance plasticity (Miyata et al., 2012). Since the PNNs are more densely located around FS (PV) INs, this also suggests that PNNs may influence the input onto FS (PV) INs in the regulation of the critical period for ocular dominance plasticity.

1.4 The role that FS (PV) INs plays in the regulation of ocular dominance plasticity and orientation tuning

A specific group of GABAergic interneurons, the fast-spiking parvalbumin-positive interneurons (FS (PV) INs), are the most abundant interneurons in the mouse neocortex (Xu et al., 2010), and

have been implicated in the developmental regulation of synaptic plasticity. The high frequency output (8-200 Hz) is responsible for the generation of gamma oscillations (Cardin et al., 2009), which facilitates sensory processing and learning by amplifying signals and reducing noise in pyramidal cells (Sohal et al., 2009). FS (PV) INs form multiple electrical and chemical synaptic connections with other FS (PV) INs (Deans et al., 2001), which allows for generation of synchronized inhibition to local excitatory neurons. FS (PV) INs innervate the somata of pyramidal cells (perisomatic inhibition), and therefore are ideally located to exert powerful temporal and spatial control of the spiking output of principal neurons (Pouille and Scanziani, 2001; Goldberg et al., 2008; Kulman et al., 2010). As FS (PV) INs mediate feed-forward inhibition, they also truncate the duration of spike trains without impacting the initial EPSPs (Vida et al., 2006). Such truncation of spike train duration will likely impact spike timing mechanisms of synaptic plasticity, and have been previously implicated in the regulation of the critical period (Kuhlman et al., 2010; Fagiolini and Hensch 2000).

Indeed, enhancing GABAergic inhibition by diazepam can induce a precocious critical period in pre-critical period wild type mice (P15-21; Fagiolini et al., 2004). As diazepam is not specific for $GABA_AR$ subunits, using transgenic mice Fagiolini et al. (2004) showed that the absence of $\alpha1$, but not $\alpha2$, $\alpha3$, blocks a precocious critical period with diazepam, implicating the $\alpha1$-containing $GABA_ARs$ in mediating the response to diazepam. As $\alpha1$ $GABA_AR$ subunits preferentially enrich at somatic synapses receiving inputs from FS (PV) INs (Klausberger et al., 2002), this indicates FS (PV) INs may play a special role in the timing of the critical period for ocular dominance plasticity. In addition, 1 day monocular deprivation reduces spontaneous and evoked EPSCs frequency onto FS (PV) INs only in juvenile visual cortex, indicating the

importance of this microcircuit during the early phase of ocular dominance shift (Kuhlman et al., 2013).

Of course, ocular preference is not the only stimulus selectivity in the visual cortex. In the rodent primary visual cortex, ~60% of the principal neurons are orientation selective (the neuron has a strong preference for visual stimuli of a specific orientation). Hubel and Wiesel proposed a feed-forward model to explain the orientation tuning of the simple cells: a simple cell in the primary visual cortex receives feed-forward excitation from dLGN relay cells whose receptive field is aligned in parallel with the simple cell's preferred orientation. Another model was proposed later claiming that intracortical inhibition sharpens or even creates orientation tuning (Blakemore and Tobin, 1972). For many years, there has been a long-lasting debate between these two models. Controversy in the field continues in that recently, Lee et al. (2012) showed that optogenetic activation of FS (PV) INs sharpened orientation tuning and improved perceptual discrimination, while Atallah et al. (2012) used similar methods to show that manipulating FS (PV) INs activity only modestly affected the tuning properties. Although not a primary focus of my work, I will show that manipulations of spiking output from FS (PV) INs did not affect orientation tuning.

In this thesis, I will use multiple *in vivo* recording techniques, in rodents of different genotypes and with different visual experience, to study the regulation of critical period for ocular dominance plasticity. Although dark exposure can reopen the critical period in adult animals, it is not known if the visual system is sensitive to DE at all ages, a question I will ask in Chapter 2. In Chapter 3 and 4 I will test hypothesis that the timing of the critical period is determined by the

strength of excitation onto FS (PV) INs, via NARP (an activity dependent pentraxin which has been shown to accumulate AMPARs onto FS (PV) INs, Chapter 3) and via Neuregulin 1 (an activity dependent neutrophic factor which is proposed to promote excitability and excitatory synaptogenesis onto FS (PV) INs, Chapter 4). Together this work will support a new model in which excitation onto FS (PV) INs is a primary locus for the regulation of the timing of the critical period.

Chapter 2: A refractory period for rejuvenating GABAergic synaptic transmission and ocular dominance plasticity with visual deprivation

Published in Journal of Neuroscience
Huang S, Gu Y, Quinlan EM, Kirkwood A. J Neurosci. 2010 Dec 8;30(49):16636-42.
My contribution: all in vivo experiments

2.1 Introduction

In juveniles, brief monocular deprivation (MD) rapidly shifts the ocular dominance of binocular neurons away from the deprived eye. Over the course of postnatal development, brief monocular deprivation becomes increasingly ineffective. Maturation of perisomatic inhibition mediated by fast-spiking parvalbumin-positive interneurons is believed to constrain Hebbian plasticity at excitatory synapses in the visual cortex, and inhibit rapid ocular dominance plasticity (Kirkwood et al., 1995; Huang et al., 1999; Rozas et al., 2001; Jiang et al., 2005; Di Cristo et al., 2007).

In the rodent primary visual cortex, the number of perisomatic GABAergic synapses onto individual pyramidal neurons increases approximately threefold between eye opening [postnatal day 15 (P15)] and puberty (P35) (Huang et al., 1999; Morales et al., 2002; Chattopadhyaya et al., 2004). During this time, inhibitory synapses are transited from an immature state with high release probability but prone to depletion, to a mature state with a low release probability and increased fidelity of transmission (Jiang et al., 2010). The functional maturation of inhibitory synaptic transmission, mediated by an endocannabinoid-dependent long-term synaptic depression [inhibitory long-term depression (iLTD)] is complete by P35.

Acceleration of the maturation of inhibition induces a precocious critical period for ocular dominance plasticity (Huang et al., 1999; Di Cristo et al., 2007). Similarly, dark rearing decelerates the maturation of GABAergic circuits (Morales et al., 2002; Chattopadhyaya et al., 2004; Di Cristo et al., 2007; Jiang et al., 2007, 2010; Kreczko et al., 2009) and the developmental constraint on ocular dominance plasticity (Cynader, 1983; Mower and Christen, 1985; Fagiolini et al., 1994; Guire et al., 1999). However, dark exposure (DE) or suppression of GABA synthesis at P35 does not reduce the number or strength of inhibitory synapses (Morales et al., 2002; Chattopadhyaya et al., 2007; Jiang et al., 2007). This predicts that the developmental constraint on rapid ocular dominance plasticity would be equally irreversible.

Nonetheless, several interventions have been shown to reactivate rapid ocular dominance plasticity in adulthood and implicate the down-regulation of intra-cortical inhibition in this process (Pizzorusso et al., 2002; He et al., 2006; Sale et al., 2007; Maya Vetencourt et al., 2008). Indeed, reactivation of ocular dominance plasticity in adults is induced by a $GABA_A$ receptor antagonist (Harauzov et al., 2010) and reversed by enhancing $GABA_A$ergic inhibition with a benzodiazepine (Sale et al., 2007; Maya Vetencourt et al., 2008). This work supports the view that inhibitory synaptic transmission imposes limitations on ocular dominance plasticity in adults. However, it is at odds with the view that the developmental maturation of inhibition is irreversible.

We addressed this discrepancy by examining GABAergic synaptic transmission after dark exposure, a potent and noninvasive intervention that reactivates ocular dominance plasticity in adults (He et al., 2006, 2007). Dark exposure initiated in adulthood rejuvenated inhibitory synaptic

transmission, resulting in a visual cortex with immature characteristics including robust endocannabinoid-dependent iLTD and rapid ocular dominance plasticity. Surprisingly, dark exposure initiated earlier in development did not stimulate the re-expression of iLTD or facilitate ocular dominance plasticity, demonstrating a refractory period for the rejuvenation of inhibition by visual deprivation.

2.2 Materials and Methods

2.2.1 Animals

Long–Evans rats were raised on a 12 h light/dark cycle, with food and water available ad libitum. Subjects were moved into a dark room at the indicated age (± 2 days), in which case care was provided under infrared illumination. All procedures conform to the guidelines of the U.S. Department of Health and Human Services and the Institutional Animal Care and Use Committees of Johns Hopkins University and University of Maryland.

2.2.2 Slice electrophysiology

Visual cortical slices (300 μm) were prepared as described (Kirkwood and Bear, 1994) in ice-cold dissection buffer containing (in mM): 212.7 sucrose, 5 KCl, 1.25 NaH_2PO_4, 10 $MgCl_2$, 0.5 $CaCl_2$, 26 $NaHCO_3$, 10 dextrose, bubbled with 95% O_2/ 5% CO_2 (pH 7.4). Slices were transferred to normal artificial cerebrospinal fluid (ACSF) for at least one hour prior to recording. Normal ACSF was similar to the dissection buffer except that sucrose was replaced by 124 mM NaCl, $MgCl_2$ was lowered to 1 mM, and $CaCl_2$ was raised to 2 mM.

Visualized whole-cell voltage-clamp recordings were made from layer II/III pyramidal neurons with glass pipettes filled with intracellular solution (in mM: CsCl 140, $CaCl_2$ 0.2, NaCl 8, EGTA 2, NaGTP 0.5, MgATP 4, and HEPES 10, pH 7.2). Only cells with membrane potentials < -65 mV, series resistance < 20 MΩ, and input resistance > 100 MΩ were included. Cells were excluded if input resistance changed >15% over the experiment. Data were filtered at 5 kHz and digitized at 10 kHz using Igor Pro (Wave Metrics Inc., Lake Oswego, Oregon). Synaptic currents were recorded at -60 mV in the presence of 20 μM 6-cyano-7-nitroquinoxaline-2,3-dione (CNQX) and 100 μM 2-amino-5-phosphonovaleric acid (APV), and evoked every 20 sec by stimulation of layer IV with 0.2 ms pulses delivered in pairs (inter-stimulus interval: i.s.i.= 100 msec) to compute paired-pulse depression (PPD=1-p2/p1, where p1 and p2 are the amplitude of the response to the first and second stimulation, respectively). Stimulation was delivered through concentric bipolar stimulating electrodes (FHC, Bowdoin, ME) with intensity adjusted to evoke 100-300 pA responses. Synaptic strength was quantified as the IPSC amplitude. 10 min of stable baseline (< 10% change) was required before any experimental manipulation. iLTD was induced with theta burst stimulation (TBS), consisting of 4 theta burst epochs delivered at 0.1 Hz. Each TBS epoch consisted of 10 trains of 4 pulses (100 Hz) delivered at 5 Hz. Statistical significance was assessed with one-tailed, unpaired t-test or two-way ANOVA followed by Tukey HSD post hoc analysis.

2.2.3 Monocular deprivation

Animals were anesthetized with ketamine/xylazine (50 mg/10 mg/kg, i.p.). The margins of the upper and lower lids of one eye were trimmed and sutured together. The animals were returned to their home cages for 3 days and disqualified in the event of suture opening or infection.

2.2.4 Visually evoked potentials

VEPs were recorded from the surface or layer IV of binocular visual cortex (V1b; ~ 7 mm posterior to Bregma and 4 mm lateral to the midline) with tungsten microelectrodes (0.5MΩ) relative to a ground screw in the frontal bone. V1b was exposed through a hole (~ 4mm diameter) in the skull following urethane anesthesia (1.4 mg/kg, i.p.). Electrode placement on the binocular region of V1 was confirmed by capturing a VEP in response to stimulation of the ipsilateral eye. Visual stimuli were full screen horizontal square wave gratings of 0.04 cycles degree−1 reversing at 1 Hz, with 96.28% maximal contrast and 40 cd/m2 luminosity, presented on a computer monitor 25 cm from eyes, in a darkened room. The amplitude of the primary positive (surface) or negative (layer IV) component of the VEP (~ 150 ms latency) was used to assess the cortical response to visual stimulation. VEPs were amplified (1000X), filtered (0.5 - 60Hz band pass digital filter), and averaged (100 repetitions) in synchrony with the stimulus using OpenEX software. Statistical significance was assessed with two-way ANOVA followed by Tukey HSD post hoc analysis.

2.2.5 Drug solutions

For systemic injections, diazepam and WIN 55212-2 {(R)-(+)-[2,3-Dihydro-5-methyl-3-(4-morpholinylmethyl)pyrrolo(1,2,3-de)-1,4-benzoxazin-6-yl]-1-napthalenylmethanone} were dissolved in 10% Tween 80, 20% DMSO and 70% saline to a final concentration of 1 mg/ml. Subjects received diazepam (1X/day 15 mg/kg diazepam) and WIN (2X/day 5 mg/kg) for 3 days via intraperitoneal injections. For in vitro experiments, stock solutions of AM251 [1-(2,4-dichlorophenyl)-5-(4-iodophenyl)-4-methyl-N-(1-piperidy)pyrazole-3-carboxamide] or WIN

were dissolved in DMSO and diluted in ACSF to the final concentration immediately before use. AM251, diazepam and WIN were purchased from Tocris. CNQX, APV, Tween 80 and DMSO were purchased from Sigma.

2.3 Results

2.3.1 A refractory period for the rejuvenation of GABAergic transmission

We recently described an endocannabinoid-mediated long-term depression of inhibitory synaptic transmission (iLTD) in layer II/III neurons in the visual cortex that is comparable with iLTD described in other brain regions (Chevaleyre et al., 2006; McBain and Kauer, 2009; Jiang et al., 2010). Cortical iLTD is robust in juveniles, but absent in subjects older than P35. Importantly, dark exposure initiated at P35 does not stimulate re-expression of iLTD (Jiang et al., 2010). However, dark exposure in much older subjects can reactivate ocular dominance plasticity (He et al., 2006, 2007), which prompted us to reexamine the effect of visual deprivation on synaptic plasticity at inhibitory synapses.

Pharmacologically isolated IPSCs were evoked in layer II/III pyramidal neurons by stimulating layer IV in slices of rat primary visual cortex, a configuration shown to recruit inputs mediated by fast-spiking interneurons (Jiang et al., 2010). iLTD was induced with TBS. We confirmed that iLTD was absent at P45 and that 10 d of dark exposure initiated at P35 did not stimulate iLTD re-expression [DE, 96.0 ± 3.7% of baseline 30 min after TBS; normal reared (NR), 94.0 ± 3.4%] (Fig. 2-1A). However, if dark exposure was initiated in much older subjects (P90), robust iLTD could be subsequently induced by TBS (DE, 72.9 ± 6.4%; NR, 98.3 ± 4.7%) (Fig. 2-

1B). In juveniles, iLTD requires the activation of type 1 endocannabinoid receptors (CB1Rs) and results in a decrease in paired-pulse depression. Similarly, the iLTD that was observed after dark exposure at P90 was blocked by the CB1R antagonist AM251 and was accompanied by a reduction in paired-pulse depression (Fig. 2-1 C,D).

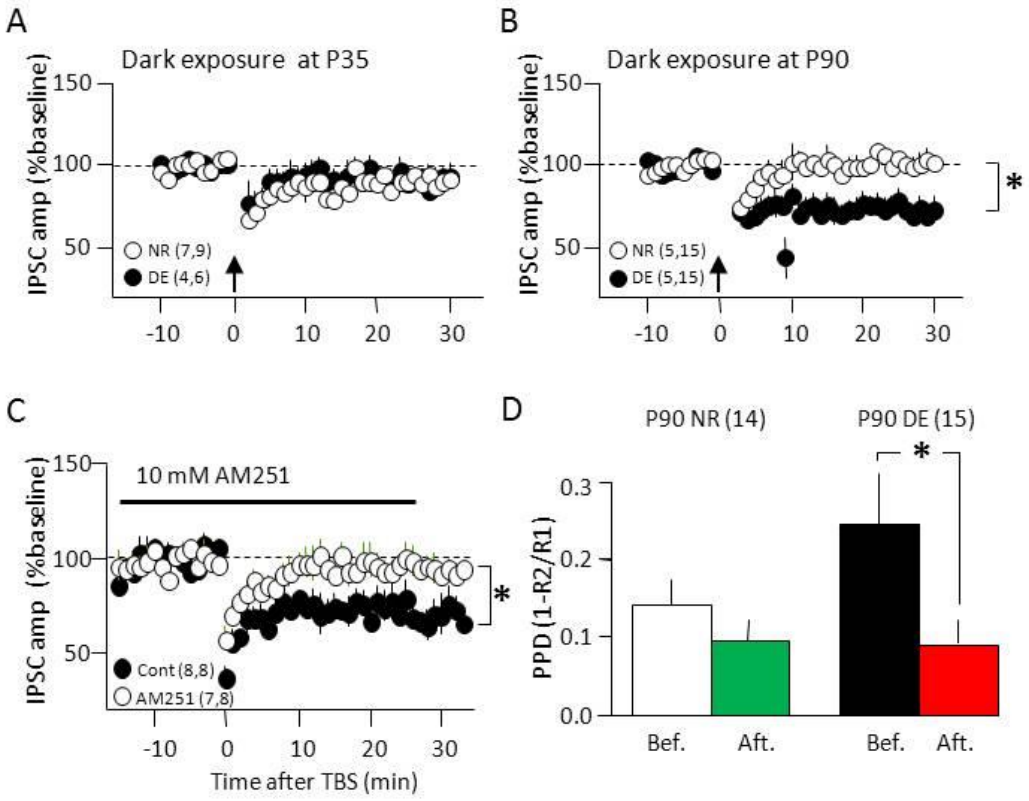

Figure 2-1. 10d DE cannot reactivate iLTD at P35 and the iLTD reactivated by dark exposure at P90 is endocannabinoid-dependent. (A, B) IPSC amplitudes recorded in layer II/III pyramidal neurons following TBS (arrow) delivered to layer IV. Absence of iLTD in response to TBS in slices prepared from normal-reared (NR) P45 (open circles, A) and P100 visual cortex (open circles, B). Ten days of dark exposure initiated at P90 (filled circles, B) but not P35 (filled circles, A) reactivated significant iLTD. *p<0.01 one tail t-test at 30 mins post TBS. (C) IPSC amplitudes recorded in layer II/III pyramidal neurons following TBS (arrow) delivered to layer IV. AM251 (filled circles) inhibits the iLTD reactivated by dark exposure at P90 (open circles). (D) Average paired pulse depression (PPD = 1-the response to second pulse/response to first pulse) recorded before and after TBS in P90 normal reared (NR) and P90 dark-exposed (DE) rats. *p<0.05 one tail t-test.

To further explore the unexpected interaction between visual deprivation and age, we examined the effects of 10 d of dark exposure initiated at ages ranging from P21 to P90 on the magnitude of iLTD and paired-pulse depression. Dark exposure enhanced iLTD if initiated at P21 (iLTD, 22.4 ± 5.3% depression from baseline), when cortical inhibitory circuitry is immature (Huang et al., 1999; Morales et al., 2002; Chattopadhyaya et al., 2004), but had little effect if initiated at P35–P49 (4.0 ± 3.7, 1.0 ± 6.6%). Nevertheless, dark exposure enabled robust iLTD if initiated at P70–P90 (18.5 ± 6.2, 28.7 ± 6.5%) (Fig. 2-2 A). The U-shaped relationship between age at initiation of DE and magnitude of iLTD contrasts with the uniformly small iLTD evoked in NR age-matched P31–P100 controls (Fig. 2-2 A). A parallel U-shaped relationship exists between the age at initiation of dark exposure and the magnitude of paired-pulse depression (Fig. 2-2 B). The loss of iLTD observed over development is accompanied by a reduction in CB1R levels and a loss of response to CB1R activation (Jiang et al., 2010). We therefore asked whether adult dark exposure reversed these processes. We found that dark exposure initiated at P90, but not P45, restored the sensitivity of the IPSC to depression by the CB1R agonist WIN (10 μm, 10 min; DE P45: 92.7 ± 7.1%; NR P45: 98.0 ± 6.6%) (Fig. 2-2 C) (DE P90: 57.4 ± 5.1%; NR P90: 88.7 ± 4.7%) (Fig. 2-2 D).

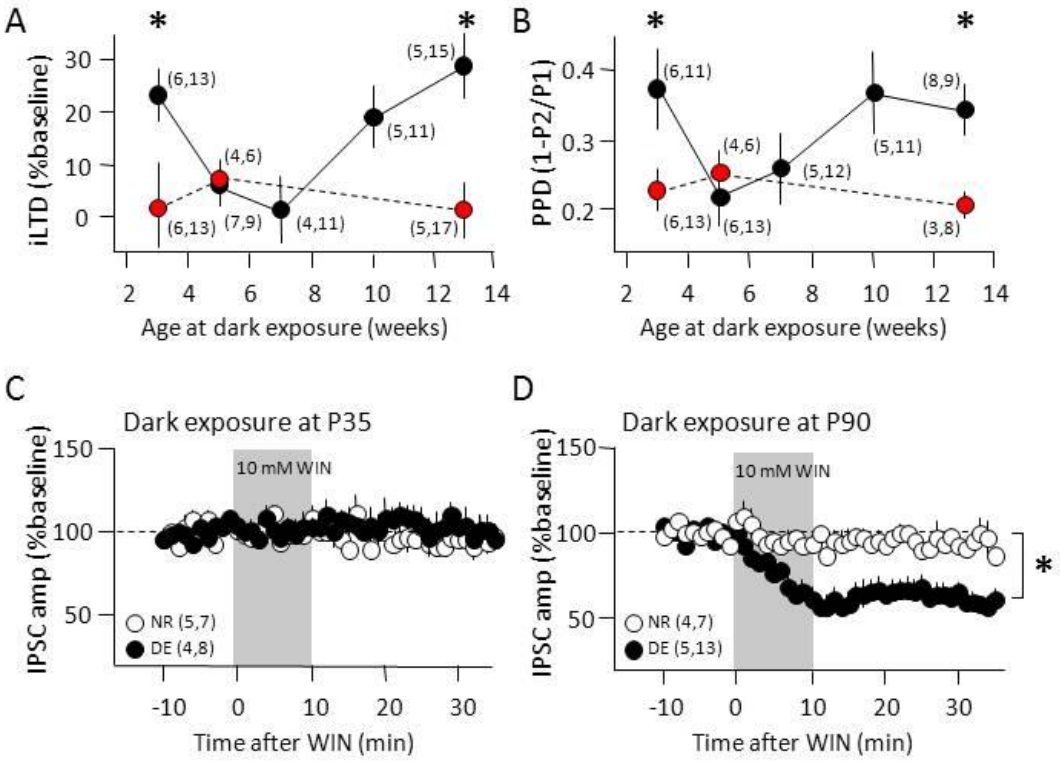

Figure 2-2. A refractory period for the rejuvenation of inhibition in the visual cortex by 10 days of dark exposure. (A) The magnitude of iLTD as a function of the age of initiation of dark exposure (filled circles) compared to age-matched normal-reared controls (open circles). Two way ANOVA ($F_{7,97}$=3.534, p=0.002), *p<0.05 in Tukey HSD post hoc. (B) The magnitude of paired pulse depression as a function of the age of initiation of dark exposure (filled circles) compared to age-matched normal-reared controls (open circles). Two way ANOVA ($F_{7,80}$=2.9193, p=0.009), *p<0.05 in Tukey HSD post hoc. (C, D) Dark exposure at P90 (C) but not P35 (D) restored the sensitivity of the IPSC to depression by the CB1R agonist WIN (grey box). *p<0.001, one tail t-test at 30 mins post TBS. The numbers in parenthesis = number of subjects, number of slices.

Similarly, quantitative PCR confirmed that DE at P90, but not P45 induced in a significant increase in the level of CB1R mRNA in the visual cortex (Fig. 2-3). Thus, dark exposure rejuvenates many aspects of inhibitory synaptic transmission but is only effective if initiated before or after a refractory period.

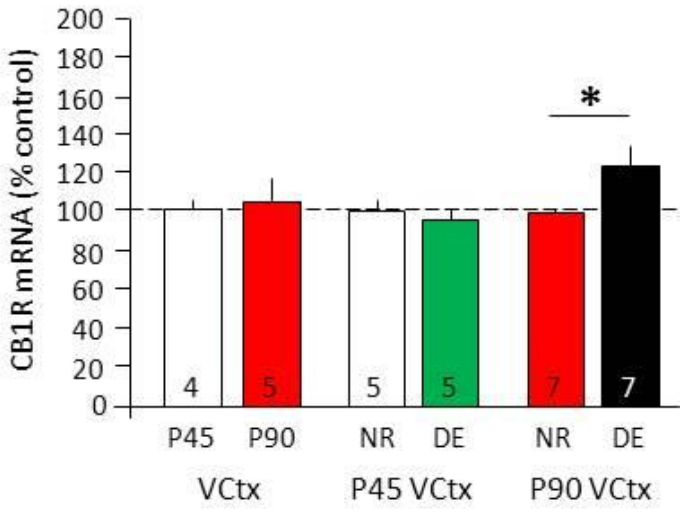

Figure 2-3. Increase in CB1R mRNA in the visual cortex following dark exposure at P90. CB1R mRNA levels were normalized to average within-experiment control (white histogram) run in parallel QT-PCR reactions. CB1R mRNA level from P90 frontal cortex (FCtx) was normalized to average P90 NR visual cortex run in parallel QT-PCR reactions. *p<0.05 one-tail t-test.

The anatomical and functional maturation of inhibition can be decelerated by dark rearing from birth but is unaffected by dark exposure initiated at P35 (Morales et al., 2002; Chattopadhyaya et al., 2007; Jiang et al., 2007). We therefore tracked changes in the maximal evoked IPSC to ask whether the density of functional inhibitory synapses onto individual pyramidal neurons could be regulated by visual experience in adulthood (Choi et al., 2002; Morales et al., 2002; Goldberg et al., 2005). Dark exposure initiated at P35–P38 did not decrease IPSC magnitude (DE: 4.32 ± 0.27 nA; NR: 4.22 ± 0.32 nA) (Fig. 2-4 A) or the input/output relationship across a range of stimulus intensities (5–100 mA; two-way ANOVA, $F(1,225) = 0.71$, $p = 0.79$). In contrast, dark exposure initiated at P90–P93 induced a significant decrease in the maximal IPSC amplitude (DE: 2.97 ± 0.37 nA; NR: 4.53 ± 0.36 nA) (Fig. 2-4 B) and a reduction in the input/out relationship (two-way ANOVA, $F(1,145) = 12.59$, $p = 0.0013$). Together, this

demonstrates a parallel refractory period for the rejuvenation of many aspects of inhibitory synaptic transmission, including endocannabinoid-dependent synaptic depression, regulation of presynaptic neurotransmitter release, and functional connectivity.

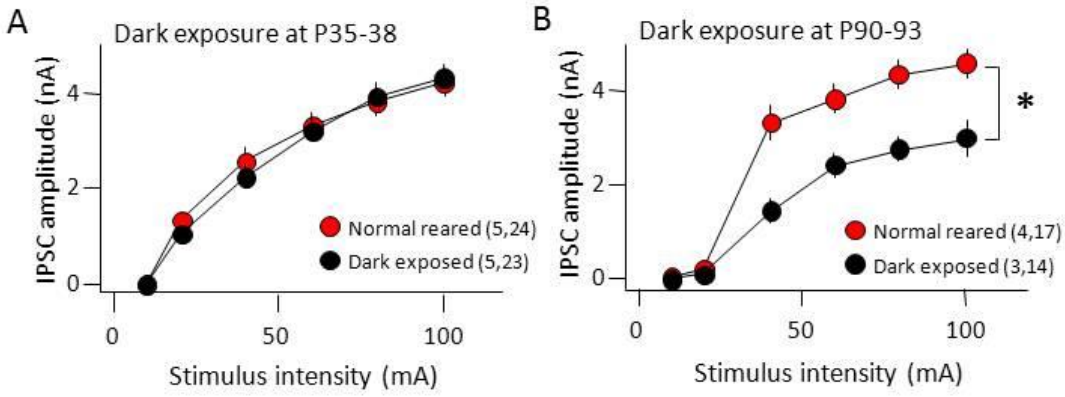

Figure 2-4. Refractory period for the reduction of maximal IPSC amplitude in the visual cortex by 10 days of dark exposure. IPSC amplitudes evoked by a range of stimulus intensities (5 - 100 A) recorded in layer II/III pyramidal neurons from slices of visual cortex following 10 days of dark exposure (DE, filled circles) and age-matched normal-reared controls (NR, open circles). Ten days of dark exposure initiated at P90 (B), but not P35 (A), reduced the maximal IPSC evoked in response to layer IV stimulation. *Two way ANOVA $F_{1,145}$=12.59, p=0.0013. Numbers in parentheses indicate the number of rats, number of slices.

2.3.2 A refractory period for the reactivation of ocular dominance plasticity

The maturation of perisomatic inhibition is widely believed to constrain Hebbian synaptic plasticity at excitatory synapses in the visual cortex and consequently reduce rapid ocular dominance plasticity (Kirkwood et al., 1995; Huang et al., 1999; Rozas et al., 2001; Di Cristo et al., 2007). Dark exposure initiated in adulthood induces a reactivation of juvenile-like ocular dominance plasticity (He et al., 2006, 2007). We therefore used VEPs in response to high contrast gratings (0.04 cycles/degree reversing at 1 Hz) to ask whether there is a refractory period for the reactivation of ocular dominance plasticity by dark exposure. The rodent visual system has a contralateral bias, resulting in twofold larger VEP amplitudes in response to stimulation of the

contralateral eye relative to the ipsilateral eye (VEP average ± SEM: 2.33 ± 0.22; n = 4) (Fig. 2-5 A, gray bar). Brief monocular deprivation induces a significant shift in ocular dominance if initiated before P65 (VEP amplitude C/I average ± SEM: P38, 0.96 ± 0.04; P45, 1.03 ± 0.05; P55, 0.93 ± 0.18; P65, 1.94 ± 0.05; P100, 2.33 ± 0.22) (Fig. 2-5 A). The decrease in the VEP contralateral bias was mediated by a decrease in the deprived-eye VEP and an increase in the nondeprived-eye VEP (shown for P45 subjects in Fig. 2-7 C,D). However, when brief monocular deprivation is preceded by 10 d of DE, a significant shift in ocular dominance was observed in all ages up to P100 (DE P38, 0.74 ± 0.06; DE P45, 1.00 ± 0.04; DE P55, 1.15 ± 0.07; DE P65, 0.89 ± 0.08; DE P100, 0.86 ± 0.08) (Fig. 2-5 A). To separate the effects of dark exposure from baseline ocular dominance plasticity, we normalized the VEP amplitudes from dark-exposed subjects to age-matched normal-reared controls. A U-shape is observed in the relationship between the age at initiation of dark exposure and the deprived-eye depression and the nondeprived-eye potentiation induced by monocular deprivation (Fig. 2-5 B). Thus, dark exposure enhances ocular dominance plasticity but is only effective if initiated before or after a refractory period.

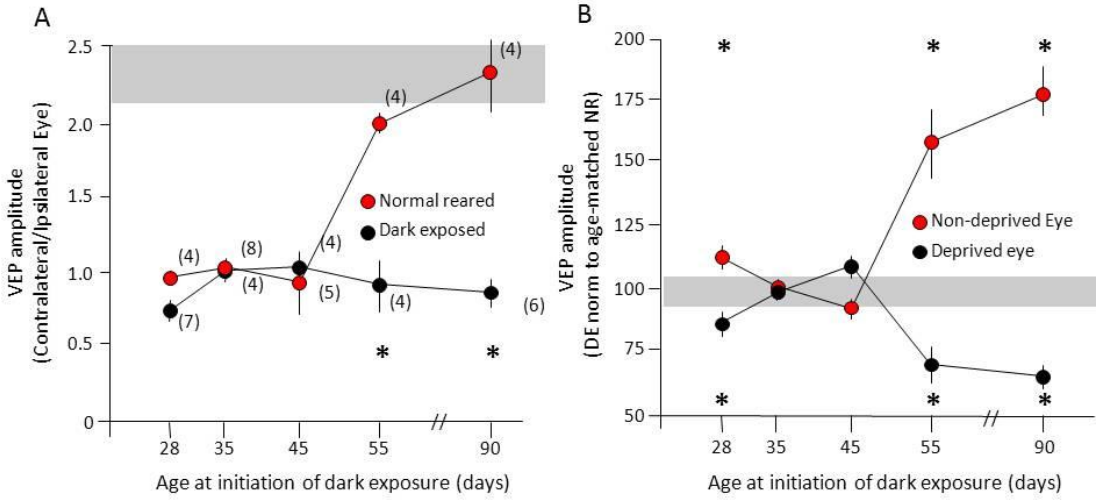

Figure 2-5. Refractory period for the reactivation of ocular dominance plasticity by 10 days of dark exposure (A) Contralateral bias (VEP amplitude C/I) following monocular deprivation as a function of the age at initiation of 10 days of dark exposure (filled circles) compared to age-matched normal reared controls

(open circles). VEPs were recorded from the surface of the binocular region of the right visual cortex following 3 days of left eye deprivation; two way ANOVA ($F_{4,40}$=25.22, p<0.0001). (B) Normalization of DE VEP amplitudes to age-matched, normal reared controls. The refractory period is seen in the response of the deprived eye (filled circles) and non-deprived eye (open circles) to monocular deprivation. Two way ANOVA ($F_{4,40}$=55.4, p<0.0001). *p<0.05 versus age-matched NR in Tukey HSD post hoc. Gray boxes indicate normal range of VEP C/I.

2.3.3 Endocannabinoid-mediated regulation of inhibitory synapse maturation and ocular dominance plasticity

We hypothesized that the rejuvenation GABAergic circuits was necessary for the reactivation of ocular dominance plasticity in adults. Therefore, we used two complementary methods to ask whether enhancement of GABAergic inhibition would reduce the reactivation of ocular dominance plasticity by dark exposure at P90. In the juvenile visual system, activation of CB1 receptors with the agonist WIN accelerates the maturation of GABAergic inhibition (Jiang et al., 2010). To ask whether the rejuvenation of GABAergic inhibition by dark exposure at P90 is reversed by CB1R activation, we administered WIN during the last 3 d of a 10 d period of dark exposure (two times per day for 3 d; 5 mg/kg, i.p.). Administration of WIN resulted in a loss of iLTD (WIN: 95.5 ± 7.0% of baseline; vehicle: 75.6 ± 5.11%) (Fig. 2-6 A) and an increase in the maximal IPSC amplitude in P90 DE subjects (WIN: 3.08 ± 0.20 nA; vehicle: 2.40 ± 0.22 nA) (Fig. 2-6 B), suggesting that WIN stimulated the maturation of GABAergic inhibition. Similarly, the reactivation of ocular dominance plasticity by dark exposure at P90 was significantly reduced by systemic injection of WIN (two times per day for 3 d; 5 mg/kg, i.p.). Importantly, enhancement of $GABA_AR$ currents with diazepam (one time per day, 15 mg/kg, i.p.) for the last 3 d of dark exposure completely blocked the reactivation of ocular dominance plasticity at P100 (layer IV VEP amplitude C/I: P90 no MD, 2.06 ±0.26; P90 MD, 2.41 ±0.20; P90 DE plus Veh, 1.11 ±0.05; P90 DE plus WIN, 1.67 ±0.13, p = 0.0072 vs MD plus DE plus Veh; P90 DE plus DZ, 2.04 ±

0.04, p < 0.0001 vs MD plus DE plus Veh in Tukey's HSD post hoc) (Fig. 2-6 C). WIN significantly reduced and diazepam completely eliminated the decrease in deprived-eye VEP and the increase in nondeprived-eye VEP induced by monocular deprivation in P90 DE subjects, and these changes were equally reflected in VEPs recorded from layer IV and the surface of the binocular region of the primary visual cortex (Fig. 2-7 A,B).

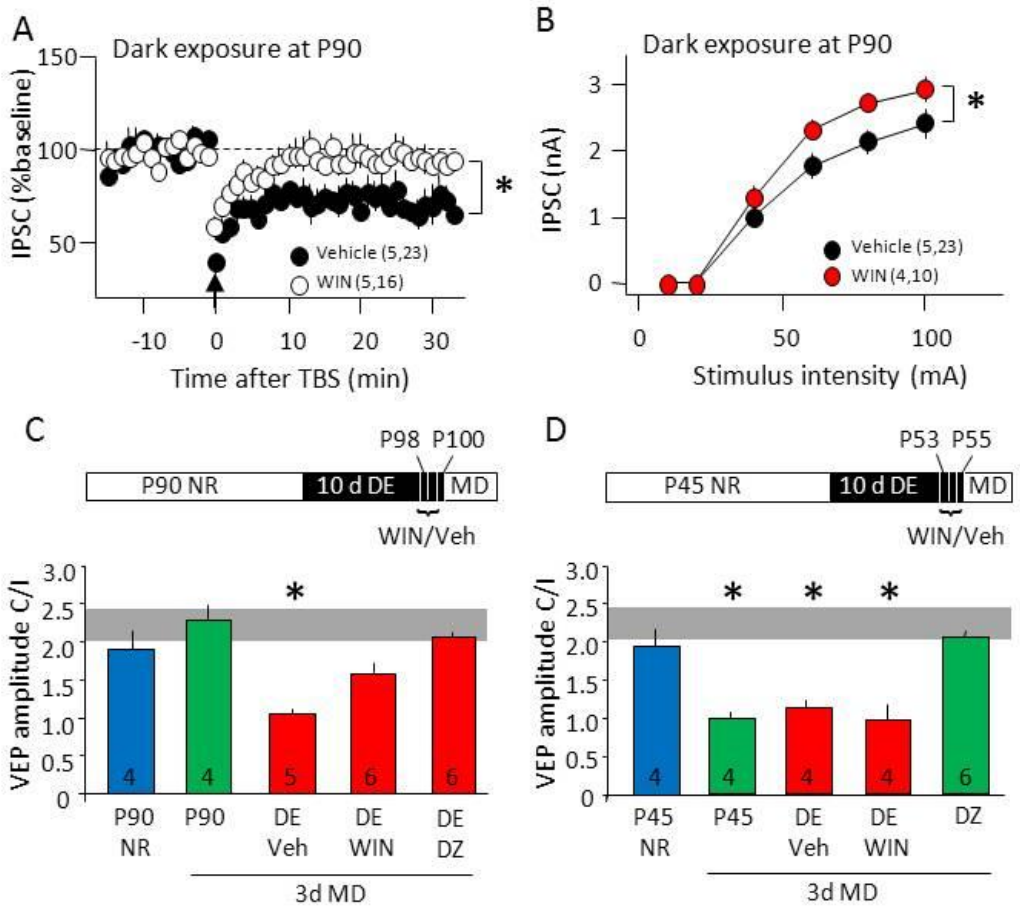

Figure 2-6. Systemic administration of the CB1R agonist WIN (open circles) but not vehicle (filled circles) reverses the effect of adult dark exposure (A-B) IPSC amplitudes in layer II/III pyramidal neurons following TBS (arrow) delivered to layer IV. (A) WIN reversed the iLTD typically observed in dark-exposed P90 subjects, * p=0.031, one-tail t-test (B) WIN reversed the decrease in IPSC amplitude typically observed in dark-exposed, P90 subjects, *p=0.028, one tail t-test. (C) Inset: P90 experimental design. The ocular dominance plasticity reactivated by dark exposure at P90 is attenuated by diazepam and WIN. (One way ANOVA ($F_{4,24}$=12.212, p<0.0001). (D) Inset: P45 experimental design. The ocular dominance plasticity present in P45 NR subjects is inhibited by diazepam, but unaffected by dark exposure or WIN. (One way ANOVA ($F_{4,21}$=30.42, p<0.0001). *p<0.05 versus age-matched NR in Tukey HSD post

hoc. VEPs were recorded from layer IV of the binocular region of the right visual cortex following 3 days of left eye deprivation.

This suggests that an immature state of inhibitory synaptic transmission, induced by dark exposure in adults, permits the reactivation of ocular dominance plasticity. Curiously, however, we observed significant ocular dominance plasticity at P55, despite the evidence that perisomatic inhibition is mature at this age (Kirkwood et al., 1995; Hensch et al., 1998; Huang et al., 1999; Rozas et al., 2001; Di Cristo et al., 2007; Jiang et al., 2010). To ask whether the persistence of ocular dominance plasticity was due to submaximal inhibition, $GABA_AR$ currents were enhanced with diazepam. Systemic diazepam (one time per day for 3 d; 15 mg/kg, i.p.; initiated at P53) inhibited ocular dominance plasticity in P55 subjects. As expected, neither dark exposure or WIN administration (two times per day for 3 d; 5 mg/kg, i.p.; during the last 3 d of dark exposure) regulated ocular dominance plasticity at this age (layer IV VEP amplitude C/I P45 no MD, 1.96 ± 0.18; P45 MD, 1.00 ± 0.05; P45 DE plus Veh, 1.12 ± 0.11; P45 DE plus WIN, 0.94 ± 0.14; P45 DZ, 2.03 ± 0.03) (Fig. 2-6 D). Diazepam, but not dark exposure or WIN, inhibited the decrease in deprived-eye VEP and the increase in nondeprived-eye VEP induced by monocular deprivation in P45 subjects, which was equally reflected in VEPs recorded from layer IV and the surface of the binocular region of the primary visual cortex (Fig. 2-7 C,D). This suggests that, at P55, inhibitory circuitry has developed both functionally and anatomically but is not maximally recruited by visual experience.

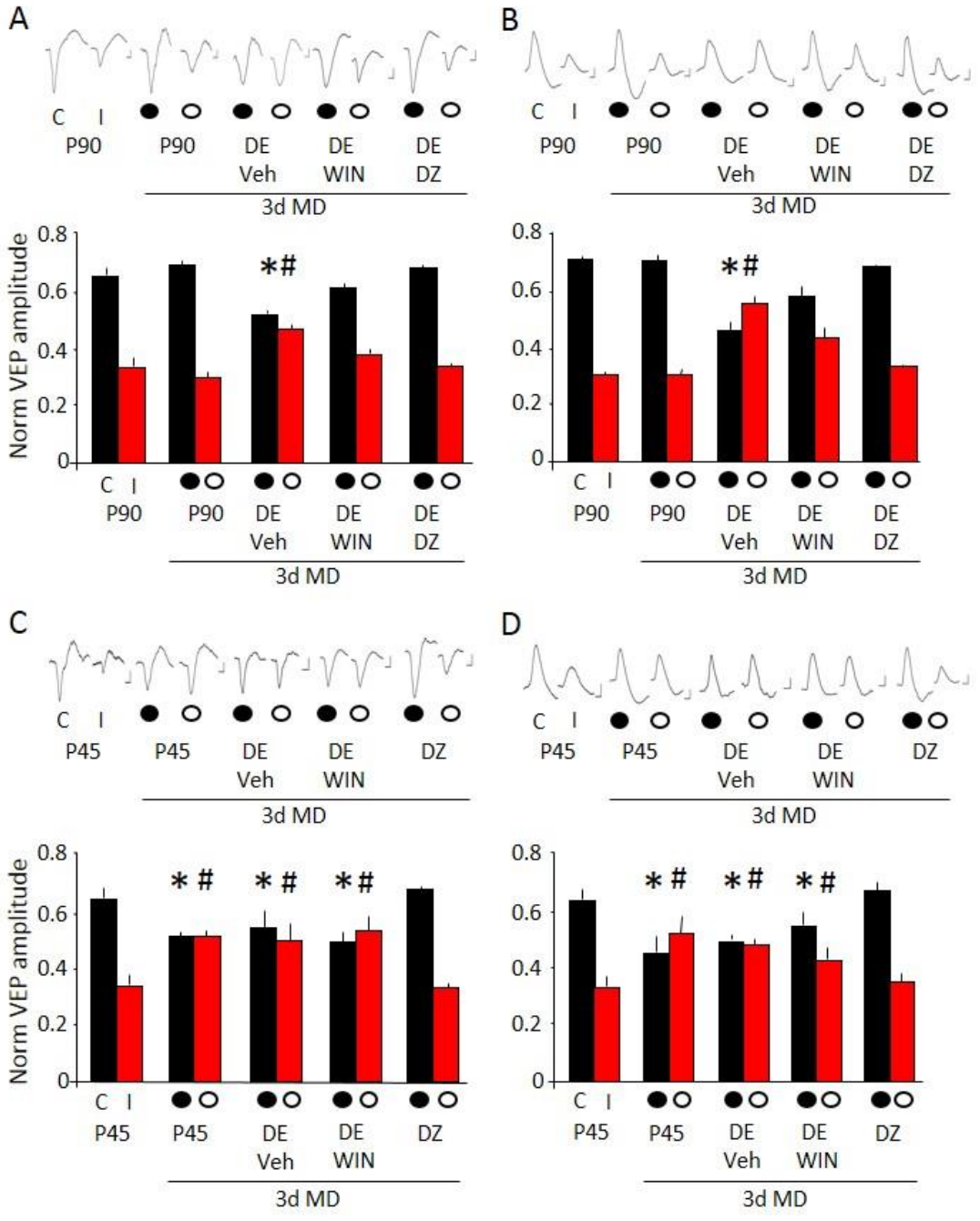

Figure 2-7. Parallel regulation of adult ocular dominance plasticity by the CB1R agonist WIN and diazepam revealed by layer IV and surface VEPs (A,B) VEPs recorded from layer IV (A) and the surface of the binocular visual cortex (B). The deprived eye depression (closed circles) and non-deprived eye potentiation (open circles) induced by monocular deprivation in P90 DE subjects are significantly reduced by WIN and completely eliminated by diazepam (DZ; One way ANOVA ($F_{4,24}$=16.91, $p<0.0001$). Inset: Representative VEP waveforms recorded from layer IV (A) and the surface (B) of the contralateral binocular visual cortex in response to stimulation of the deprived and non-deprived eyes. (C,D) VEPs recorded from layer IV (C) and the surface of the binocular visual cortex (D). The deprived eye depression and the non-deprived eye potentiation induced by monocular deprivation in P45 subjects are inhibited by

diazepam, but unaffected by dark exposure or WIN (One way ANOVA ($F_{4,21}$=10.75, p=0.0003). Inset: Representative VEP waveforms recorded from layer IV (C) and the surface (D) of the contralateral binocular visual cortex in response to stimulation of the deprived and non-deprived eyes. Scale bars: horizontal 50ms, vertical 50μV. *p<0.05 versus age-matched control contralateral eye, #p<0.05 versus age-matched control ipsilateral eye in Tukey HSD post hoc.

2.4 Discussion

Dark exposure initiated in adulthood reactivates robust ocular dominance plasticity in the mammalian visual cortex. Here, we show that a critical step in the reactivation of ocular dominance plasticity in adults is the rejuvenation of inhibitory synaptic transmission, resulting in a decrease in functional inhibitory synaptic density, a decrease in paired-pulse depression, and a re-expression of endocannabinoid-dependent iLTD. Pharmacological acceleration of the maturation of inhibition, through activation of CB1Rs, reverses the re-expression of iLTD and the reactivation of ocular dominance plasticity in dark-exposed adults. However, dark exposure initiated earlier in postnatal development does not rejuvenate inhibitory synaptic transmission or facilitate rapid ocular dominance plasticity, demonstrating the presence of a refractory period for the regulation of synaptic plasticity by visual deprivation. The refractory period for the rejuvenation of inhibitory synaptic transmission demonstrates the existence of constraints on the regulation of synaptic function by visual deprivation. In addition, it suggests that the efficacy of therapeutic interventions used to promote ocular dominance plasticity may increase with age.

An important outstanding issue is the location of the synapses that underlie the ocular dominance plasticity observed in dark-exposed adults. Several lines of evidence implicate a role of layer II/III circuits in the reactivation of ocular dominance plasticity. The activation of CB1Rs, which has been implicated in the plasticity of neuronal circuits in cortical layer III, but not layer IV (Crozier et al., 2007; Liu et al., 2008; Li et al., 2009; Yoon et al., 2009), significantly reduces

the reactivation of ocular dominance plasticity by dark exposure in adults. Similarly, pyramidal neurons in layer III, which receive substantial excitation from thalamic afferents, exhibit a rejuvenation of inhibitory synaptic transmission after dark exposure in adulthood. Importantly, excitatory synapses onto layer II/III pyramidal neurons retain the capacity to express Hebbian plasticity in adulthood (Jiang et al., 2007), but induction is constrained by GABAergic inhibition (Kirkwood and Bear, 1995; Jang et al., 2009). Together, this suggests that the reduction of inhibition onto layer II/III pyramidal contributes to the reactivation of ocular dominance plasticity by dark exposure.

2.4.1 The rejuvenation of inhibitory synaptic transmission

The experience-dependent maturation of inhibition was previously thought to be irreversible, as visual deprivation during postnatal development retards rather than reverses the developmental progression at inhibitory synapses (Morales et al., 2002; Chattopadhyaya et al., 2004; Di Cristo et al., 2007; Jiang et al., 2007). However, here we show that dark exposure in adulthood rejuvenates inhibitory circuits. Immature inhibition, characterized by sparse synapses with a high density of presynaptic CB1Rs and a high probability of GABA release, is seen in the visual cortex of juveniles and dark-exposed adults. Postnatal visual experience stimulates the maturation of inhibition through an endocannabinoid-dependent long-term depression of GABA release. In contrast, mature inhibition is characterized by dense synapses that no longer express CB1Rs and have a low probability of GABA release (Jiang et al., 2010).

The mechanism by which dark exposure induces the rejuvenation of inhibitory synaptic transmission and the reactivation of ocular dominance plasticity in adults is not yet known. In

response to the reduction in synaptic activity induced by dark exposure, preexisting inhibitory synapses in the adult visual cortex may revert to a more immature phenotype, accompanied by an increase in CB1R expression and an increase in presynaptic release probability. Alternatively, dark exposure may increase the turnover of GABAergic terminals by promoting the degradation of factors that restrict axonal outgrowth, such as myelin-derived signaling molecules (McGee et al., 2005) or chondroitin sulfate proteoglycans (Pizzorusso et al., 2002). Interestingly, a significant increase in the condensation of extracellular matrix components into perineuronal nets occurs between P45 and P65 (Pizzorusso et al., 2002), which may impart increased resistance to experience-dependent degradation of a restrictive extracellular environment and contribute to the refractory period.

2.4.2 The role of inhibition in the developmental constraint of ocular dominance plasticity

The late maturation of inhibitory circuitry relative to excitatory circuitry creates a window in postnatal development that is permissive for experience-dependent synaptic plasticity in the visual system. Perisomatic inhibition mediated by fast spiking interneurons exerts a powerful influence on the excitability and plasticity of postsynaptic targets. Although a threshold level of inhibition is necessary to initiate the critical period for ocular dominance plasticity early in postnatal development (Hensch et al., 1998; Huang et al., 1999), a subsequent increase in the strength of perisomatic inhibition has been implicated in the constraint of ocular dominance plasticity later in development (Kirkwood et al., 1995; Rozas et al., 2001; Di Cristo et al., 2007). However, here we show that ocular dominance plasticity is robust after postnatal day 35, the time point at which perisomatic inhibition reaches maturity in the rodent cortex (Huang et al., 1999; Rozas et al., 2001;

Morales et al., 2002; Chattopadhyaya et al., 2004). A similar persistence of rapid ocular dominance plasticity beyond the expected age of the maturation of inhibition has been observed in cats and mice (Mower and Guo, 2001; Pham et al., 2004; Lehmann and Löwel, 2008). Interestingly, ocular dominance plasticity at P45 could be inhibited by enhancing $GABA_A$ receptor function with diazepam, but not by accelerating the maturation of inhibitory synaptic transmission with the CB1R agonist WIN. This suggests that, at P45, inhibitory synapses are present and mature, but ocular dominance plasticity persists because activity at inhibitory synapses is not maximally recruited by visual experience at this age.

Chapter 3: Obligatory role for the immediate early gene

NARP in critical period plasticity

Published in Neuron
Gu Y, Huang S, Chang MC, Worley P, Kirkwood A, Quinlan EM. Neuron. 2013 Jul 24;79(2):335-46.
My contribution: all in vivo experiments

3.1 Introduction

Understanding the processes that initiate and terminate critical periods for receptive field plasticity is a subject of intense investigation. The initiation of the critical period for ocular dominance plasticity is widely believed to be triggered by the maturation of inhibitory synapses targeting the somata of principal neurons in the visual cortex (Hensch et al., 1998; Huang et al., 1999; Di Cristo et al., 2007). Increased perisomatic inhibition would reduce excitability in principal neurons, enabling mechanisms of activity-dependent synaptic plasticity to discriminate between inputs from the two eyes (Jiang et al., 2007; Toyoizumi and Miller, 2009; Kuhlman et al., 2010). The activation of inhibitory GABA receptors would also limit activity at NMDA receptors and restrict subsequent induction of synaptic plasticity at excitatory synapses onto principal neurons (Kirkwood and Bear, 1994; Rozas et al., 2001; Artola and Singer, 1987; Jang et al., 2009).

The evidence supporting the idea that maturation of inhibition determines the timing of the critical period is based on experimental manipulations of inhibitory output. For example, promotion of the early maturation of inhibitory synapses onto principal neurons induces a precocious initiation of the critical period (Huang et al., 1999; Di Cristo et al., 2007; Sugiyama et al., 2008). Similarly, premature expression of ocular dominance plasticity is enabled by

enhancement of inhibitory output with diazepam, a positive allosteric modulator of ligand-bound $GABA_A$ receptors (Seighart, 1995; Fagiolini and Hensch, 2000). Conversely, direct or indirect reduction of the strength of inhibitory output restores ocular dominance plasticity in post-critical period adults (He et al., 2006; Sale et al., 2007; Harazouv et al., 2010). However, recent evidence suggests a disconnection between the maturation of inhibitory output and the termination of the critical period for ocular dominance plasticity (Huang et al., 2010). The maturation of perisomatic inhibition, characterized by a plateau in inhibitory synaptic density, IPSC amplitudes and the loss of endocannabinoid-dependent iLTD, reaches adult levels ~ postnatal day 35 (P35) in the rodent visual cortex (Morales et al., 2002; Huang et al., 1999; Di Cristo et al., 2007; Jiang et al., 2010). Nonetheless, robust juvenile-like ocular dominance plasticity persists beyond P35 (Sawtell et al., 2003; Fischer et al., 2007; Heimel et al., 2007; Lehmann and Lowel, 2008; Sato and Stryker, 2008). Importantly, enhancing inhibitory output with diazepam blocks ocular dominance plasticity in late postnatal development (Huang et al., 2010). This suggests that inhibitory synapses are functional at this age, but are not efficiently recruited by visual experience.

The possibility that the recruitment of inhibitory circuitry might control the timing of the critical period for ocular dominance plasticity prompted us to examine the regulation of excitatory inputs onto interneurons in the visual cortex. We focused specifically on the recruitment of inhibition mediated by FS (PV) INs, which mediate the majority of perisomatic inhibition, and therefore exert powerful control of neuronal spiking output. We studied mice lacking the gene for NARP (neuronal activity-regulated pentraxin a.k.a. NP2) an immediate early gene that is rapidly expressed in the visual cortex in response to light exposure following dark adaptation (Tsui et al., 1996). NARP is a calcium-dependent lectin that is secreted by pyramidal neurons, and accumulates at excitatory synapses onto FS (PV) INs where it forms an AMPAR-binding complex with NP1

and NPR (O'Brien et al., 1999; Xu et al., 2003; Chang et al., 2010). NARP accumulation onto FS (PV) INs is inhibited by degradation of the proteoglycans of the perineuronal net (Chang et al., 2010), a manipulation previously shown to enhance ocular dominance plasticity in adults (Pizzorusso et al., 2002; 2006). Importantly, NARP $^{-/-}$ mice are unable to scale EPSCs onto FS (PV) INs in response to changes in synaptic activity (Chang et al., 2010), demonstrating the importance of NARP in activity-dependent plasticity at these synapses.

NARP $^{-/-}$ mice therefore provide a unique opportunity to examine how excitatory drive onto FS (PV) INs contributes to the timing of the critical period for ocular dominance plasticity. We found that NARP $^{-/-}$ mice have a reduction in the number of excitatory synaptic inputs onto FS (PV) INs, while inhibitory synapses onto pyramidal neurons are unchanged. The reduction in excitatory drive onto FS (PV) INs renders the visual cortex of NARP $^{-/-}$ mice hyper-excitable, and unable to express ocular dominance plasticity. Nonetheless, other forms of synaptic plasticity, which are prominent in the pre-critical stage of development, are normal in NARP $^{-/-}$ mice. Importantly, ocular dominance plasticity can be triggered at any age in NARP $^{-/-}$ mice by enhancing inhibitory output with diazepam. Thus the ability to recruit inhibition, rather than the strength of inhibitory synapses, plays a central role in the initiation of the critical period for ocular dominance plasticity.

3.2 Materials and methods

3.2.1 Animals

Wild-type and NARP$^{-/-}$ mice (Bjartmar et al., 2006) were of C57BL/6, 129/SVJII mixed genetic

background. All subjects were raised on a 12 hr light/dark cycle, with food and water available ad libitum. All procedures conform to the guidelines of the U.S. Department of Health and Human Services and the Institutional Animal Care and Use Committees of the University of Maryland and Johns Hopkins University. Monocular deprivation was performed under ketamine/xylazine anesthesia (50 mg/10 mg/kg, i.p.). The margins of the upper and lower lids of one eye were trimmed and sutured together. The animals were returned to their home cages and disqualified in the event of suture opening or infection.

3.2.2 In vitro electrophysiology

Visual cortical slices (300 μm) were prepared as described (Huang et al., 2010) in ice-cold dissection buffer containing 212.7 mM sucrose, 5 mM KCl, 1.25 mM NaH_2PO_4, 10 mM $MgCl_2$, 0.5 mM $CaCl_2$, 26 mM $NaHCO_3$, 10 mM dextrose, bubbled with 95% O_2/5% CO_2 (pH 7.4). Slices were transferred to normal artificial cerebrospinal fluid (ACSF) for at least 1 hr prior to recording. Normal ACSF was similar to the dissection buffer except that sucrose was replaced by 124 mM NaCl, $MgCl_2$ was lowered to 1 mM, and $CaCl_2$ was raised to 2 mM.

Visualized dual whole-cell voltage-clamp recordings were made from pairs of FS (PV) INs and pyramidal neurons with glass pipettes filled with 130 mM K-gluconate, 0.2 mM $CaCl_2$, 8 mM NaCl, 2 mM EGTA, 0.5 mM NaGTP, 4 mM MgATP, and 10 mM HEPES (pH 7.2). Only cells with membrane potentials <−65 mV, series resistance <20 MW, input resistance >100 MW (with <15% variation over the experiment) were studied. Data were filtered at 5 kHz and digitized at 10 kHz using Igor Pro (Wave Metrics). uEPSCs were recorded in voltage clamp in the FS (PV) INs at −70 mV and evoked by suprathreshold somatic current injection (2 ms) in presynaptic pyramidal neurons. uIPSCs were recorded in voltage clamp in pyramidal neurons at 0 mV and evoked by

suprathreshold somatic current injection (2 ms) in presynaptic FS (PV) INs (Jiang et al., 2010). At least 20 responses evoked at 0.1 Hz with paired pulse stimulation (interstimulus interval: 50 ms for Pyr→FS [PV] IN pairs; 100 ms for FS [PV] IN→Pyr pairs) were used to confirm a synaptic connection and to compute the amplitudes of the unitary responses.

Mean variance analysis was performed on responses evoked by 15 stimulus trains (5 or 10 stimuli at 50 Hz) delivered at 20 s intervals. The uEPSC amplitude was measured for each stimulus, and the mean (I) and variance (Var) were plotted against each other. Synaptic parameters including number of release sites (N) and quantal size (q) were obtained by fitting the data to the parabola: Var = qI − I2/N as previously described (Scheuss and Neher, 2001). We considered only those cases in which the R2 value of the fit was >0.5.

3.2.3 In vivo electrophysiology

In vivo electrophysiology was performed under isoflurane anesthesia (~1.5% in 100% O_2 via modified nose cone). The dura covering binocular visual cortex was exposed through a hole (~3 mm diameter) in the skull. The exposed brain was kept moist with artificial cerebral spinal fluid (ACSF), and the room humidity was supplemented (ZD300Y0, Zenith). Subjects were retained in a stereotaxic device in a darkened room (without visual stimulation) between measurements. Body temperature was maintained at 37 ℃ via circulating water heating pad (T/PUMP; Gaymar Industries), monitored with a rectal probe (BAT-12; Sensortek). A broad-band signal was collected from the lateral aspect (binocular region) of the primary visual cortex (site of largest ipsilateral eye VEP, typically 3.3 mm lateral to the intersection of lambda and the midline), with a tungsten microelectrode (0.5 MΩ) relative to a ground screw in the frontal bone (Figure S3). Laminar placement of the electrode was confirmed by time to VEP peak and the shape of the VEP

waveform: layer II/III, ~250 μm below the pia + primary positive peak, time-to-peak ~130 ms (average ± SEM 131.76 ± 5.88 ms, n = 7); layer IV, ~450 μm below the pia + primary negative peak, time-to-peak ~105 ms (107.38 ± 3.17 ms, n = 6). A 50 Hz low pass filter was used to isolate VEPs in response to 1 Hz reversals of full screen 100% contrast gratings (0.04 cycles/degree and 40 cd/m2 luminosity) presented on a computer monitor 25 cm from eyes. To estimate spatial acuity, the VEP amplitude was plotted against the spatial frequency of the visual stimulus (0.04–0.6 cycles/degree), and the linear regression was extrapolated to zero VEP amplitude. To estimate contrast sensitivity, the VEP amplitude was plotted against the contrast of the visual stimulus (20%–100%). VEPs were averaged in synchrony with the visual stimulus using OpenEX software (TDT).

A 700–7 kHz band-pass filter was used to isolate multiunit activity, which was sorted into single units based on waveform shape and principal component analysis (OpenEx software; TDT). Spontaneous firing rates were measured over 100 s in response to blank screen. Evoked spiking rates were measured in response to visual stimulus in preferred orientation (from nine orientations ranging from 0° (vertical) to 180°). Duration of evoked single unit activity was determined by comparison with 50 ms prestimulus baseline. Orientation selectivity index = (response evoked by preferred – orthogonal orientation)/(preferred + orthogonal orientation). Orientation tuning was determined by plotting spiking activity against stimulus orientation from −90° to 90° from preferred orientation. Single unit activity was assigned to cortical lamina based on shape of VEP waveform.

Plasticity of VEP amplitude induced by repetitive visual stimulation was assessed under continuous isoflurane anesthesia (~1.5% in 100% O_2). Sixty minutes after recording baseline

VEPs (evoked by 100 reversals of 0.04 cycles/degree; 100% contrast vertical and horizontal gratings; reversing at 1 Hz), high-frequency visual stimulation (5–10 Hz reversals of same gratings; 1,000 reversals) was delivered at a single orientation (vertical). Sixty minutes after delivery of high-frequency visual stimulation, VEPs were acquired with baseline stimulation (1 Hz) in response to vertical and horizontal gratings. Low-frequency visual stimulation (1 Hz reversals of same gratings; 1,000 reversals) was delivered at a single orientation (vertical). Twelve hours, 15 hr, and 18 hr after delivery of low-frequency visual stimulation, VEPs were acquired with baseline stimulation (1 Hz) in response to vertical and horizontal gratings.

3.2.4 Drugs

Diazepam (Sigma) was dissolved in 10% Tween 80, 20% DMSO, and 70% saline to a final concentration of 2 mg/ml. Spiking rates in diazepam are reported 45 min after administration.

3.3 Results

3.3.1 Reduced excitatory drive onto FS (PV) INs in NARP $^{-/-}$ mice.

To ask how the absence of NARP impacted excitatory synaptic drive onto inhibitory interneurons, we crossed NARP $^{-/-}$ mice with G42 mice, which express GFP in fast spiking, parvalbumin positive interneurons (FS (PV) INs; Jiang et al., 2010). Unitary excitatory postsynaptic currents (uEPSCs) were recorded pairs of pyramidal (Pyr) and FS (PV) interneurons from layer II/III in slices of visual cortex prepared from three week old (postnatal day 21 – 25) NARP $^{-/-}$ and age-matched wild type mice (Fig 3-1A, B). In the absence of NARP, the probability of connectivity between any Pyr->FS (PV) IN pair was significantly reduced (connection probability average ± SEM: NARP$^{-/-}$

0.47 ±0.06, n = 9 mice, 72 pairs; WT 0.73 ±0.06, n=12, 52; p= 0.0007, Fisher exact test; Fig 3-1D). However, in connected pairs, the uEPSC amplitude was normal ($NARP^{-/-}$ 82.2 ±16.3 pA, n = 9, 33; WT 72.0 ±13.0%, n=10, 35; p=0.62, t-test; Fig 3-1B, E). Importantly, the absence of NARP did not affect connectivity from FS (PV) INs onto pyramidal cells (Fig 3-1G-L). No differences were detected between wild type and $NARP^{-/-}$ mice in either the probably of connectivity (p=0.20; Fig 3-1J), the amplitude of the unitary IPSC evoked by direct depolarization of the FS (PV) IN (p=0.69; Fig 3-1K) or the paired pulse response ratio (p=0.83; Fig 3-1L). Thus, the absence of NARP specifically reduced the connectivity from pyramidal neurons onto FS (PV) INs, while the connectivity from FS (PV) IN onto pyramidal neurons was unimpaired.

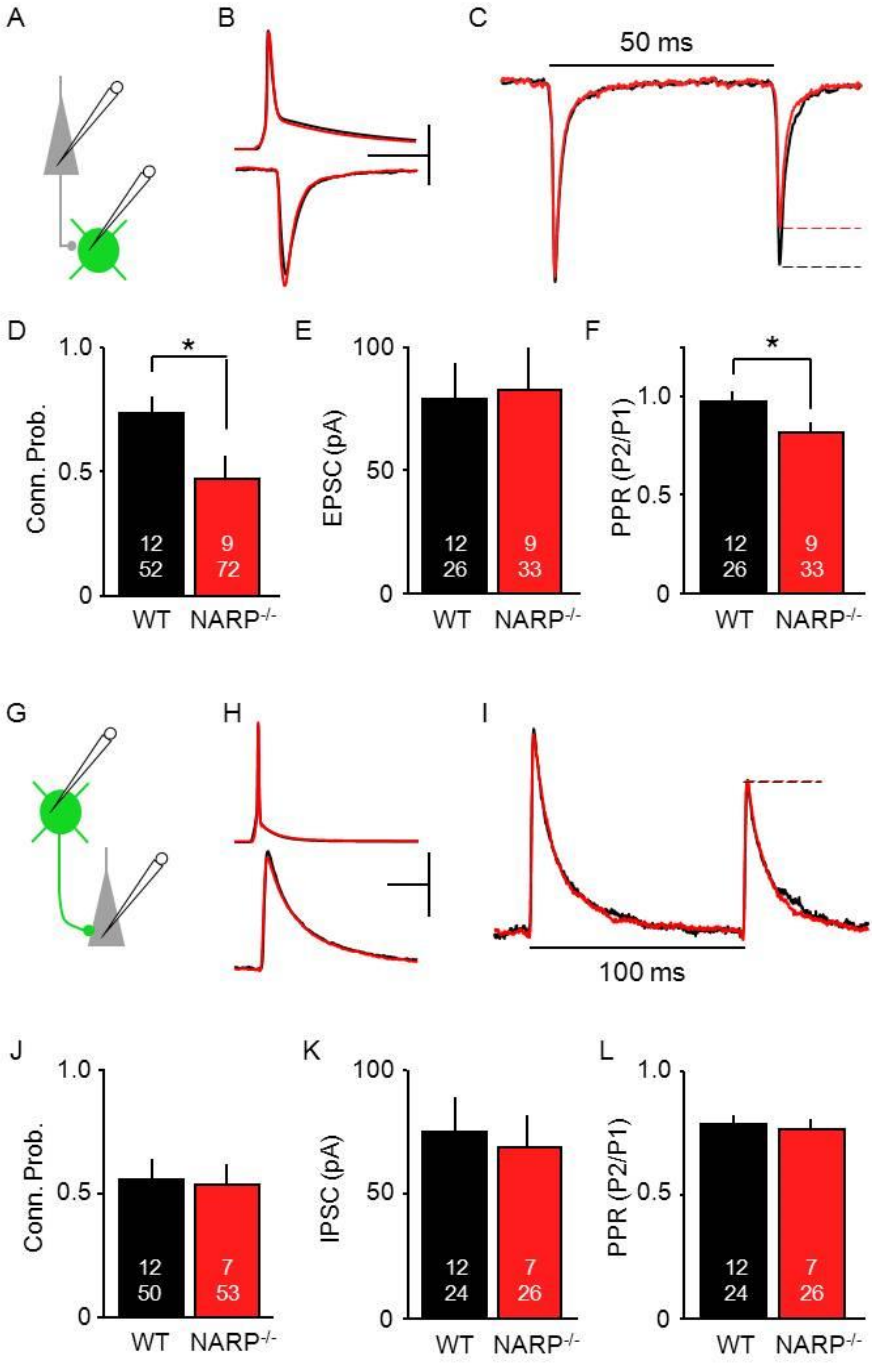

Figure 3-1. Altered Connectivity between Layer II/III Pyramidal Neurons and FS (PV) INs in the Visual Cortex of NARP$^{-/-}$ Mice (A–F) uEPSCs in FS (PV) IN (green) evoked by action potentials in a nearby pyramidal neuron (gray). (A) Experimental schematics. (B) Average of all responses recorded in connected Pyr→FS (PV) IN pairs (20 responses/pair) from P21–P25 NARP$^{-/-}$ (red) and age-matched wild-type mice (black). Top: action potentials in pyramidal neurons; bottom: uEPSCs in FS (PV) INs. Scale bar represents 50 mV, 50 pA, 10 ms. (C) Average uEPSC evoked with paired pulse stimulation, normalized to first uEPSC (NARP$^{-/-}$, red; WT, black). Effects of NARP deletion on the probability of finding (D) a

connected pair, (E) the uEPSC amplitude, and (F) the paired pulse-response ratio. (G–L) uIPSCs in pyramidal neuron (gray) evoked by action potentials in a nearby FS (PV) IN (green). (G) Experimental schematics. (H) Average of all responses recorded in connected FS (PV) IN→Pyr neuron pairs (20 responses/pair). Top: action potentials in FS (PV) INs; bottom: uIPSCs in pyramidal neurons. Scale bar represents 40 mV, 40 pA, 10 ms. (I) Average uIPSC evoked with paired pulse stimulation, normalized to first uIPSC ($NARP^{-/-}$, red; WT, black). Effects of NARP deletion on the probability of finding (J) a connected pair, (K) the uIPSC amplitude, and (L) the paired-pulse response ratio. The number of mice and cell pairs is presented in each bar. $^{*}p < 0.01$, t test.

As a first estimation of neurotransmitter release probability, we examined the paired-pulse response ratio (PPR) of the uEPSCs in Pyr->FS (PV) IN pairs. We found that the PPR was decreased in NARP $^{-/-}$ mice ($NARP^{-/-}$ 0.80 ±0.04, n = 4, 17; WT 0.99 ±0.05, n=10, 35; p= 0.007, t-test; Fig 3-1C, F), suggesting that the excitatory synapses that persist may have enhanced presynaptic function. This prompted us to ask if the absence of NARP affects quantal parameters such as quantal size (Q), the number of presynaptic release sites (N) and the presynaptic release probability (P) at the remaining Pyr ->FS (PV) IN synapses. To obtain these parameters, we performed a mean- variance analysis of the uEPSC evoked by 50 Hz trains of 5 or 10 action potentials in the pyramidal neuron, as described (Fig 3-2A; Scheuss et al 2001; Huang et al 2010). This analysis allows quantal parameters (N, P, Q) to be estimated from the parabola fit to the relationship between mean and variance of the uEPSCs within the train (Fig 3-2B, see methods). We first tested the validity of this approach by increasing extracellular [Ca^{2+}] from 2 mM to 4 mM. As expected, this resulted in an increase in the magnitude of the uEPSC (paired t-test: p=0.008, n=6 pairs) that was associated with an increase in release probability (p<0.001), but no change in quantal size (p=0.307) or the number of release sites (p=0.426). Alternatively, the addition of a low dose of the glutamate receptor antagonist kynurenic acid (200 mM) resulted in a decrease the magnitude of the uEPSC (paired t-test: p=0.039; n=6 pairs) that was associated with a decrease quantal size (p=0.008), but no change in release probability (p=0.807) or the number of release

sites (p=0.722; Fig 3-3). Application of the mean-variance approach to Pyr->FS (PV) IN uEPSCs in NARP $^{-/-}$ mice (postnatal day 21- 25) revealed a decrease in the number of presynaptic release sites (N; NARP$^{-/-}$ 11.8 ±2.0, n = 7,15; WT 31.5 ±7.1, n=5, 205; p=0.016, t-test; Fig 3-2C) associated with an increase in presynaptic release probability (P; NARP$^{-/-}$ 0.66 ±0.05, n = 7,15; WT 0.46 ±0.06, n=5, 20; p=0.010, t-test; Fig 2D), but no change in quantal size (Q: NARP$^{-/-}$ 18.2 ±2.4, n = 7.15; WT 14.2 ±2.3, n=5, 20; p=0.231, t-test; Fig 3-2E). Together, this demonstrates a net reduction in the excitatory drive onto FS (PV) INs in the visual cortex of NARP$^{-/-}$ mice.

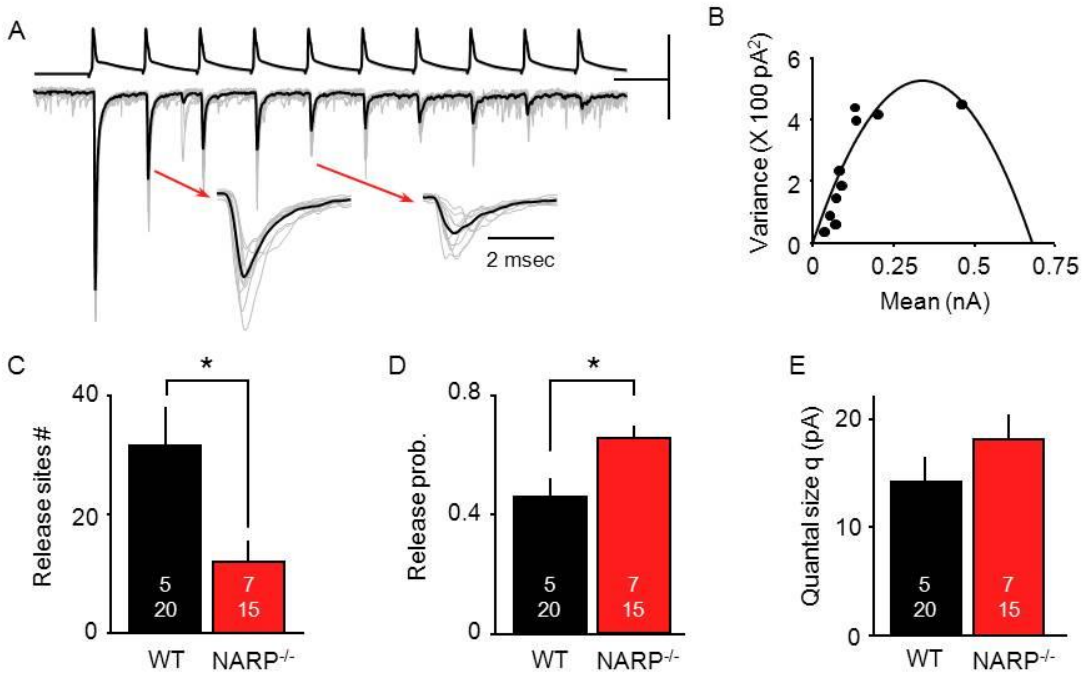

Figure 3-2. NARP Deletion Reduces the Number of Release Sites and Increases the Release Probability at Pyr to FS (PV) IN Connections (A) Representative experiment illustrating the estimation of synaptic parameters through a mean variance analysis of uEPSCs evoked by 50 Hz trains (of 10 pulses). Fifteen consecutive trials (gray) are superimposed, along with averaged response (black). Scale bars represent 200 mV, 200 pA, 20 ms. Expanded uEPSCs, indicated by arrows, were evoked by the second and fifth pulse of the trains. (B) The relationship between mean uEPSC amplitude and variance for each of the ten uEPSCs within the train was fitted with a parabola. (C–E) Synaptic parameters estimated from the parabolic fit in NARP$^{-/-}$ (red) and WT mice (black) include (C) the number of release sites, (D) the release probability, and (E) the quantal size. The number of mice and cell pairs is presented in each bar. *p < 0.01, t test.

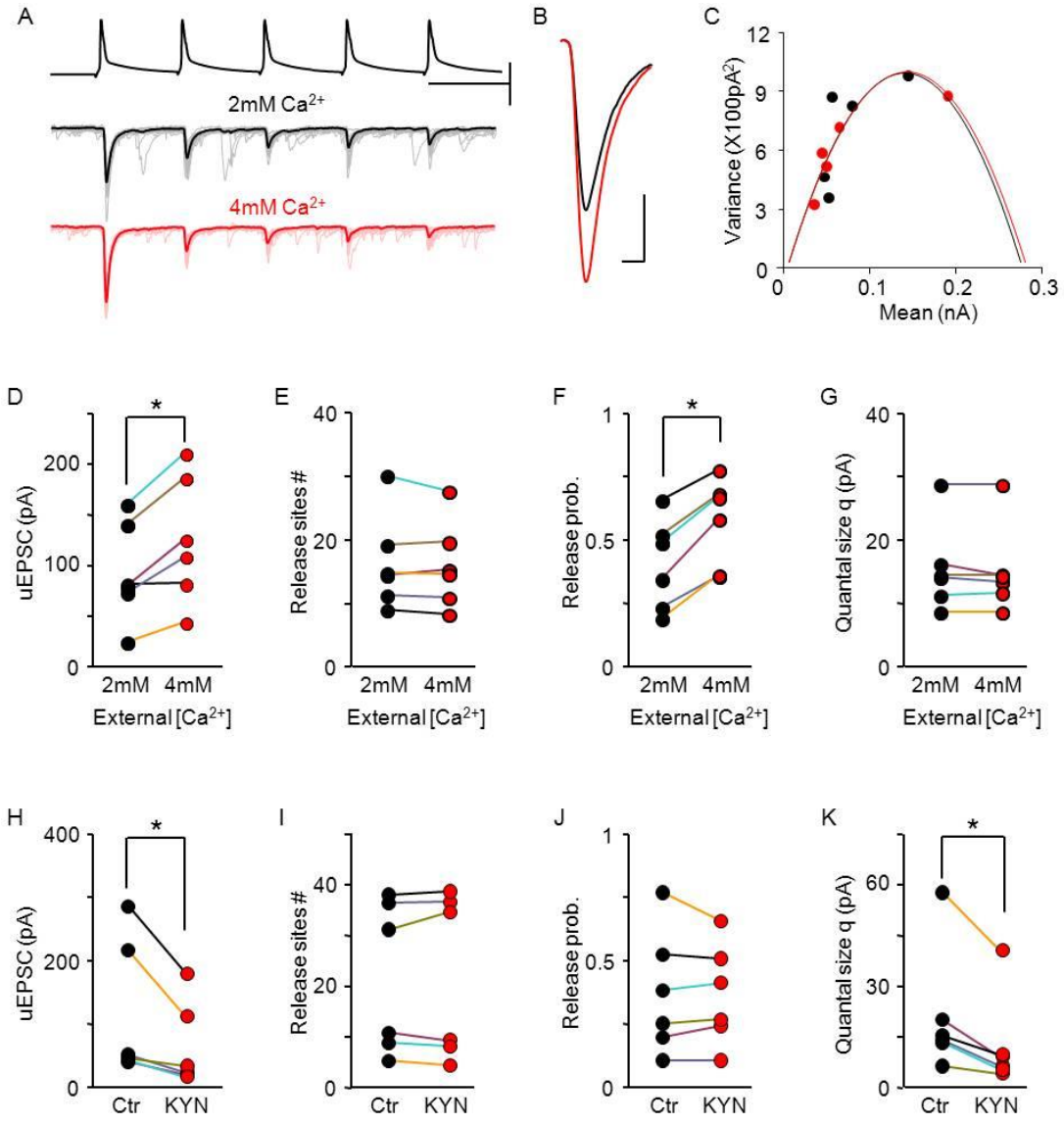

Figure 3-3. Validation of the mean variance analysis for determination of unitary EPSC synaptic parameters. (A) Representative experiment illustrating the estimation of synaptic parameters with a mean variance analysis of uEPSCs evoked by 50 Hz trains (5 pulses). Superimposed traces are 15 consecutive trials (thin lines), along with averaged response (thick lines) recorded in 2 mM Ca^{2+} (black) and 4 mM Ca^{2+} (red). Scale bars: 80 mV, 100 pA, 20 msec. The increase in external Ca^{2+} increased the uEPSC magnitude (B), but did not change the mean-variance relationship (C). Scale bars in B: 50 pA, 10 msec. (D)-(G). Summary of the effect of Ca^{2+} on the uEPSC magnitude (D), the number of release sites (E), the release probability (F) and the quantal size (G) in 2 mM Ca^{2+} (black) and 4 mM Ca^{2+} (red). (H)-(K) Summary of the effect of kynurenic acid on the uEPSC magnitude (H), the number of release sites (I), the release probability (J) and the quantal size (K) before (black) and after kynurenic acid (200 mM). * $p < 0.02$, paired t-test.

To ask how the reduction in excitatory input from proximal pyramidal neurons onto FS (PV) INs impacts total functional excitatory input or inhibitory output, we examined the maximal, extracellularly-evoked IPSC in pyramidal neurons (eIPSC; Fig 3-4 A-C), and the maximal extracellularly-evoked EPSC in FS (PV) IN (eEPSC; Fig 3-4 D-F). This allows an estimation of the combined strength of all available inputs, which we have previously used to characterize developmental changes in the strength of inhibition onto pyramidal neurons (Huang et al., 1999; Morales et al., 2002; Jiang et al., 2007; Huang et al., 2010). In these experiments, the stimulating electrode was placed in layer IV, which effectively recruits horizontal inputs onto layer II/III neurons (Morales et al., 2002). These experiments were performed at postnatal day 35 (± 2 days), when the maturation of inhibitory output is complete in wild types. In pyramidal neurons we observed a similar input/output relationship for the eIPSC in NARP$^{-/-}$ and wild type mice (one way ANOVA, $F_{1, 335}= 0.16$, p=0.689; Fig 3-4B) and similar amplitude of the maximal eIPSC (NARP$^{-/-}$ 5.4 ± 0.4 pA, n = 3, 15; WT 5.2 ± 0.4, n=3, 15; p=0.5, t-test; Fig 3-4C). In contrast, the input/output relationship for the eEPSC was significantly different in NARP $^{-/-}$ and wild type mice (one way ANOVA, $F_{1, 299}=10.93$, p=0.0011; Fig 3-4E), and the amplitude of the maximal eEPSC was significantly reduced (NARP$^{-/-}$ 3.35 ± 0.12 pA, n = 3, 24; WT 2.76 ± 0.17, n=3, 24; p=0.010, t-test; Fig 3-4F). Thus the absence of NARP decreased the strength of total excitatory drive onto FS (PV) INs, without affecting the strength of inhibitory output evoked by depolarization of FS (PV) INs.

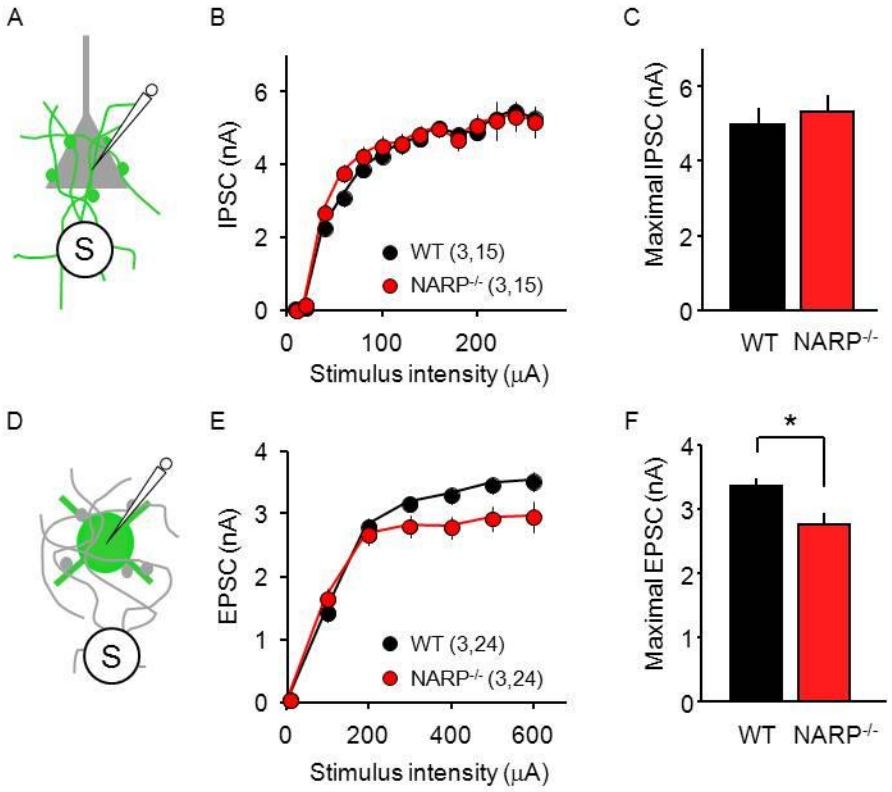

Figure 3-4. Normal Inhibitory Input onto Pyramidal Cells but Reduced Excitatory Input onto FS (PV) INs in NARP$^{-/-}$ Mice (A–C) Extracellularly evoked IPSCs (eIPSCs) recorded in pyramidal neurons are normal in P35 NARP$^{-/-}$ mice. (A) Pharmacologically-isolated eIPSCs were recorded in layer II/III pyramidal neurons, evoked by extracellular stimulation of the underlying layer IV. (B) Input-output relationship for eIPSCs in NARP$^{-/-}$ (red) and WT controls (black). (C) Maximal IPSC computed by averaging eIPSC amplitudes evoked by the three largest stimulus intensities. (D–F) Extracellularly evoked EPSCs (eEPSCs) recorded in FS (PV) INs are reduced in P35 NARP$^{-/-}$ mice. (D) Pharmacologically isolated eEPSCs were recorded in layer II/III FS (PV) INs, evoked by extracellular stimulation of the underlying layer IV. (E) Input-output relationship for eEPSCs in NARP$^{-/-}$ (red) and WT controls (black). (F) Maximal EPSC computed by averaging eEPSC amplitudes evoked by the three largest stimulus intensities. Number of mice and neurons in parentheses in (B) and (E). $^{*}p < 0.02$; t test.

3.3.2 Hyper-excitable visual cortex in NARP $^{-/-}$ mice

We predicted that the decrease in excitatory drive from pyramidal neurons to FS (PV) INs in NARP $^{-/-}$ mice would reduce the ability to recruit fast perisomatic inhibition and increase overall cortical excitability. To test this hypothesis, we examined single unit spiking output in the binocular region of the primary visual cortex of P28 mice *in vivo*. In NARP $^{-/-}$ mice, visually-evoked activity of

neurons in layer II/III (response to 1 Hz reversals of 0.04 cycles/degree; 100% contrast gratings; presented at preferred orientation) had a larger average spike rate (median evoked activity ± SEM (spikes/second): WT 2.45 ±0.32, n=6,16; NARP $^{-/-}$ 4.32 ±0.34, n=6,21, Fig 3-5D) an earlier time to peak (average time to peak ± SEM (msecs): WT 132 ±6, n=6,16; NARP $^{-/-}$ 117 ±7, n=6,21; WT + DZ 153 ±4, n=6,25; NARP $^{-/-}$ + DZ, 139 ±4, n=6,17, one way ANOVA, $F_{3,57}$=8.449, p<0.001; Fig 3-5E) and a longer duration (average msecs ± SEM: WT 76 ±5, n=6,16; NARP $^{-/-}$ 101 ±6, n=6,21; WT + DZ 54 ±3, n=6,25; NARP $^{-/-}$ + DZ 78 ±5, n=6,17; one way ANOVA, $F_{3,57}$=32.370, p<0.001; Fig 3-5F) than wild types. To ask if enhancing inhibitory output could reverse this cortical hyper-excitability, we administered diazepam, a positive allosteric modulator of ligand-bound $GABA_A$ receptors (Sieghart, 1995). Acute diazepam (15 mg/kg, i.p.) significantly reduced the average spike rate, the time to peak and the response duration of visually-evoked activity in NARP $^{-/-}$ and wild type mice (evoked: WT + DZ 1.16 ±0.13, n=6,25; NARP $^{-/-}$ + DZ 2.98 ±0.40, n=6,17, Kruskal-Wallis test, H(3)=37.812, p<0.001, Fig 4D; spontaneous: WT + DZ 0.44 ±0.06, n=6,25, NARP $^{-/-}$ + DZ 0.87 ±0.09, n=6,17, Kruskal-Wallis test, H(3)=28.980, p<0.001). In all cases we observed parallel changes in spontaneous and evoked neuronal firing rates, resulting in no net change in signal to noise ratio (evoked activity / (evoked activity + spontaneous activity) average ± SEM: WT 0.74 ±0.03, n=6,16; NARP $^{-/-}$ 0.75 ±0.03, n=6,21; WT + DZ 0.74 ±0.03, n=6,25; NARP $^{-/-}$ + DZ 0.80 ±0.03, n=6,17; Kruskal-Wallis test, H(3)=2.201, p=0.532). Similar enhancement of visually-evoked and spontaneous activity was observed in neurons from layer IV of NARP $^{-/-}$ mice (Fig 3-6), indicating widespread hyper-excitability in the primary visual cortex of NARP $^{-/-}$ mice.

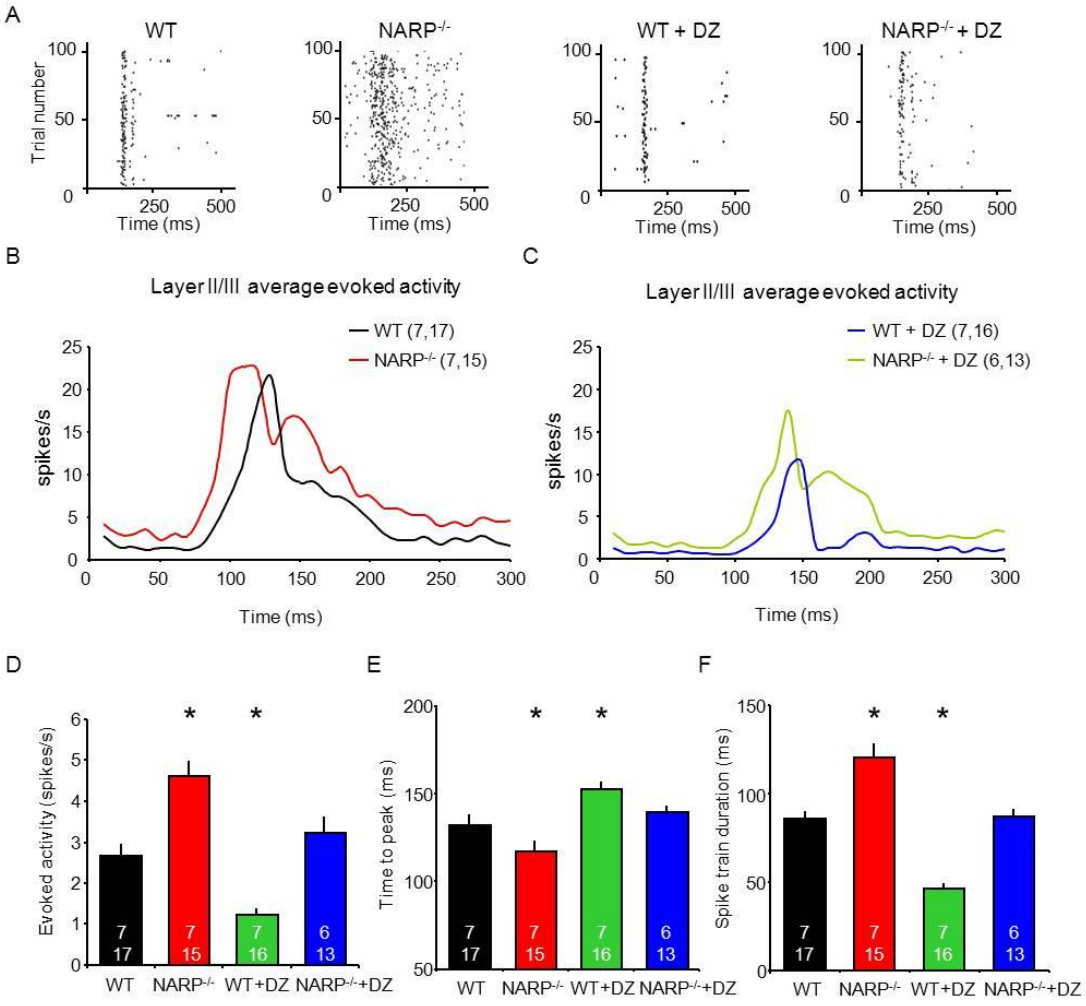

Figure 3-5. Enhanced Neuronal Excitability in Layer II/III of NARP$^{-/-}$ Visual Cortex (A) Representative raster plots of neuronal activity acquired in layer II/III of P28 visual cortex of wild-type, NARP$^{-/-}$, wild-type + diazepam, and NARP$^{-/-}$ + diazepam mice. In each case, activity is shown in response to 100 presentation of visual stimulus in preferred orientation (1 Hz reversals of 0.04 cycles/degree; 100% contrast gratings, starting at time 0). (B) Poststimulus time histograms of average evoked activity of wild-type and NARP$^{-/-}$ mice in response to visual stimulus in preferred orientation. Kruskal-Wallis test, H = 9.366, p = 0.002. (C) Poststimulus time histograms of average-evoked activity of wild-type + diazepam and NARP$^{-/-}$ + diazepam in response to visual stimulus in preferred orientation. Kruskal-Wallis test, H = 21.01, p < 0.001. (D) Median-evoked activity from layer II/III of P28 visual cortex. Kruskal-Wallis test, H(3) = 37.812, p < 0.001, *p < 0.05 Mann-Whitney post hoc versus wild-type controls. (E) Time-to-peak-evoked activity from layer II/III of P28 visual cortex. One-way ANOVA ($F_{3,57}$ = 8.449, p < 0.001), *p < 0.05 Bonferroni post hoc versus wild-type controls. (F) Spike train duration from layer II/III of P28 visual cortex. One-way ANOVA ($F_{3,57}$ = 32.370, p < 0.001), *p < 0.05 Bonferroni post hoc versus wild-type controls.

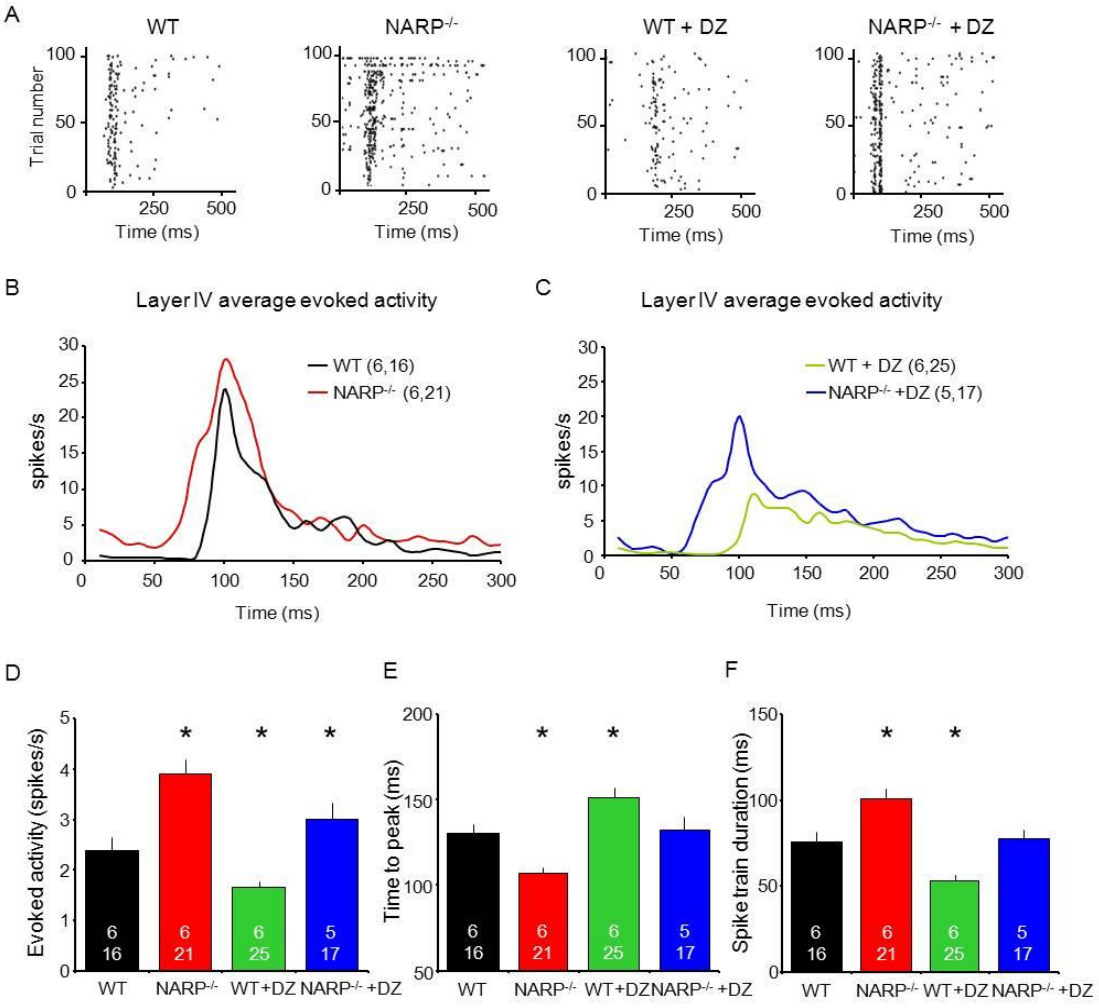

Figure 3-6. Enhanced neuronal excitability in layer IV of NARP$^{-/-}$ visual cortex. (A) Representative raster plots of neuronal activity acquired in layer IV of P28 visual cortex of wild type, NARP$^{-/-}$, wild type + diazepam and NARP$^{-/-}$ + diazepam mice. In each case, activity is shown in response to visual stimulus in preferred orientation (1 Hz reversals of 0.04 cycles/degree; 100% contrast gratings, starting a time 0). (B) Post-stimulus time histograms of average evoked activity of wild type (black) and NARP$^{-/-}$ (red) mice in response to visual stimulus in preferred orientation. n = (subjects, neurons), Kruskal-Wallis test, H = 7.24, p = 0.007. (C) Post-stimulus time histograms of average evoked activity of wild type + diazepam (green) and NARP$^{-/-}$ + diazepam (blue) mice in response to visual stimulus in preferred orientation. n = (subjects, neurons), Kruskal-Wallis test, H = 7.643, p = 0.006. (D) Median (+/- S.E.M.) visually-evoked activity recorded in layer IV of P28 mice. Kruskal-Wallis test, $H(3)$ = 31.533, $p < 0.001$, * $p < 0.05$ Mann-Whitney post hoc versus wild type controls. (E) Average (+/- S.E.M.) time to peak of visually-evoked activity recorded in layer IV of P28 mice. One way ANOVA F(3,75) = 12.267, $p < 0.001$, * $p < 0.05$ Bonferroni's post hoc versus wild type controls. (F) Average (+/- S.E.M.) spike train duration recorded in layer IV of P28 mice. One way ANOVA F(3,75) = 21.505, $p < 0.001$, * $p < 0.05$ Bonferroni's post hoc versus wild type controls.

3.3.3 Normal vision in NARP $^{-/-}$ mice

We used visually evoked potentials (VEPs) to ask if the absence of NARP and the resulting increase in cortical excitability, impacted visual acuity or visual cortical plasticity. Visual acuity was estimated by extrapolating the linear regression of the VEP amplitude versus the spatial frequency of the visual stimulus (range from 0.04 – 0.6 cycles/degree) to 0 mV (Porciatti et al., 1999). In these experiments, we used VEPs recorded from the surface of the binocular visual cortex, to focus on synaptic potentials generated in superficial laminae (Katzner et al., 2009). We found that juvenile (P30) NARP $^{-/-}$ mice had an estimated spatial acuity of 0.48 ±0.04 cycles/degree (average ± SEM, n=5), which was indistinguishable from age-matched wild type controls (0.49 ±0.02 cycles/degree, n=5; p=0.86, t-test; Fig 3-7A). Manipulation of the visual stimulus from 20 to 100% contrast revealed similar contrast sensitivity in NARP $^{-/-}$ and wild type vision (Two way repeated measures ANOVA, $F_{1,6} = 0.003$, p=0.955; Fig 3-7B).

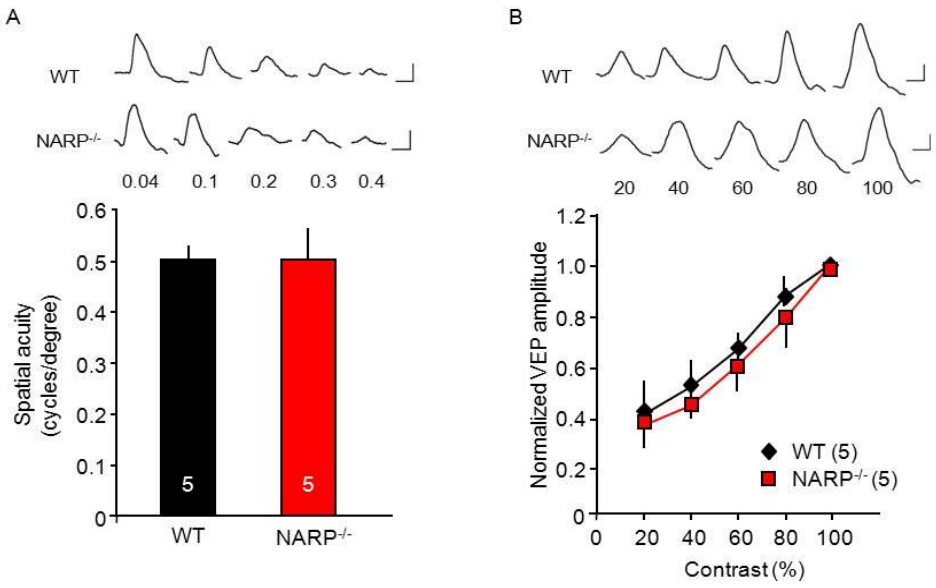

Figure 3-7. Normal Vision in NARP$^{-/-}$ Mice (A) Comparable spatial acuity in NARP$^{-/-}$ mice and age-matched (P30) wild-types. Spatial acuity is extrapolated from the linear regression of VEP amplitude versus spatial frequency of the visual stimulus. (B) Comparable contrast sensitivity in NARP$^{-/-}$ mice and age-matched (P30) wild-types.

To ask if the absence of NARP disrupts the organization of the visual cortex, we quantified ocular preference and retinotopy over the medio-lateral extension of V1. To examine ocular preference, we calculated the ratio of VEP amplitudes in response to separate stimulation of the contralateral and ipsilateral eye (Fig 3-8). In both wild type and NARP $^{-/-}$ mice, recordings medial to the binocular region of the primary visual cortex revealed responses to contralateral eye stimulation only, as expected of monocular visual cortex. Recordings from a narrow area, ranging from ~ 3.0 – 3.5 mm lateral to the intersection of lambda and bregma, revealed responses to visual stimulation of both eyes, as expected of binocular visual cortex. Recordings lateral to the binocular region of the primary visual cortex revealed a loss of contralateral preference, as expected for the lateral medial region of secondary visual cortex (Rossi et al., 2001). Retinotopy was also similar in wild type and NARP $^{-/-}$ mice. The area of visual space resulting in the largest VEP amplitude moved along the visual field azimuth, from contralateral visual field to the meridian as the recording site was moved laterally across the binocular region of the primary visual cortex, and reversed toward the contralateral visual cortex as the recording site moved laterally from the binocular region of the primary visual cortex into LM (Fig 3-8D). The orientation selectivity and orientation tuning of NARP $^{-/-}$ mice was also similar to wild types (Fig 3-9). Thus many aspects of visual system organization and function are normal in NARP $^{-/-}$ mice.

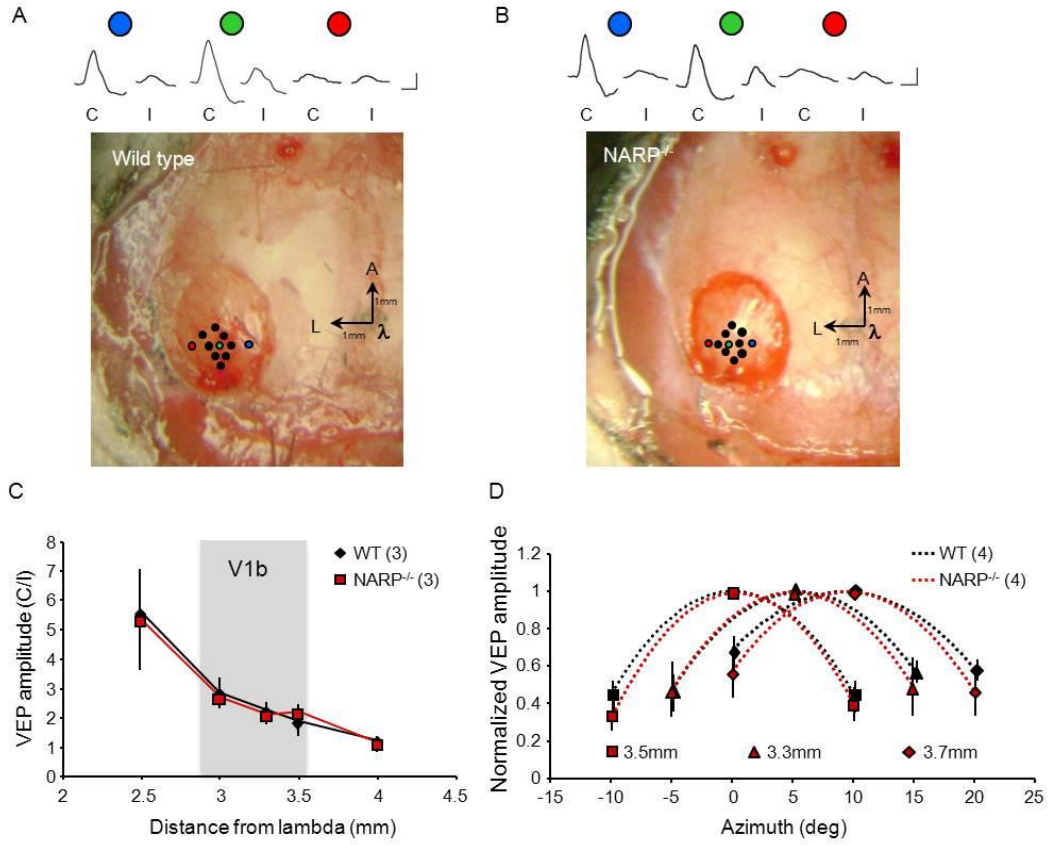

Figure 3-8. Normal ocularity and retinotopy in NARP$^{-/-}$ mice. Representative VEPs in response to stimulation of the contralateral (C) and ipsilateral (I) eye recorded at multiple sites along the medio-lateral aspect of visual cortex in a wild type (A) and NARP$^{-/-}$ mouse (B). Recording site ~ 2.8 mm lateral to intersection of lambda (λ) and midline (blue), is near the V1b/V1m border (WT, C/I = 3.64, ipsilateral VEP 14 μV; NARP$^{-/-}$, C/I = 5.65, ipsilateral VEP 26 μV). The recording site yielding the largest ipsilateral VEP, typically 3.3 mm lateral to lambda (green) was used for comparison of contralateral bias across genotypes (WT, C/I = 2.46, ipsilateral VEP 69 μV; NARP$^{-/-}$, C/I = 2.17, ipsilateral VEP 60 μV). Recording site ~3.8 mm lateral to lambda (red) is near the V1b/LM border (WT C/I = 1.24, ipsilateral VEP 17 μV; NARP$^{-/-}$ C/I = 0.98, ipsilateral VEP 22 μV). Scale bars in (A) and (B): 50 ms, 50 μV. (C) Similar distribution of ocular preference along the medio-lateral dimension of the visual cortex in wild type (black) and NARP$^{-/-}$ (red) mice. VEP C/I: WT, 2.5 mm, 5.61 ±1.36, 3.0 mm, 2.85 ±0.51, 3.3 mm, 2.26 ±0.28, 3.5 mm, 1.91 ±0.54, 4.0 mm, 1.25 ±0.01, n=3 subjects; NARP$^{-/-}$, 2.5 mm, 5.37 ±1.72, 3.0 mm, 2.69 ±0.38, 3.3 mm, 2.12 ±0.04; 3.5 mm, 2.22 ±0.16, 4.0 mm, 1.16 ±0.21, n=3 subjects. Two way ANOVA, F(1,4) = 0.2805, p = 0.886. (D) Similar retinotopic organization in the visual cortex of wild type (black) and NARP$^{-/-}$ (red) mice. VEP responses to windowed visual stimuli (10 degrees; horizontal gratings reversing at 1Hz) at different visual field azimuths (from -10 to +20 degrees from visual meridian) at 3 recording sites (3.3 mm, 3.5 mm and 3.7 mm lateral to midline) in wild type and NARP$^{-/-}$ mice. n = 4 subjects. VEP amplitudes are normalized to the maximal VEP recorded at that site, and the relationship between amplitude and visual field azimuth was fitted with a second-order polynomial (dotted line). Two-way ANOVA, 3.3 mm, F(1,1) = 0.2576, p = 0.62; 3.5 mm, F(1,1) = 0.1528, p = 0.7; 3.7 mm, F(1,1) = 0.1984, p = 0.66.

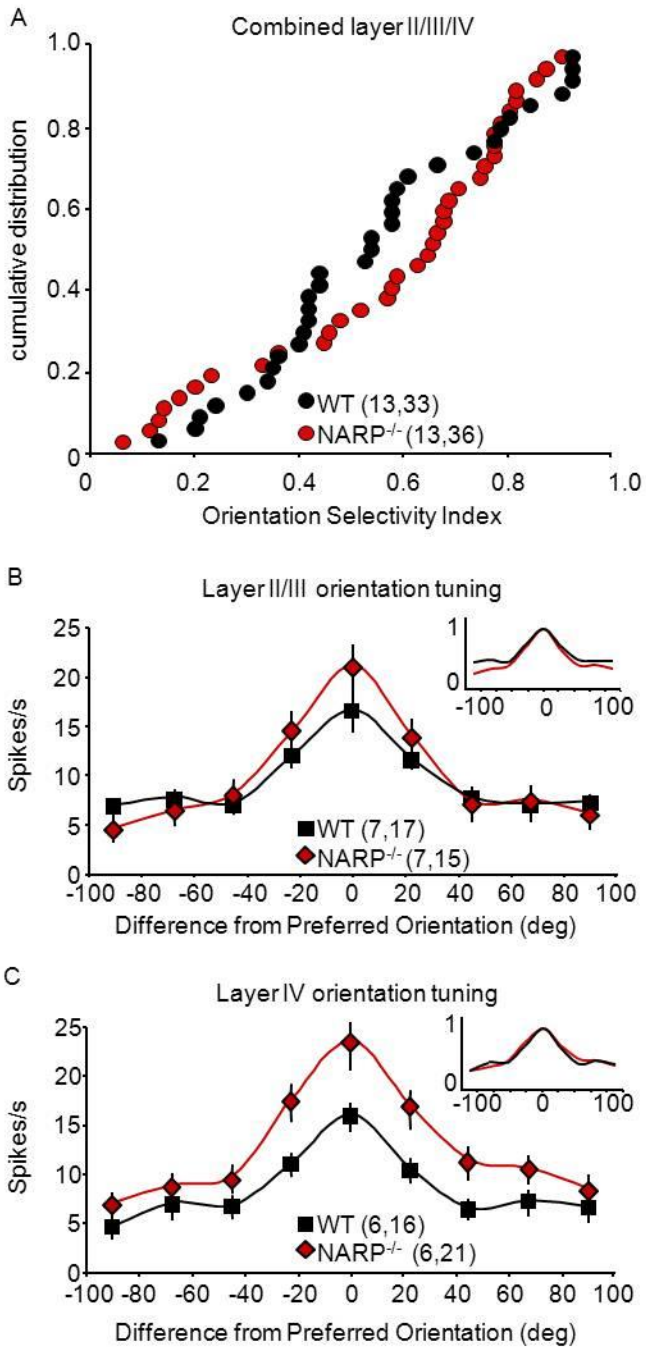

Figure 3-9. Normal orientation selectivity and orientation tuning in NARP$^{-/-}$ mice. (A) Similar orientation selectivity of visually-evoked unit activity in wild type (black) and NARP$^{-/-}$ (red) mice. Orientation selectivity index = (response evoked by visual stimulus in preferred orientation - orthogonal orientation) / (pref + ortho). n = (subjects, neurons), KS test: D = 0.2525, p = 0.1899. (B) Similar orientation tuning width of neurons in layer II/III of binocular visual cortex in wild type (black) and NARP$^{-/-}$ (red) mice. The preferred orientations are aligned at 0 degrees. n = (subjects, neurons). Inset: orientation tuning normalized by maximal responses in each genotype. (C) Similar orientation tuning width of neurons in layer IV of binocular visual cortex in wild type (black) and NARP$^{-/-}$ (red) mice. The preferred orientations are aligned at 0 degrees. n = (subjects, neurons). Inset: orientation tuning normalized by maximal responses in each genotype.

The binocular primary visual cortex of rodent has a contralateral bias that depends on early binocular visual experience (McCurry et al., 2010). To ask if NARP $^{-/-}$ mice retained normal experience-dependent regulation of VEP contralateral bias, we examined VEP contralateral bias at the site in binocular visual cortex that yielded the largest ipsilateral eye VEP (typically 3.3 mm

lateral to the intersection of lambda and bregma). Dark-rearing from birth to postnatal day 30 (P30) prevented the expression of the VEP contralateral bias in both genotypes. Similarly, bringing dark-reared subjects (at P30) into a normal lighted environment (3 days) increased the contralateral bias to the normal range (VEP amplitude contralateral eye/ipsilateral eye, average ± SEM: wild type DR 1.26 ±0.03, n=4; DR+L 2.05 ±0.03, n=4; one way ANOVA, $F_{2,10}$=273.61, p<0.001, Fig 3-10A; NARP $^{-/-}$ DR 1.29 ±0.02, n=6; DR+L 2.12 ±0.04, n=6; one way ANOVA, $F_{2,14}$=72.947, p<0.001, Fig 3-10B). In both NARP $^{-/-}$ and wild type mice, the experience-dependent regulation of VEP contralateral bias was mediated by changes in the amplitude of the contralateral eye VEP (Fig 3-10 C-D). Thus the expression of a form of synaptic plasticity that is dependent on early visual experience is intact in NARP $^{-/-}$ mice.

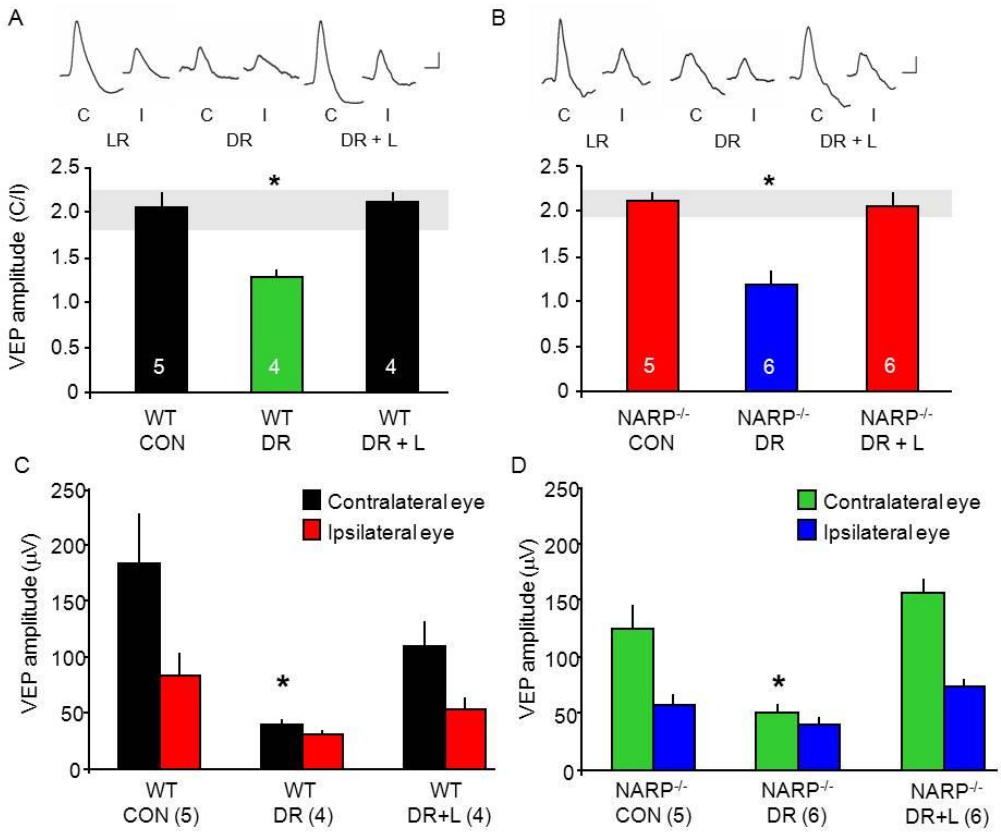

Figure 3-10. Normal experience-dependent regulation of VEP contralateral bias in NARP$^{-/-}$ mice. (A) Two-fold VEP contralateral bias in P30 wild-types (CON). Dark rearing (DR) from birth to P30 significantly inhibits the experience-dependent expression of VEP contralateral bias. Exposing dark-reared subjects to 3 days of normal lighted environment (DR + L) at P28 increases the VEP contralateral bias to the normal range (gray horizontal bar). One-way ANOVA ($F_{2,10} = 273.61$, $p < 0.001$). (B) VEP contralateral bias is normal in P30 NARP$^{-/-}$ mice (CON). Dark rearing (DR) from birth to P30 significantly inhibits the experience-dependent expression of VEP contralateral bias. Exposing dark-reared subjects to 3 days of light (DR + L) at P28 increases VEP contralateral bias to the normal range (gray horizontal bar). One-way ANOVA ($F_{2,14} = 72.947$, $p < 0.001$); $^{*}p < 0.01$ Bonferroni post hoc versus control. Inset: representative VEP waveforms. Scale bars represent 50 ms, 50 μV. **(**C) Two-fold larger VEP amplitudes in response to stimulation of the contralateral eye (black) versus ipsilateral eye (red) in P30 wild type controls (CON, n = 5). Dark-rearing from birth (DR, n = 4) inhibited the experience-dependent enhancement of the contralateral eye VEP. Exposure to normal lighted environment after dark-rearing (DR + L, n = 4) stimulated an increase in the contralateral eye VEP. One way ANOVA F(2,10) = 4.793, $p < 0.05$; * $p < 0.05$ Bonferroni's post hoc versus WT CON. (D) Normal, two-fold larger VEP amplitude in response to stimulation of the contralateral eye (green) versus ipsilateral eye (blue) in P30 NARP$^{-/-}$ controls (CON, n = 5). Dark-rearing from birth (DR, n = 6) inhibited the experience-dependent enhancement of the contralateral eye VEP. Exposure to normal lighted environment after dark-rearing (DR + L, n = 6) stimulated an increase in the contralateral eye VEP. One way ANOVA F(2,10) = 14.875, $p < 0.001$; * $p < 0.05$ Bonferroni's post hoc versus NARP$^{-/-}$ CON.

3.3.4 Absence of ocular dominance plasticity in NARP $^{-/-}$ mice

To ask how the absence of NARP affects ocular dominance plasticity, we examined the response to brief (3 days) and prolonged (7 days) monocular deprivation (MD) on the VEP contralateral bias initiated at P25, the peak of the critical period (Fagiolini et al., 1994; Gordon and Stryker, 1996; Fagiolini and Hensch, 2000). As expected, both brief and prolonged monocular deprivation of the dominant contralateral eye significantly decreased the VEP contralateral bias in juvenile wild type mice (VEP amplitude contralateral eye/ipsilateral eye average ± SEM: no MD 2.19 ± 0.03, n=5; 3d MD 1.32 ± 0.05, n=4; 7d MD 1.18 ± 0.04, n=5; Fig 3-11). In contrast, no shift in ocular dominance was observed in juvenile NARP $^{-/-}$ mice following either brief or prolonged monocular deprivation (no MD 2.16 ± 0.10, n=5; 3d MD 1.91 ± 0.07, n=6; 7d MD 1.92 ± 0.07, n=6). Importantly, enhancing inhibitory output with diazepam (15 mg/kg, 1x/day) enabled ocular dominance plasticity in juvenile NARP $^{-/-}$ mice (5d MD+DZ 1.09 ± 0.08, n=5). No shift in ocular

dominance was observed following diazepam alone (VEP amplitude contralateral eye/ipsilateral eye, average ± SEM: NARP $^{-/-}$ + DZ no MD, 2.08±0.11, n=3, t-test versus NARP $^{-/-}$ no MD, p=0.61).

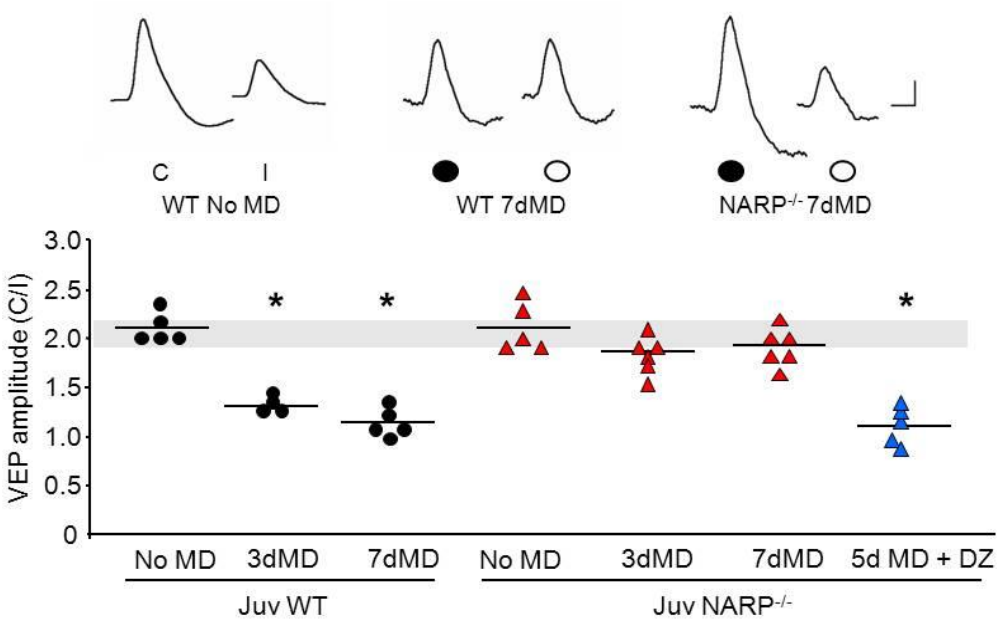

Figure 3-11. Absence of Ocular Dominance Plasticity in Juvenile NARP$^{-/-}$ Mice Brief (3 days) and prolonged (7 days) monocular deprivation of the dominant, contralateral eye induced a significant decrease in the VEP contralateral bias in juvenile (P25) wild-type, but not NARP$^{-/-}$ mice. Diazepam (DZ, for 5 days initiated at P25) enabled ocular dominance plasticity in NARP$^{-/-}$ mice. One-way ANOVA ($F_{6,29} = 51.187$, $p < 0.001$); $^{*}p < 0.05$ Bonferroni post hoc versus WT no MD control. Normal VEP contralateral bias is depicted by gray horizontal bar. Inset: representative VEP waveforms. C, contralateral eye; I, ipsilateral eye. Scale bars represent horizontal 50 ms, vertical 50 μV.

Ocular dominance plasticity persists into adulthood in wild type mice (Sawtell et al., 2003; Sato and Stryker, 2008) and may utilize mechanisms distinct from those recruited by monocular deprivation earlier in development (Pham et al., 2004; Fischer et al., 2007; Ranson et al., 2012). To ask if adult NARP $^{-/-}$ mice could express ocular dominance plasticity, we examined the response to monocular deprivation for 7 days beginning at P90 (Fig 3-12). However this manipulation did

not induce a shift in ocular dominance in NARP $^{-/-}$ mice (VEP amplitude contralateral eye/ipsilateral eye average ± SEM: adult NARP $^{-/-}$ no MD 2.15±0.13, n=5; 7d MD 1.93±0.09, n=7). To confirm the absence of ocular dominance plasticity in NARP $^{-/-}$ mice, we examined the VEP contralateral bias after chronic monocular deprivation (80 days beginning at P21). Surprisingly, the normal ocular dominance of NARP $^{-/-}$ mice persisted following chronic monocular deprivation (VEP amplitude contralateral eye/ipsilateral eye average ± SEM: cMD 2.00±0.11, n=5). Increasing inhibitory output with diazepam for the last 5 days of chronic monocular deprivation enabled an ocular dominance shift in adult NARP $^{-/-}$ mice (15 mg/kg, i.p.; cMD + DZ 1.17±0.10, n=6; Fig 3-12). As expected, adult wild type mice expressed a significant shift in contralateral bias in response to prolonged (7 days) and chronic (80 days) monocular deprivation (VEP amplitude contralateral eye/ipsilateral eye average ± SEM: adult WT no MD 2.04±0.20, n=5; 7d MD 1.14±0.13, n=5; cMD 0.99±0.17, n=3), which was unaffected by diazepam in adulthood (cMD + DZ 0.98±0.09, n=4). Thus, in the absence of NARP, the visual system is unable to respond to monocular deprivation, despite functional inhibitory output.

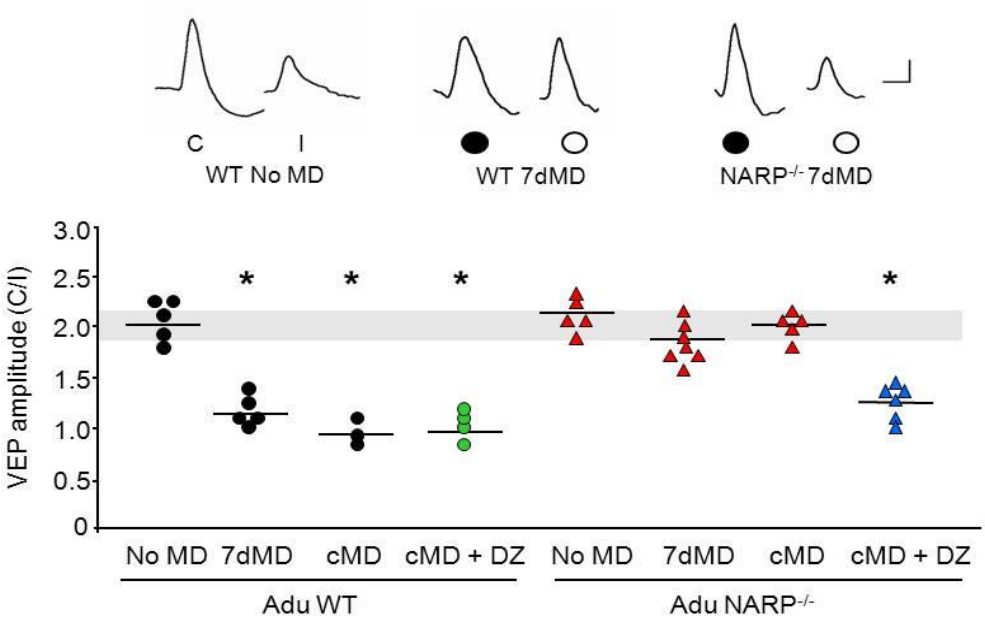

Figure 3-12. Absence of Ocular Dominance Plasticity in Adult NARP$^{-/-}$ Mice Prolonged monocular deprivation (7 days) of the dominant, contralateral eye initiated in adulthood (P90) and chronic monocular deprivation (from P21–P100) induced a significant decrease in the VEP contralateral bias in adult wild-type, but not NARP$^{-/-}$ mice. Diazepam (DZ, during the last 5 days of chronic MD) enabled ocular dominance plasticity in chronically deprived NARP$^{-/-}$ mice, but does not change the ocular dominance shift in wild-type mice. One-way ANOVA ($F_{7,32} = 18.706$, $p < 0.001$); $^{*}p < 0.05$ Bonferroni post hoc versus WT no MD. Normal VEP contralateral bias is depicted by gray horizontal bar. Inset: representative VEP waveforms. C, contralateral eye; I, ipsilateral eye. Scale bars represent 50 ms, 50 μV.

3.3.5 Differential response of NARP $^{-/-}$ mice to low frequency versus high frequency visual stimulation

Although NARP $^{-/-}$ mice do not express ocular dominance plasticity, other forms of experience-dependent synaptic plasticity, such as the plasticity of the VEP contralateral bias, remain intact (Fig 3-10). To further explore the range of deficits in synaptic plasticity in NARP $^{-/-}$ mice, we examined the response to repetitive visual stimulation, previously shown to induce robust changes in VEP amplitudes *in vivo* (Sawtell et al., 2003; Frenkel et al., 2006; Ross et al., 2008; Cooke and Bear, 2010; Beste et al., 2011). High frequency visual stimulation (10 Hz reversals of 0.04 cycles/degree, 100% contrast, vertical gratings) induced a rapid enhancement of the VEP amplitude in P30 NARP $^{-/-}$ and wild type mice (VEP amplitude 60 mins post-stimulation normalized to pre-stimulation: WT 1.48 ±0.12, n=5; NARP $^{-/-}$ 1.41 ±0.06, n=5; two way ANOVA, $F_{1,1}$=0.316, p=0.584; Fig 3-13A). The enhancement in VEP amplitude was dependent on the temporal frequency of the visual stimulation, as visual stimulation at an intermediate temporal frequency (5 Hz) did not affect VEP amplitudes in either genotype (VEP amplitude 60 mins post-stimulation normalized to pre-stimulation: WT 1.00 ±0.03, n=3; NARP $^{-/-}$ 0.97 ±0.10, n=3). The increase in VEP amplitude induced by 10 Hz visual stimulation was specific for the orientation of the visual stimulus, as no VEP enhancement was observed in response to a rotated grating (10 Hz:

WT 0.96±0.05, n=5; NARP $^{-/-}$ 0.94±0.06, n=5; 5 Hz: WT 0.94±0.03, n=3; NARP $^{-/-}$ 0.97±0.08, n=3; two way ANOVA, $F_{1,1}$=0.002, p=0.968; Fig 3-13B). In contrast,, low frequency visual stimulation (1 Hz reversals of 0.04 cycles/degree, 100% contrast vertical gratings) induced a slowly emerging increase in VEP amplitude in wild type mice (VEP amplitude post/pre stimulation: 12h 0.98±0.14; 15h 1.32±0.12; 18h 1.45±0.08; n=5), that was inhibited by diazepam (12h 0.91±0.01; 15h 0.91±0.04; 18h 1.13±0.01; n=5, two way ANOVA with repeated measures, $F_{1,8}$=18.288, p=0.003; *p<0.01 versus wild type control; Fig 3-13C). As previously reported, the enhancement of VEP amplitude was selective for the orientation of the visual stimulus, as no increase in VEP amplitude was observed in response to a rotated grating (12h 0.88±0.12; 15h 0.99±0.04; 18h 0.94±0.06, n=5; Fig 3-13D; Cooke and Bear, 2010). However, the slow, stimulus-selective response plasticity was absent in NARP $^{-/-}$ mice (12h 0.82±0.12; 15h 0.93±0.11; 18h 1.01±0.06; n=5; Fig 8E), but could be enabled by diazepam (12h 1.14±0.06; 15h 1.53±0.12; 18h 1.55±0.13; n=5, two way ANOVA with repeated measures, $F_{1,8}$=12.247, p=0.008; *p<0.01 versus NARP -/- control; Fig 3-13E). The response enhancement evoked in the presence of diazepam was selective for the orientation of the familiar visual stimulus (12h 0.68±0.06; 15h 0.79±0.05; 18h 0.99±0.02; n=5; Fig 3-13F). Thus, the absence of NARP completely eliminates the expression of

several essential form of experience-dependent synaptic plasticity, while other aspects of circuit function and plasticity remain unchanged.

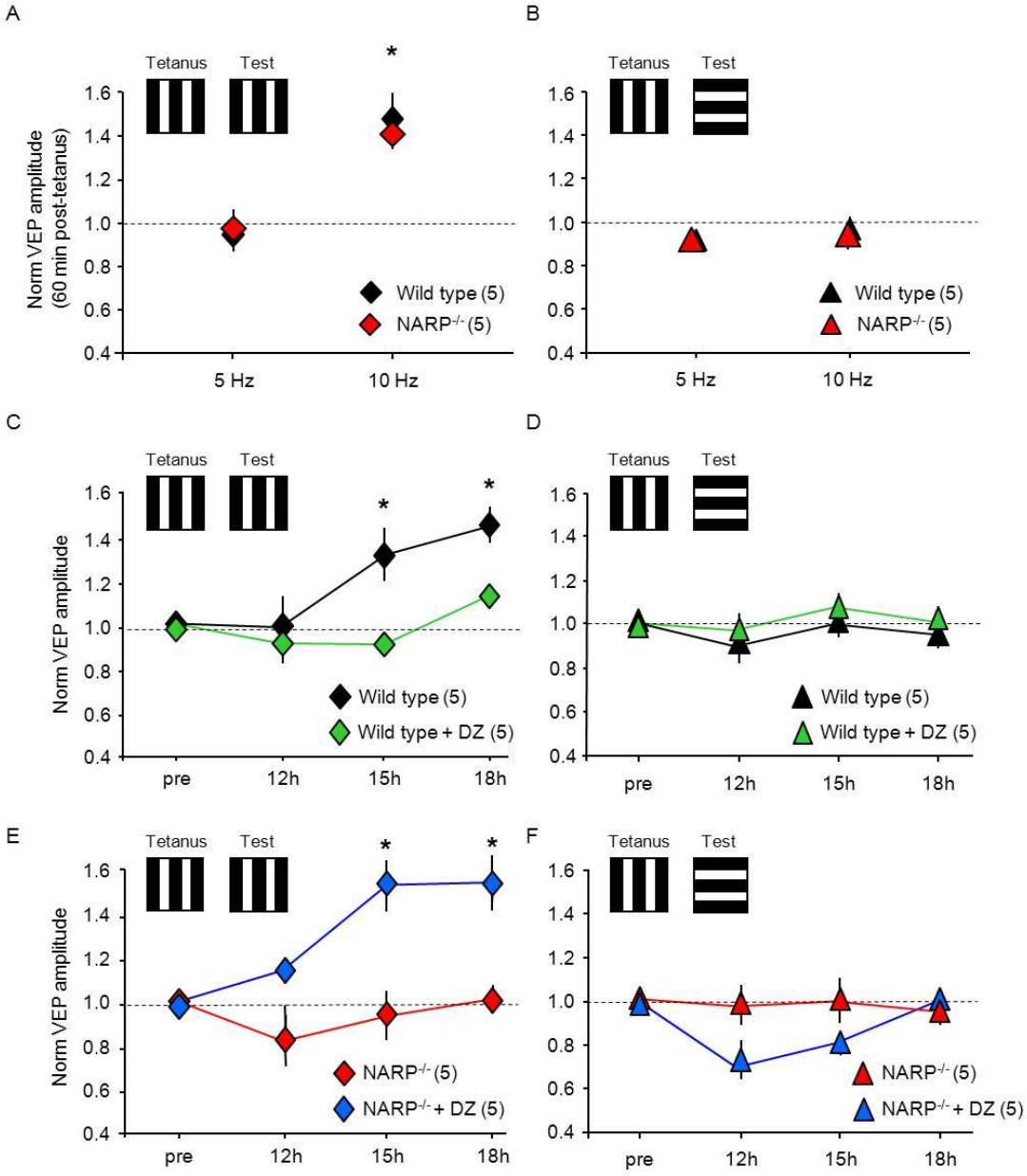

Figure 3-13. Differential Response of NARP$^{-/-}$ Mice to Low- versus High-Frequency Visual Stimulation (A) High-frequency visual stimulation (10 Hz reversals of 0.04 cycle/degree 100% contrast vertical gratings) induced a rapid increase in VEP amplitude in P30 wild-type and NARP$^{-/-}$ mice, but 5 Hz reversals were ineffective $^{*}p < 0.05$ t test versus prestimulation baseline. (B) Enhancement of VEP amplitude following high-frequency visual stimulation did not transfer to a visual stimulus of a novel orientation. (C) Low-frequency visual stimulation (1 Hz reversals of 0.04 cycle/degree 100% contrast

vertical gratings) induced a slow increase in VEP amplitude in P30 wild-type mice (black symbols), which was inhibited by diazepam (15 mg/kg, i.p.; 30 min prior to stimulation; green symbols). Two-way repeated-measures ANOVA ($F_{1,8} = 18.288$, $p = 0.003$); $^{*}p < 0.01$ Bonferroni post hoc versus prestimulation. (D) Enhancement of VEP amplitudes following low-frequency visual stimulation did not transfer to a visual stimulus of a novel orientation. (E) Low-frequency visual stimulation (1 Hz reversals of 0.04 cycle/degree 100% contrast vertical gratings) did not change VEP amplitudes in P30 NARP$^{-/-}$ mice (red symbols). Administration of diazepam (30 min prior to stimulation), enabled the enhancement of VEP amplitudes by low-frequency visual stimulation (blue symbols; 15 mg/kg, i.p.). Two-way repeated-measures ANOVA ($F_{1,8} = 12.247$, $p = 0.008$); $^{*}p < 0.01$ Bonferroni post hoc versus prestimulation. (F) The enhancement of VEP amplitudes in NARP$^{-/-}$ mice by low-frequency visual stimulation enabled by diazepam did not transfer to a visual stimulus of a novel orientation.

3.4 Discussion

Transgenic deletion of NARP allowed us to demonstrate that the strength of excitatory drive onto FS (PV) INs plays a central role in the initiation of the critical period for ocular dominance plasticity. Transgenic deletion of the immediate early gene NARP decreases the number of excitatory synaptic connections onto FS (PV) INs, thereby decreasing net excitatory drive onto neurons that mediate the majority of perisomatic inhibition. Importantly, net inhibitory drive from FS (PV) INs is unchanged in NARP$^{-/-}$ mice. Nonetheless, the visual cortex of NARP $^{-/-}$ mice is hyper-excitable, and unable to express several cardinal forms of synaptic plasticity, including ocular dominance plasticity, which are typically robust during an early postnatal critical period. Pharmacological reduction of the hyper-excitability in NARP $^{-/-}$ mice compensates for the deficit in the recruitment of inhibition, and allows the expression of ocular dominance plasticity. We propose that NARP-dependent recruitment of inhibition from FS (PV) INs is necessary to ensure the precision of pyramidal cell activity necessary to engage these forms of synaptic plasticity (Jiang et al., 2007; Toyoizumi and Miller, 2009; Kuhlman et al., 2010). The NARP-dependent enhancement of excitatory drive onto FS (PV) INs is therefore an important, novel locus for the regulation of the critical period for ocular dominance plasticity.

3.4.1 Role of NARP in initiation of the critical period

NARP is selectively enriched at excitatory synapses onto FS (PV) INs (Chang et al., 2010), the fast-spiking basket cells which mediate rapid feed-forward and feed-back inhibition onto neuronal somata (Kawaguchi and Kubota, 1997; Ascoli et al., 2008). Perisomatic inhibition from FS (PV) INs is therefore ideally located to exert powerful temporal and spatial control of the spiking output of principal neurons (Pouille and Scanziani, 2001; Goldberg et al., 2008; Kulman et al., 2010). Indeed, it has been proposed that a supra-threshold level of perisomatic inhibition is necessary to promote the synaptic plasticity between principal neurons that initiates the critical period for ocular dominance plasticity (Huang et al., 1999; Di Cristo et al., 2007). Alternatively, plasticity at synapses that mediate feedback inhibition onto principal neurons in the visual cortex has been proposed to mediate the shift in ocular dominance induced by monocular deprivation (Maffei et al., 2006). Changes in interneuron excitability and ocularity have been reported in response to monocular deprivation (Yazaki-Sugiyama et al., 2009; Gandhi et al., 2008; Kameyama et al., 2010). Our work suggests for the first time that a critical step in the initiation of the critical period is the recruitment of inhibition through NARP-dependent enhancement of excitatory drive onto FS (PV) INs. The deficit in the ability to recruit inhibition prevents the induction of ocular dominance plasticity in NARP $^{-/-}$ mice, despite the presence of normal perisomatic inhibition. Importantly, sensory experience has been shown to strengthen excitation from thalamic afferents onto feed-forward inhibitory interneurons in layer IV of rodent barrel cortex (Chittajallu and Isaac, 2010), and in the visual cortex, these inputs are remodeled by monocular deprivation (Kuhlman et al., 2011).

3.4.2 Absence of critical period plasticity in NARP $^{-/-}$ mice

Monocular deprivation prior to the initiation of the critical period (~ P18 in rodents) is ineffective, demonstrating that a developmental change in visual cortical circuitry is necessary to initiate ocular dominance plasticity. In the absence of NARP, the visual system is retained in a hyper-excitable state that is reminiscent of this pre-critical period. The method that we used to assess ocular dominance plasticity, examination of the contralateral bias of VEPs evoked by simple visual stimuli, has a lower threshold for the detection of changes induced by MD than other methods, such as change in visual acuity (Prusky and Douglas, 2003; Heimel et al., 2007). In addition, our VEP recordings were performed in superficial layers of the visual cortex, where ocular dominance plasticity is expressed long into postnatal development in wild types (Fischer et al., 2007; Heimel et al., 2007; Lehmann and Lowel, 2008; Sato and Stryker, 2008). Despite this, we saw no evidence for a shift in ocular dominance in NARP $^{-/-}$ mice, including in response to monocular deprivation of unusually long duration (> ten weeks). This suggests that the visual system cannot compensate for the absence of NARP, and is unable to recruit the inhibition necessary to enable ocular dominance plasticity**.** We cannot rule out the possibility that monocular deprivation in NARP $^{-/-}$ mice induces changes in the strength of synapses outside the recording radius of our electrode.

3.4.3 Visual function and pre-critical period plasticity are normal in NARP $^{-/-}$ mice

Previous work has identified an important role for neuronal pentraxins in the refinement of retinogeniculate synapses in the dLGN (Bjartmar et al., 2006). The ipsilateral eye input to the dLGN of NARP $^{-/-}$ (a.k.a. NP2), was slightly expanded at P10 compared to age matched WTs, but this expansion was mild compared to NP1/2 double KO mice. Despite the initial deficit in the refinement of retinogeniculate synapses, the binocular inputs to the dLGN of P30 NP1/2 KO mice become more segregated by P30. In our experiments, the single deletion of NARP (NP2) did not

disrupt the macro-organization of V1. Indeed, the anatomical boundaries between V1b and V1m and LM were similar in wild type and NARP $^{-/-}$ mice, and no differences were observed in retinotopy within V1b or the distribution of ocular preference along the medio-lateral aspect of the primary visual cortex. Although other aspects of visual system organization not tested here may be disrupted in NARP $^{-/-}$ mice, our results clearly demonstrate that many aspects of visual cortex organization are unimpaired despite the deficit in the recruitment of inhibition. In addition, many aspects of visual function that mature before or during the critical period, including contralateral bias, spatial acuity and contrast sensitivity, were normal in NARP$^{-/-}$ mice (Huang et al., 1999; Prusky and Douglas, 2004; Heimel et al., 2007). The absence of a change in visual acuity was not unexpected, as the parallel increase in evoked and spontaneous single unit activity in NARP $^{-/-}$ visual cortex mice predicts that visual detection thresholds would remain unchanged. Similarly, other transgenic manipulations that induce hyper-excitability in the visual cortex (i.e. GAD 65 $^{-/-}$; Hensch et al., 1998) have normal retinotopy and orientation selectivity, while manipulations that decrease inhibition in the visual cortex (i.e., dark-exposure, environmental enrichment) are not accompanied by a loss of spatial acuity (He et al., 2007; Sale et al., 2007).

Interestingly, not all forms of experience-dependent synaptic plasticity are absent in NARP $^{-/-}$ mice. NARP $^{-/-}$ mice retain the ability to express experience-dependent enhancement of the VEP contralateral bias, which is dependent on early binocular visual experience and reflects the complement of thalamocortical projections serving each eye (McCurry et al., 2010; Coleman et al., 2009). In addition, NARP $^{-/-}$ mice retain the ability to express experience-dependent enhancement of VEP amplitudes in response to high frequency (10 Hz) visual stimulation. Normal long term potentiation (in response to 100 Hz stimulation) and long term depression (in response to 3 Hz stimulation) of the hippocampal Schaffer collateral pathway also persists in hippocampus

of double (NP1 and NP2) knockout mice (Bjartmar et al., 2006). This suggests that these forms of synaptic plasticity do not require gating by fast inhibition or can be engaged by a lower level of inhibitory output. Brief monocular deprivation during the critical period induces a rapid depression of synapses serving the deprived eye and a slow strengthening of synapses serving the non-deprived eye (Sawtell et al., 2003; Frenkel and Bear, 2004; Tagawa et al., 2005; Sato and Stryker, 2008). Importantly, despite the persistence of some forms of experience-dependent synaptic potentiation, we did not observe a strengthening of non-deprived eye synapses, even following unusually long durations of monocular deprivation. The potentiation of the inputs serving the non-deprived eye may be constrained in NARP $^{-/-}$ mice by the absence of deprived eye depression, which has been proposed to be required to first lower the threshold for strengthening of synapses serving the non-deprived eye (Smith et al., 2010).

3.4.4 Unique phenotype of NARP $^{-/-}$ mouse

There are important differences in the phenotype of the NARP $^{-/-}$ mouse from other transgenic models with deficits in ocular dominance plasticity. Transgenic manipulations that impair synaptic plasticity at excitatory synapses onto pyramidal neurons, such as deletion of the activity-regulated cytoskeletal protein arc, block the expression of ocular dominance plasticity along with a wide range of other forms of homeostatic and hebbian plasticity (McCurry et al., 2010). On the other hand, transgenic manipulations that result in hyper-excitability of the visual cortex, such as deletion of the synaptic isoform of the GABA synthetic enzyme GAD65, impair both GABAergic synaptic transmission (Choi et al., 2002) and the response to brief monocular deprivation (Hensch et al., 1998). Nonetheless, slightly longer durations of monocular deprivation can reliably induce ocular dominance shift in the visual system of GAD 65 $^{-/-}$ mice (Fagiolini and Hensch, 2000).

Ocular dominance plasticity is absent in NARP $^{-/-}$ mice, even in response to prolonged duration of monocular deprivation, suggesting that the visual cortex is unable to compensate for the absence of NARP. Nonetheless, several forms of experience-dependent synaptic plasticity, such as plasticity of the VEP contralateral bias and the response to high frequency visual stimulation, are retained. The unique phenotype of the NARP $^{-/-}$ mouse underscores the importance of the recruitment of fast inhibition, via regulation of excitatory drive onto FS (PV) INs, in the induction of fundamental forms of experience-dependent synaptic plasticity in the mammalian visual cortex**.**

Chapter 4: Regulation of cortical excitability and ocular dominance plasticity via NRG1-ErbB4 signaling

Manuscript in preparation.
My contribution: all experiments

4.1 Introduction

The developmental constraint on ocular dominance plasticity is thought to underlie the inability to recover from amblyopia in adults. Understanding the mechanisms for the initiation and termination of the critical period for ocular dominance plasticity may lead to insights in potential treatments for amblyopia. The temporal regulation of the critical period for ocular dominance plasticity was previously thought to be dependent on the strength of inhibition onto the somata of principal neurons in the visual cortex (Huang et al., 1999; Fagiolini and Hensch, 2000; Di Cristo et al., 2007). However, ocular dominance plasticity, in the absence of barbiturate anesthesia, exists far beyond the maturation of perisomatic inhibition (~ postnatal day 35 in rodents) (Pham et al., 2004; Huang et al., 2010). Importantly, ocular dominance plasticity during the later critical period can also be inhibited by benzodiazepines, a positive allosteric modulators of ligand bound $GABA_A$Rs. Together this suggests that a late critical period exists in which perisomatic inhibition is mature, but activity in GABAergic interneurons is not fully recruited by visual experience (Pham et al., 2004; Gu et al., 2013).

Indeed, we recently used transgenic deletion of the immediate early gene NARP to demonstrate the importance of maturation of excitatory drive onto FS (PV) INs in the initiation of the critical period. NARP is a soluble protein that is synthesized by pyramidal neurons and

released by activity (Tsui et al., 1996). NARP is highly enriched at excitatory synapses onto FS (PV) INs, where it forms a complex with the transmembrane proteins NR1 and NPR (Xu et al., 2003). NARP binds to the lectin binding site of chondroitin sulfate proteoglycans (CSPG; Tsui et al., 1996), and thereby tethers membrane surface AMPARs to the extracellular matrix. In the absence of NARP, hippocampal synapses lose the ability to bidirectionally scale synaptic strength in response to prolonged increase or decrease in activity (Chang et al., 2010). Importantly, in the absence of NARP, the connection probability between pyramidal neurons and FS (PV) INs is significantly reduced, resulting in a hyper-excitable cortex (Gu et al., 2013). This hyper-excitability prevents the expression of ocular dominance plasticity, even in response to chronic (> 100 days) monocular deprivation. Reducing neuronal excitability with diazepam, a positive allosteric modulator of ligand bound $GABA_A$Rs, enabled expression of ocular dominance plasticity in the NARP $^{-/-}$ mouse. This identified excitatory synaptic drive onto FS (PV) INs as an important locus for the regulation of the critical period.

The strength of excitatory drive onto FS (PV) INs is also regulated by monocular deprivation. Indeed, 1 day monocular deprivation in juvenile mice rapidly reduces the frequency of spontaneous and evoked EPSCs onto FS (PV) INs in visual cortex, suggesting that reduction in excitatory drive onto FS (PV) INs is an early step in the changes in circuitry underlying ocular dominance shift (Kuhlman et al., 2013). Brief MD in juvenile (P27-28) rats induces an ocular dominance shift in spiking output from both excitatory and inhibitory neurons in superficial layers of V1b, but the shift is more pronounced in inhibitory neurons in older subjects with prolonged MD (P60, Kameyama et al., 2010). We sought to manipulate excitability of FS (PV) INs, to test the hypothesis that manipulating the excitability of FS (PV) INs can maintain the cortical

excitability in a permissive range for the expression of ocular dominance plasticity. This work focused on the NRG1-ErbB4 signaling pathway, as pharmacological tools exist that can cross the blood-brain barrier, and therefore may be generalizable to an amblyopic population.

NRG1 is a neurotrophic factors that is either synthesized as a membrane anchored precursor, which is released into the synaptic cleft via cleavage by BACE1 (Savonenko et al., 2008) or neuropsin (Tamura et al., 2012), or synthesized without a transmembrane domain and directly secreted into the extracellular space (Falls, 2003). The processing and release of NRG1 is up-regulated in response to neuronal activity (Ozaki et al., 2004; Mei and Xiong 2008). Accumulating evidence suggests that the primary cellular targets of NRG1 is excitation onto FS (PV) INs, as the cognate receptor ErbB4, the only NRG1 receptor with active tyrosine kinase activity, is enriched in fast-spiking parvalbumin-positive interneurons (Lai and Lemke, 1991; Yau et al., 2003; Abe et al., 2011; Vullhorst et al., 2009).

Indeed, acute application of NRG1 in cortical slices from P28 rodents increases the excitability of FS (PV) INs and decreases excitability of principal neurons. Acute application of NRG1 induces tyrosine phosphorylation, and subsequent reduction in voltage threshold of the Kv1.1 channel, resulting in increased spiking frequency of FS (PV) INs (Li et al., 2011). These acute effects of NRG1 on FS (PV) INs were not blocked by pharmacological inhibition of synaptic input, indicating direct non-synaptic enhancement of excitability. In contrast the decrease in spiking frequency of pyramidal neurons induced by acute NRG1 is blocked by picrotoxin, indicating indirect suppression of pyramidal neuron excitability via enhanced inhibition. Deletion of ErbB4 in FS (PV) INs reduces the susceptibility to pentyl and pilocarpine-induced seizures, and

ErbB4 expression is reduced in human epileptogenic tissue (Li et al., 2011), suggesting that NRG1-ErbB4 signaling influences circuit excitability, by regulating the excitation onto interneurons.

Prolonged NRG1 treatment also influences neuronal excitability, but through a different mechanism. Prolonged NRG1 treatment of low density cortical neuron in culture increases both the number and size of PSD-95 puncta and the frequency and amplitude of miniature EPSCs (mEPSCs) in GABAergic interneurons, suggesting that prolonged NRG1 stimulates the formation of new synapses and strengthens existing synapses (Ting et al., 2011). Prolonged NRG1 increases the tyrosine phosphorylation of PSD-95, which reduces the degradation of this important scaffold protein. The enhanced stability would result in an increase in PSD-95 concentration, and enhanced synaptic strength by increasing binding sites for synaptic *transmembrane AMPA regulatory proteins* (*TARPs;* Dakoji et al., 2003). Additionally, a tyrosine kinase cascade initiated by NRG1 binding to ErbB4 could activate ERK (Liu et al., 2007) and PI3K pathways (Law et al., 2012), which target subunits of the AMPAR to promote trans-synaptic insertion, priming, and discourage endocytosis (Qin et al., 2005; Lee et al., 2003). ERK and PI3K pathways can also activate the dendritic translation factors which promote the synthesis of synaptic receptors and scaffolding proteins, and maintain the long-lasting modification of the synapses (Derkach et al., 2007; Cammalleri et al., 2003). Indeed, cortical GABAergic neurons treated with NRG1 exhibited a significant increase in surface GluR1 immunoreactivity at putative synaptic sites on dendrites (Abe et al., 2011). The recruitment and stabilization of AMPARs is an important step involved in many aspects of functional maturation and activity-dependent strengthening of these synapses (McMahon and Diaz, 2011; Ting et al., 2011). Similarly, a function blocking peptide (Ecto-ErbB4)

reduces the number and size of excitatory synapses onto FS (PV) INs, implicating a role of endogenous NRG1 in basal synapse formation (Ting et al., 2011).

Importantly, the effects of prolonged NRG1 on synapse formation and strengthening are specific to excitatory synapses onto GABAergic INs (Ting et al., 2011). Indeed, postnatal deletion of ErbB4 decreases mEPSC frequencies on FS (PV) INs, without changes mIPSC frequencies (versus P40 WT controls; Yang et al., 2013). Importantly, previous reports of effects of NRG1-ErbB4 on plasticity of excitatory synapses onto principal neurons, including the suppression of LTP and enhancement of NMDAR currents, have been proven to be indirect, due to the regulation of the strength of convergent inhibition onto principal neurons (Pitcher, 2011).

In this chapter, we use NRG1, a recombinant polypeptide containing the EGF domain of β-type Neuregulin 1, and PD 158780, a tyrosine kinase inhibitor with high specificity for ErbB4 (IC_{50}=52nM) to bidirectionally regulate the output of FS (PV) IN and regular spiking (presumptive excitatory; RS) neurons. I show that I can use these manipulation to maintain cortical excitability in a permissive range for the expression of ocular dominance plasticity.

4.2 Materials and methods

4.2.1 Animals

Wild type (WT) and NARP $^{-/-}$ mice (Bjartmar et al., 2006) were of C57BL/6, 129/SVJII mixed genetic background. All subjects were raised on a 12 h light/dark cycle, with food and water available *ad libitum.* All procedures conform to the guidelines of the U.S. Department of Health and Human Services and the Institutional Animal Care and Use Committees of the University of

Maryland. Monocular deprivation (MD) was performed under ketamine/xylazine anesthesia (50 mg/10 mg/kg, i.p.). The margins of the upper and lower lids of one eye were trimmed and sutured together. The animals were returned to their home cages and disqualified in the event of suture opening or infection. For dark exposure (DE), animals were kept in a complete darkened room; care was made with infrared goggles.

4.2.2 In vivo electrophysiology

In vivo electrophysiology was performed under isoflurane anesthesia (~1.5% in 100% O_2 via modified nose cone). The dura covering binocular visual cortex was exposed through a hole (~ 3 mm diameter) in the skull. The exposed brain was kept moist with artificial cerebral spinal fluid (ACSF (in mM): 124 NaCl, 5 KCl, 1.25 NaH_2PO_4, 1 $MgCl_2$, 2 $CaCl_2$, 26 $NaHCO_3$, 10 dextrose, bubbled with 95% O_2/ 5% CO_2 (pH 7.4)), and the room humidity was supplemented (ZD300Y0, Zenith). Subjects were retained in a stereotax in a darkened room (without visual stimulation) between measurements. Body temperature was maintained at 37 degrees C via circulating water heating pad (T/PUMP, Gaymar Industries Inc.), monitored with a rectal probe (BAT-12, Sensortek Inc.). A broad-band signal was collected from the lateral aspect (binocular region) of the primary visual cortex (site of largest ipsilateral eye VEP, typically 3 mm lateral to the intersection of lambda and the midline), with a tungsten microelectrode (0.5 MΩ) relative to a ground screw in the frontal bone. 50 Hz low pass filter was used to isolate VEPs in response to 1 Hz reversals of full screen 100% contrast gratings (0.04 cycles/degree and 40 cd/m^2 luminosity) presented on a computer monitor 25 cm from eyes. VEPs were averaged in synchrony with the visual stimulus using OpenEX software (TDT).

700-7k Hz band pass filter was used to isolate multi-unit activity, which was sorted into single-units based on waveform shape and principal component analysis (OpenEx software; TDT). The individual waveform samples were aligned by most negative point, and normalized amplitudes from -1 to 1. Units were then classified as fast or regular spiking based on parameters of the averaged waveforms (Niell and Stryker, 2008). Two parameters were used for discrimination: the height of the positive peak relative to the initial negative trough, and the slope of the waveform 0.5 ms after the initial trough. Two linearly separable clusters were found, corresponding to narrow-spiking (putative inhibitory, fast-spiking) and broad-spiking (putative excitatory, regular-spiking) neurons. Spontaneous firing rates were measured over 100 seconds in response to blank screen. Evoked spiking rates were measured in response to visual stimulus in preferred orientation (from 9 orientations ranging from 0 degrees (vertical) to 180 degrees). Orientation tuning was determined by plotting spiking activity against stimulus orientation from -90 to 90 degrees from preferred orientation.

4.2.3 Drug solutions

PD 158780 (Tocris) was dissolved in 10% Tween 80, 20% DMSO and 70% saline to a final concentration of 2 mg/ml. NRG1 (R&D systems) was dissolved in 100% saline to a final concentration of 10 ng/ml.

4.3 Results

4.3.1 Regulation of neuronal excitability and inhibition of ocular dominance plasticity during the critical period with NRG1

The strength of excitatory drive onto FS (PV) INs has been proposed to be critical in recruitment of inhibition necessary for the expression of ocular dominance plasticity. To ask if manipulations of NRG1-ErbB4 signaling pathway can be used to manipulate the spiking output of FS and RS neurons and subsequent ocular dominance plasticity, we administrated NRG1 peptide (10 ng/kg, i.p., twice a day for 3 days) to wild type mice at the peak of the critical period (P30), and recorded spontaneous and visually-evoked single unit activity. Systemic delivery of NRG1 did not affect the peak/trough ratio (RS neurons average ± SEM; WT juveniles: 0.78±0.17, WT juveniles + NRG1 0.87±0.21; FS neurons; WT juveniles: 0.59±0.12, WT juveniles + NRG1 0.61±0.07; Fig. 4-1A left) or the end slope of single unit waveforms (RS neurons average ± SEM; WT juveniles 0.0004±0.006, WT juveniles + NRG1 0.011±0.004; FS: WT juveniles -0.074±0.008, WT juveniles + NRG1 -0.072±0.008; Fig. 4-1A middle). Indeed, single unit waveforms sorted into two distinct clusters based on these two parameters, representing regular spiking units (putative excitatory neurons, green Fig. 4-1A, right) and fast spiking units (putative parvalbumin-positive inhibitory neurons, blue Fig. 4-1A, right).

However, NRG1 treatment induced an increase in visually evoked (left) and spontaneous (right) firing rates in FS (PV) INs (spikes/s, blue; visually-evoked, WT juveniles: 6.58±0.35, WT juveniles + NRG1: 7.67±0.46; spontaneous, WT juveniles: 2.15±0.17, WT juveniles + NRG1: 2.56±0.19; Fig 4-1B), and a corresponding decrease in visually evoked (left) and spontaneous (right) firing rates in RS neurons (spikes/s, green; visually-evoked, WT juveniles: 2.39±0.21, WT juveniles + NRG1 1.30±0.14; spontaneous, WT juveniles: 0.99±0.13, WT juveniles + NRG1 0.44±0.07; Fig. 4-1B). This is consistent with the previously description of NRG1 in strengthening excitation onto FS (PV) INs (Ting et al., 2011). However, the changes in neuronal excitability resulting from NRG1 administration did not affect the orientation tuning of RS or FS neurons in primary visual cortex (Fig. 4-2). This is consistent with our previous work showing that changes in neuronal excitability resulting from genetic ablation of NARP, an AMPAR-binding protein that

is enriched at excitatory synapses on FS (PV) INs, does not change the orientation tuning of neurons in primary visual cortex (Gu et al., 2013).

The increase in output from FS (PV) INs and the subsequent decrease in output from RS neurons at the closure of the critical period is expected to drive cortical excitability down from permissive range necessary to express ocular dominance plasticity. To address this question, we explored the response to 3 days of monocular deprivation (MD) following NRG1 administration. At this age, 3 days of MD induced a robust shift in neuronal responses away from the deprived eye, revealed as a decrease in the ocular dominance index (red; ODI =(Contralateral Eye VEP – Ipsilateral Eye VEP)/(C+I)) relative to non-MDed controls (blue). However, NRG1 administration concurrent with 3 days MD inhibited the response to 3 days of MD (green; *$H(2)=11.94$, $p<0.01$, Kruskal-Wallis test; Fig. 4-1C). This demonstrates that systemic administration of NRG1 during the critical period reduces cortical excitability and inhibits subsequent ocular dominance plasticity.

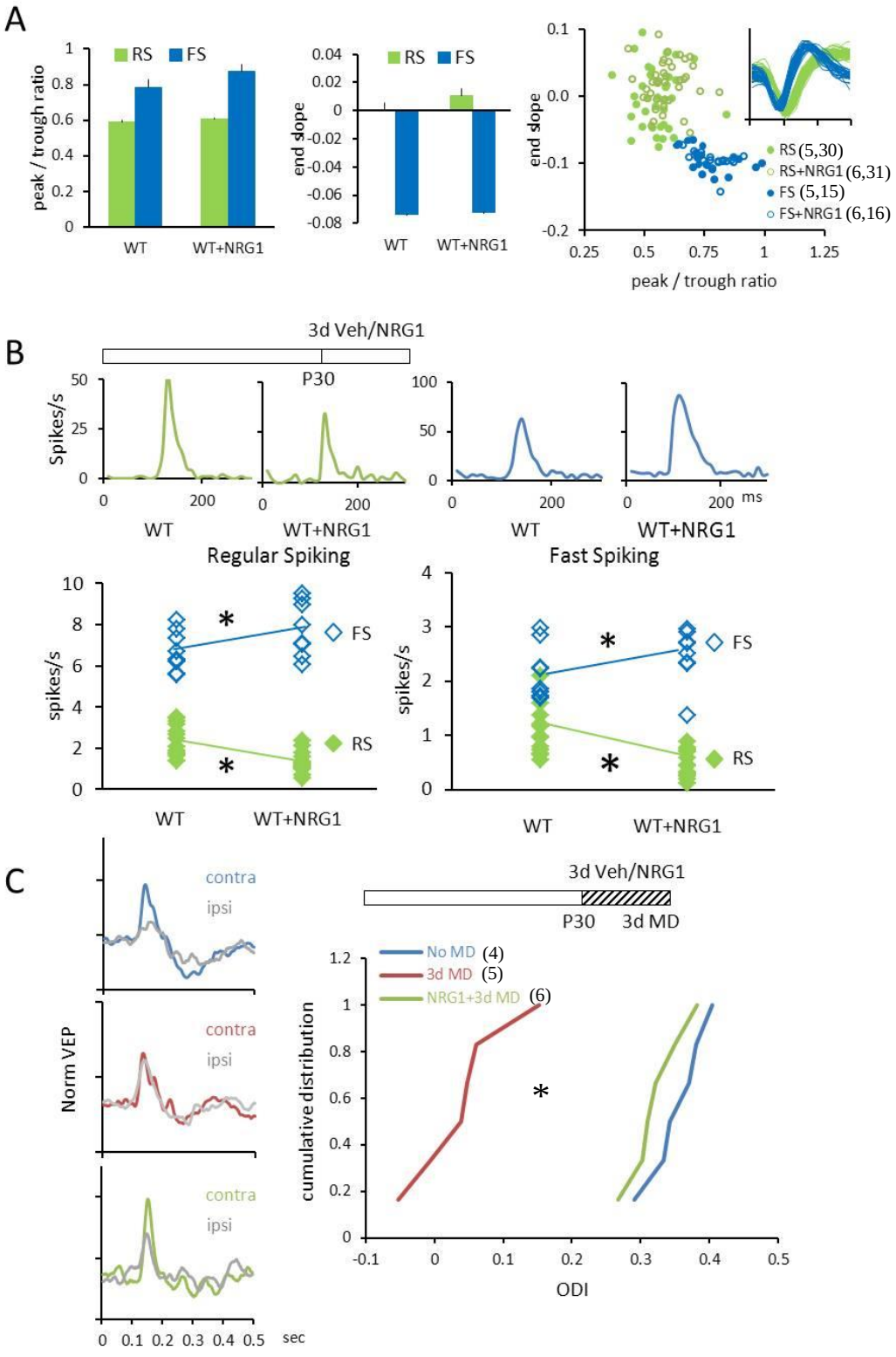

Figure 4-1. Regulation of spiking output and inhibition of ocular dominance plasticity in juvenile (P30) wild type mice with NRG1. (A) NRG1 has no effect on spiking waveform parameters of both RS and FS. Left, average peak / trough ratio of RS (green) and FS (blue) waveforms with or without NRG1 treatment in juvenile (P30) wild type mice. Middle, average end slope of RS and FS waveforms with or

without NRG1 treatment in juvenile (P30) wild type mice. Right, plotting unit waveform end slope against peak / trough ratio, each spot represent one single unit, green spot represent RS, blue spot represent FS. Insert, spike waveforms normalized by amplitude from -1 to 1, green traces represent RS, blue traces represent FS. (B) NRG1 decreased evoked and spontaneous firing rates of RS (green closed diamond) and increased evoked and spontaneous firing rates of FS (blue open diamond) in juvenile wild type mice. Upper, representative PSTH for RS and FS with or without NRG1 treatment. Down left, evoked spiking, right, spontaneous spiking. *one-tail unpaired t-test, $p<0.05$. Lines connect averages. (C) Cumulative distribution of ocular dominance index (ODI) of VEP amplitudes recorded from juvenile wild type mice. 3 day MD decreased VEP ODI, which was reversed by NRG1. *Kruskal-Wallis test, $H(2)=11.94$, $p<0.01$. Left, representative contralateral and ipsilateral VEP waveform in no MD (top), 3 day MD (middle) and NRG1+3 day MD (bottom) wild type mice.

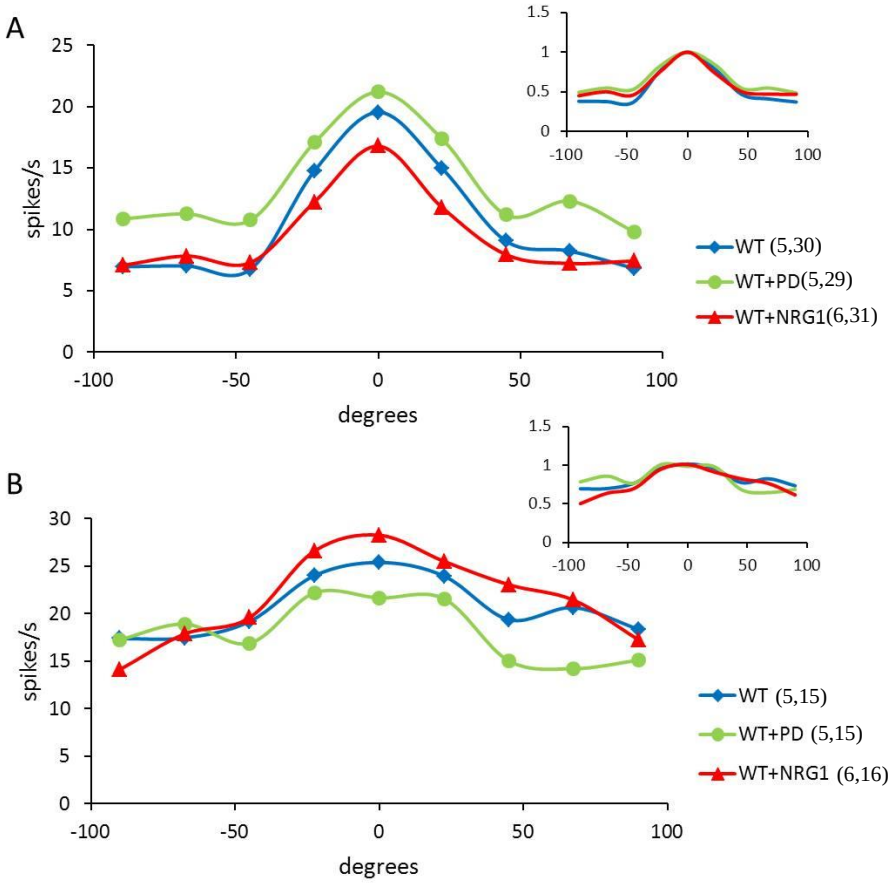

Figure 4-2. Orientation tuning of RS and FS are not affected by PD 158780 and NRG1 administration. (A) Similar orientation tuning curves for RS in the visual cortex of wild type adults (blue), WT with ErbB4 inhibitor PD 158780 (green) and WT with NRG1 (red). The preferred orientations are aligned at 0 degrees. Inset: orientation tuning normalized by maximal responses in each group. (B) Similar orientation tuning curves for FS in the visual cortex of wild type adults (blue), WT with PD 158780 (green) and WT with NRG1 (red). The preferred orientations are aligned at 0 degrees. Inset: orientation tuning normalized by maximal responses in each group.

4.3.2 Regulation of neuronal excitability and ocular dominance plasticity in NARP $^{-/-}$ mice and dark exposed wild type adult mice with NRG1

We have previously shown that the visual cortex of NARP $^{-/-}$ mice does not express ocular dominance plasticity at any age, even in response to prolonged occlusion (Gu et al., 2013). Indeed, NARP $^{-/-}$ mice display a decrease in visually evoked (left) and spontaneous (right) firing rates in FS (PV) INs (spikes/s, blue; visually-evoked, WT: 7.52 ±0.34, NARP$^{-/-}$: 5.57 ±0.16; spontaneous, WT: 2.34 ±0.06, NARP$^{-/-}$: 1.82 ±0.11; Fig. 4-3), and a corresponding increase in visually-evoked (left) and spontaneous (right) firing rates in RS neurons (spikes/s, green; visually-evoked, WT: 2.38 ±0.20, NARP$^{-/-}$: 4.34 ±0.27; spontaneous, WT: 0.39 ±0.07, NARP$^{-/-}$ 1.82 ±0.17; Fig. 4-3).

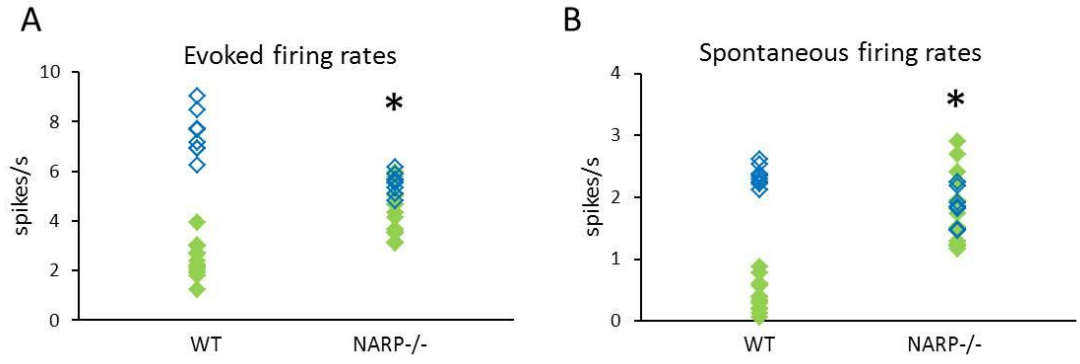

Figure 4-3. Regulation of spiking output by knocking out NARP. (A) Increased evoked firing rates of RS (green closed diamond) and decreased evoked firing rates of FS (blue open diamond) in NARP -/- mice compared to wild type mice. *one-tail unpaired t-test, $p<0.05$. (B) Increased spontaneous firing rates of RS (green closed diamond) and decreased spontaneous firing rates of FS (blue open diamond) in NARP $^{-/-}$ mice compared to wild type mice. *one-tail unpaired t-test, $p<0.05$.

This phenotype is consistent with our previous observation of a reduction in connection probability and excitatory drive onto FS (PV) INs in the NARP $^{-/-}$ visual cortex (Gu et al., 2013). To ask if the regulation of neuronal excitability via NRG1 could reverse the hyper-excitability in the visual cortex of NARP $^{-/-}$ mice, we administrated NRG1 peptide to NARP $^{-/-}$ mice. Systemic delivery of NRG1 to NARP $^{-/-}$ mice did not affect the peak/trough ratio (Fig. 4-4A top) or the end slope (Fig. 4-4A bottom) of single unit waveforms from RS or FS neurons. However, the visually-

evoked firing rates of FS (PV) INs were increased (spikes/s, NARP $^{-/-}$ 5.57 ±0.16, NARP $^{-/-}$ + NRG1 6.43 ±0.30; Fig. 4-4B, blue) and RS neurons were decreased (spikes/s, NARP $^{-/-}$ 4.34 ±0.27, NARP $^{-/-}$ + NRG1 3.09 ±0.20; Fig 4-4B, green) following NRG1 treatment. Spontaneous firing rates were similarly increased in FS (PV) INs and decreased in RS neurons (spikes/s, FS: NARP $^{-/-}$ 1.82 ±0.11, NARP $^{-/-}$ + NRG1 2.14 ±0.07; RS: NARP $^{-/-}$ 1.82 ±0.17, NARP $^{-/-}$ + NRG1 0.91 ±0.08, not shown).

The increase in output from FS (PV) INs and the decrease in output from RS neurons following NRG1 administration might be expected to drive cortical excitability in NARP $^{-/-}$ mice down into the permissive range for ocular dominance plasticity. Indeed, 3 days of MD, which is normally ineffective in NARP $^{-/-}$ mice (red MD, blue no MD NARP $^{-/-}$), induced a robust shift in ocular dominance when administered concurrently with NRG1 (green; *$H(2)=18.38$, $p<0.001$; Kruskal-Wallis test; Fig. 4-4C). Thus cortical excitability and subsequent ocular dominance plasticity can be rescued in NARP $^{-/-}$ mice with NRG1.

We have previously demonstrated that the developmental reduction in cortical excitability and loss of ocular dominance plasticity can be rescued in adult rats with 10 days of dark exposure (DE, He et al., 2006). Similarly 10 days of dark exposure regulates neuronal excitability and rescues ocular dominance plasticity in adult wild type mice (Fig. 4-4E-F). However, the effects of DE can be occluded by knocking out NARP (Fig. 4-5). To ask if the effects of dark exposure can be reversed by NRG1, we systemically delivered NRG1 for the last 3 days of the 10 day dark exposure. NRG1 administration did not affect the peak/trough ratio or the end slope of single unit waveforms from RS or FS neurons (Fig. 4-4D). However, NRG1 administration during the last 3 days of 10 day DE reversed the DE-induced changes in neuronal excitability, increasing the

visually-evoked firing rates of FS IN (spikes/s, WT+DE 6.64±0.16; DE + NRG1 7.87±0.11; Fig. 4-4E, blue) and decreasing in RS neurons (spikes/s, WT+DE 3.58±0.13; DE + NRG1 2.16±0.05; Fig. 4-4E, green). Spontaneous firing rates were similarly increased in FS (PV) INs and decreased in RS neurons (spikes/s, FS: WT+DE 1.74±0.07, DE + NRG1 2.11±0.07; RS: WT+DE 1.22±0.04, DE + NRG1 0.48±0.04, not shown). DE decreased the firing rates of WT adults to critical period level, while NRG1 administration reversed the firing rates back to WT adult level (data in Fig. 4-1 and 4-7). Similarly, the robust shift in ODI observed in DE WT adults is reversed by NRG1 treatment (blue MD alone, red DE+MD, green DE+NRG1+MD; cumulative distribution of ODI; *$H(2)=15.77$, $p<0.001$, Kruskal-Wallis test, Fig. 4-4F).

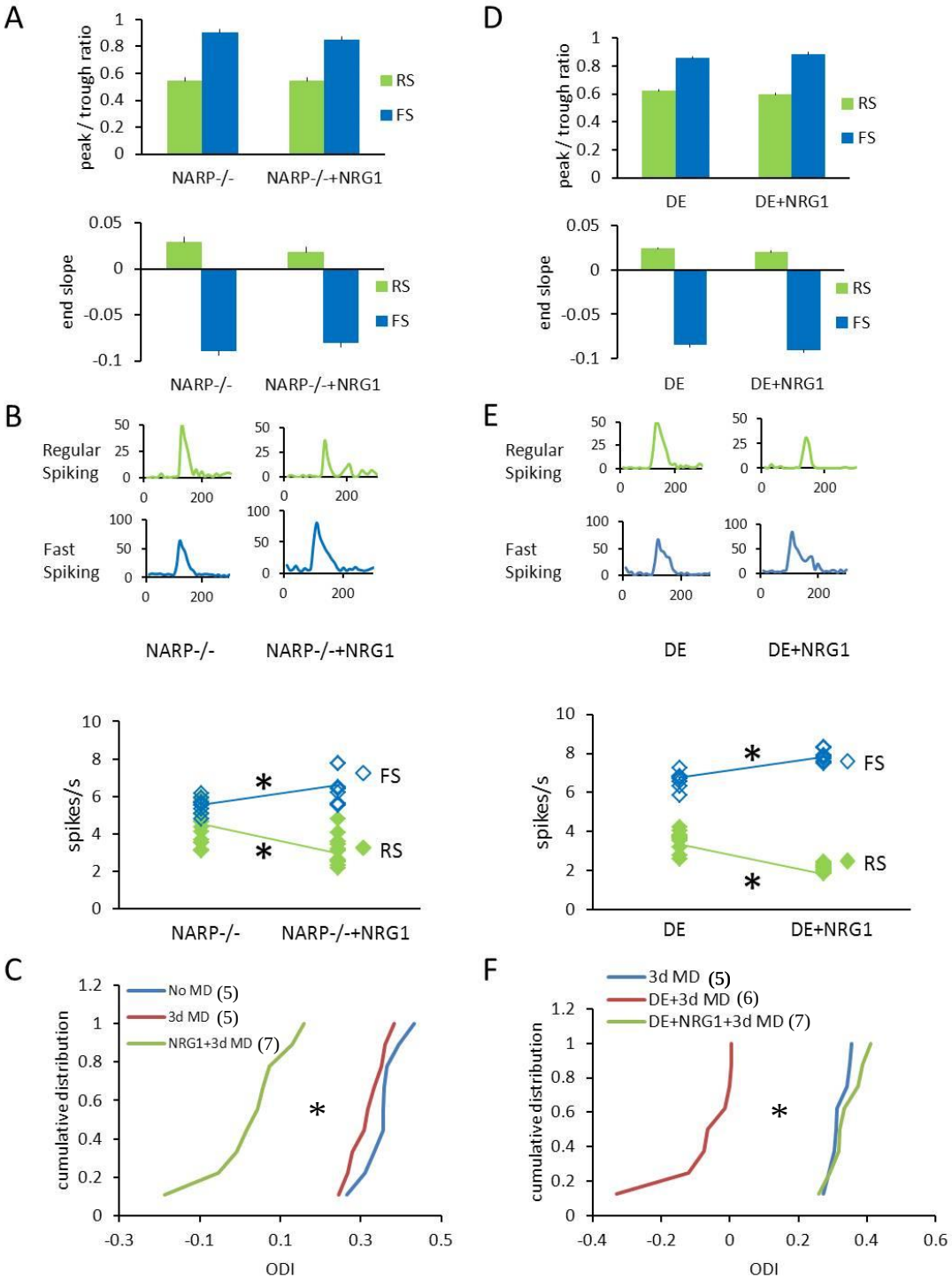

Figure 4-4. Rescue of ocular dominance plasticity in NARP $^{-/-}$ and reversal of DE effects in adult WT with NRG1. (A) NRG1 has no effect on spiking waveform parameters of both RS and FS in NARP $^{-/-}$ mice. Top, average peak / trough ratio of RS (green) and FS (blue) waveforms with or without NRG1 treatment in NARP $^{-/-}$ mice. Bottom, average end slope of RS and FS waveforms with or without NRG1 treatment in NARP $^{-/-}$ mice. (B) NRG1 decreased evoked firing rates of RS (green closed diamond) and increased evoked

firing rates of FS (blue open diamond) in NARP $^{-/-}$ mice. *one-tail unpaired t-test, $p<0.05$. Lines connect averages. Insert, representative PSTH for RS and FS with or without NRG1 treatment. (C) Cumulative distribution of ocular dominance index (ODI) of VEP amplitudes recorded from NARP $^{-/-}$ mice. 3 day MD decreased VEP ODI in NARP $^{-/-}$ only with NRG1. *Kruskal-Wallis test, $H(2)=18.38$, $p<0.001$. (D) NRG1 has no effect on spiking waveform parameters of both RS and FS in DE adult WT mice. Top, average peak / trough ratio of RS (green) and FS (blue) waveforms with or without NRG1 treatment in adult WT mice. Bottom, average end slope of RS and FS waveforms with or without NRG1 treatment in adult WT mice. (E) NRG1 decreased evoked firing rates of RS (green closed diamond) and increased evoked firing rates of FS (blue open diamond) in adult WT mice after 10 day DE. *one-tail unpaired t-test, $p<0.05$. Lines connect averages. Insert, representative PSTH for RS and FS with or without NRG1 treatment. (F) Cumulative distribution of ocular dominance index (ODI) of VEP amplitudes recorded from adult WT mice. 3 day MD decreased VEP ODI in adult WT after 10 day DE, which was reversed by NRG1. *Kruskal-Wallis test, $H(2)=15.77$, $p<0.001$.

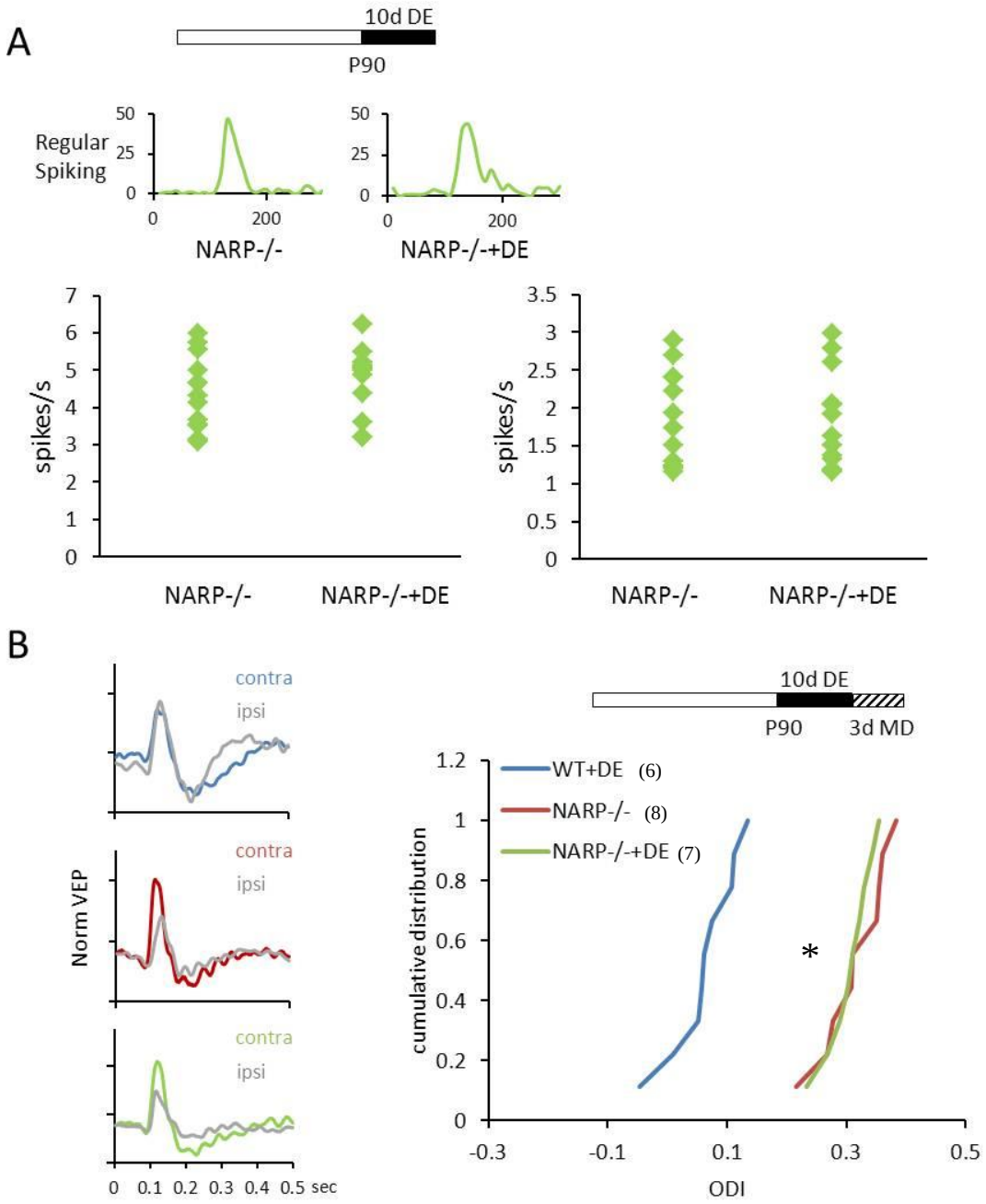

Figure 4-5. DE effects are occluded in NARP $^{-/-}$ mice. (A) 10 days of DE did not change the evoked and spontaneous firing rates of RS (green closed diamond) in NARP$^{-/-}$ mice. Upper, representative PSTH for RS with or without 10 days DE. Down left, evoked spiking, right, spontaneous spiking. *one-tail unpaired t-test, p>0.05. (B) Cumulative distribution of ocular dominance index (ODI) of VEP amplitudes recorded from adult wild type and NARP$^{-/-}$ mice. 3 days MD following 10 days DE decreased VEP C/I only in wild type mice. Kruskal-Wallis test, *H(2)=17.48, p<0.001. Left, representative contralateral and ipsilateral VEP waveform in WT+DE (top), NARP$^{-/-}$ (middle) and NARP$^{-/-}$+DE (bottom) mice following by 3 days MD.

4.3.3 Regulation of neuronal excitability and rescue of ocular dominance plasticity in adults with ErbB4 inhibition

The cognate receptor for NRG1 is ErbB4, a receptor tyrosine kinase that is highly enriched at excitatory synapses on FS (PV) INs (Vullhorst et al., 2009). To ask if systemic delivery of an ErbB4 inhibitor could weaken FS (PV) INs excitability, we administered PD 158780 (10 mg/kg, i.p., twice a day for 3 days), a receptor tyrosine kinase inhibitor with high specificity for ErbB4 (IC_{50}=52nM) to wild type adults (P90). The ability to cross the blood-brain barrier of PD 158780 was confirmed with the 25.1% increase of evoked spiking activity in RS neuron within 15min after acute administration (10mg/kg, i.p., Fig. 4-6). Systemic delivery of the ErbB4 inhibitor did not affect sorting of single units into two distinct clusters based on waveform (Fig. 4-7A right), the peak/trough ratio (RS: WT controls 0.59±0.11, WT+PD 158780 0.52±0.08; FS: WT controls 0.78±0.16, WT+PD 158780 0.83±0.20; Fig. 4-7A left) or the end slope (RS: WT controls 0.0004±0.005, WT+PD 158780 0.003±0.004; FS: WT controls -0.074±0.007, WT+PD 158780 -0.055±0.006; Fig. 4-7A middle). In addition, administration of the ErbB4 inhibitor did not affect the orientation tuning of RS or FS neurons in primary visual cortex (Fig. 4-2).

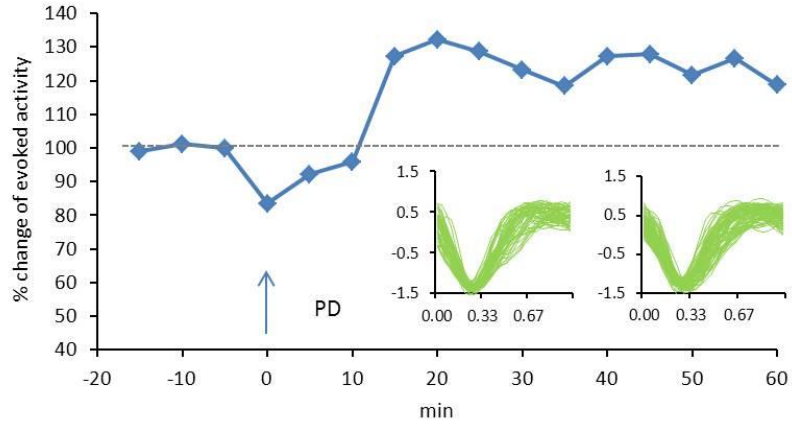

Figure 4-6. Acute effects in RS evoked spiking of PD 158780 in P90 WT mice. Average single unit activity before and after the treatment of PD 158780 in vivo. After obtaining a baseline evoked spiking activity, PD 158780 was administrated acutely (10mg/kg, i.p.) and evoked spiking activity was measured every 5 min. Evoked spiking activity gradually increased and reached plateau about 15 min after the drug treatment (increased by 25.1% compared to baseline). The evoked spiking activity remained potentiation for at least 60 min. Recording section was restricted in the 60 min time frame to avoid the induction of response enhancement due to repetitive visual stimulation. Insert, 2 example unit spike waveforms normalized by amplitude from -1 to 1. Peak / trough ratio (0.496) and end slope (-0.005) of the SU

waveform are in the range of WT RS (peak / trough 0.59±0.11, end slope 0.0004±0.005) but not in the range of FS (peak / trough 0.78±0.16, end slope -0.074±0.007).

Importantly, ErbB4 inhibition resulted in a decrease in evoked (left) and spontaneous (right) firing rates in FS neurons (spikes/s, blue; visually-evoked, controls 2.38±0.20, with PD 158780 3.65±0.11; spontaneous, controls 0.39±0.07, with PD 158780 1.31±0.06; Fig. 3B), and a corresponding increase in evoked (left) and spontaneous (right) firing rates in RS neurons (spikes/s, green; visually-evoked, controls 7.52±0.34, with PD 158780 6.05±0.13; spontaneous, controls 2.34±0.06, with PD 158780 1.79±0.07; Fig. 4-7B). This is consistent with the observation that interfering with endogenous NRG1-ErbB4 signaling reduces the amplitude and frequency of mEPSCs onto FS (PV) INs (Ting et al., 2011).

The decrease in output from FS (PV) INs and the subsequent increase in output from RS neurons in adults might be expected to drive cortical excitability back up into the permissive range for ocular dominance plasticity. To address this question, we again explored the response to 3 days of MD. At this age, 3 days of MD does not induce a shit in the ocular dominance of VEPs (red MD, blue no MD control adults). ErbB4 inhibition concurrent with 3 days of MD rescued the response to 3 days of MD in adults (green, *$H(2)=15.24$, $p<0.001$, Kruskal-Wallis test; Fig 4-7C). Thus systemic ErbB4 inhibition effectively regulates cortical excitability and subsequent ocular dominance plasticity.

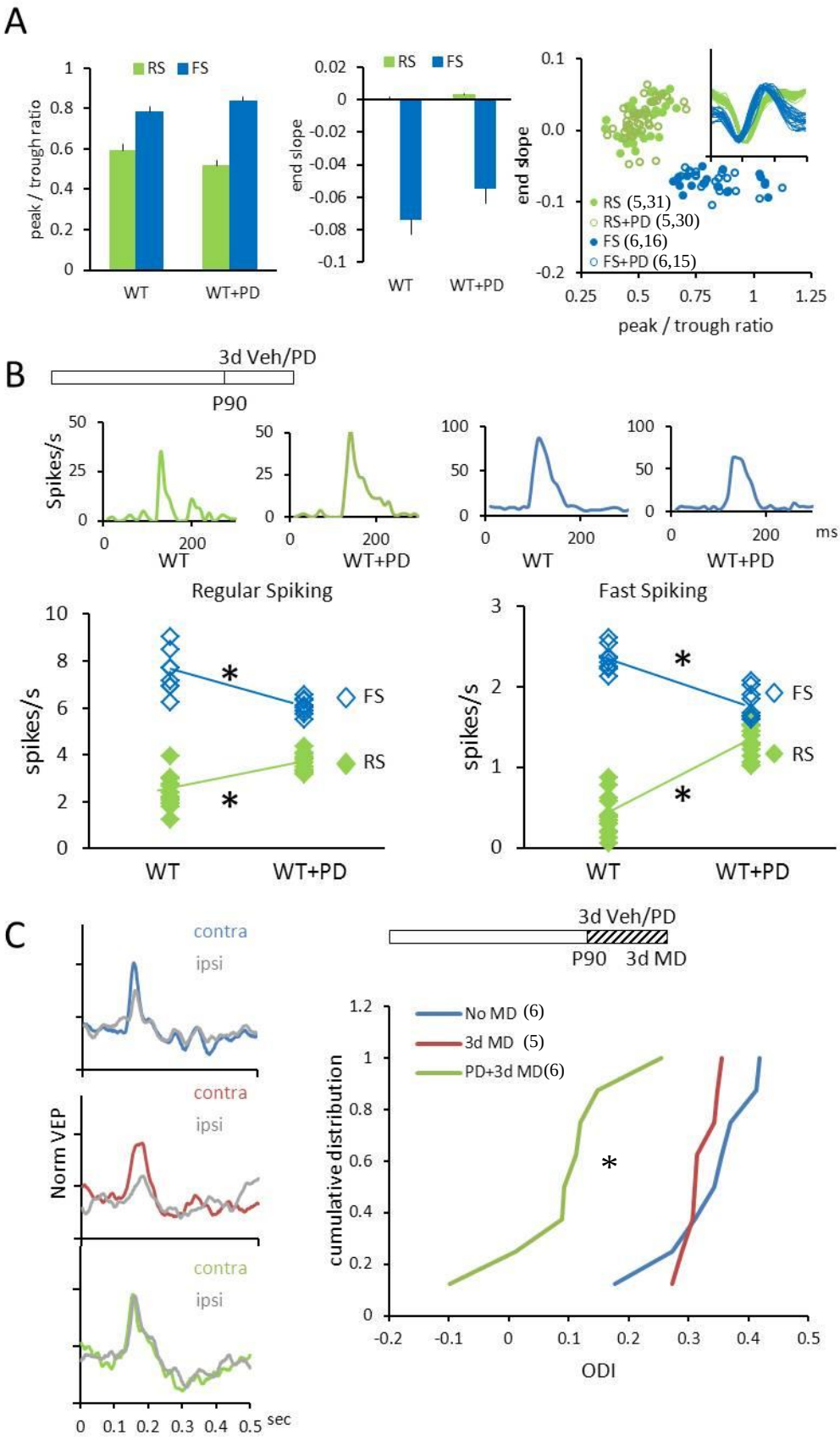
A
RS
FS
peak / trough ratio
WT
WT+PD
end slope
RS (5,31)
RS+PD (5,30)
FS (6,16)
FS+PD (6,15)
peak / trough ratio
B
3d Veh/PD
P90
Spikes/s
ms
Regular Spiking
Fast Spiking
spikes/s
C
contra
ipsi
Norm VEP
sec
3d Veh/PD
P90 3d MD
No MD (6)
3d MD (5)
PD+3d MD(6)
cumulative distribution
ODI

Figure 4-7. Regulation of spiking output and reactivation of ocular dominance plasticity in adult (P90) wild type mice with PD 158780. (A) PD 158780 has no effect on spiking waveform parameters of both RS and FS. Left, average peak / trough ratio of RS (green) and FS (blue) waveforms with or without PD 158780 treatment in adult (P90) wild type mice. Middle, average end slope of RS and FS waveforms with or without PD 158780 treatment in adult (P90) wild type mice. Right, plotting unit waveform end slope against peak / trough ratio, each spot represent one single unit, green spot represent RS, blue spot represent FS. Insert, spike waveforms normalized by amplitude from -1 to 1, green traces represent RS, blue traces represent FS. (B) PD 158780 increased evoked and spontaneous firing rates of RS (green closed diamond) and decreased evoked and spontaneous firing rates of FS (blue open diamond) in adult wild type mice. Upper, representative PSTH for RS and FS with or without PD 158780 treatment. Down left, evoked spiking, right, spontaneous spiking. *one-tail unpaired t-test, $p<0.05$. Lines connect averages. (C) Cumulative distribution of ocular dominance index (ODI) of VEP amplitudes recorded from adult wild type mice. 3 day MD decreased VEP ODI only with PD 158780. *Kruskal-Wallis test, $H(2)=15.24$, $p<0.001$. Left, representative contralateral and ipsilateral VEP waveform in no MD (top), 3 day MD (middle) and PD 158780 +3 day MD (bottom) wild type mice.

4.3.4 Regulation of cortical excitability and recovery from chronic monocular deprivation in amblyopic adults following inhibition of ErbB4

One of the consequences of the developmental reduction in cortical excitability and constraint on ocular dominance plasticity is the increasing resistance to recovery from chronic monocular deprivation with age. Indeed, we have previously reported that ocular dominance and/or visual function do not recovery spontaneously following the removal of a chronic occlusion (He et al., 2007). Chronic MD mimics the inborn cataract in the amblyopia patient, and can be used to study the potential therapies to amblyopia.

The demonstration that inhibition of ErbB4 signaling can reactivate ocular dominance plasticity led us to propose that the reactivated plasticity may be sufficient to promote the recovery from chronic monocular deprivation in adults. Mice were given monocular deprivation at eye opening (P14) which was maintained until adulthood (P100), which we have previously shown induces a severe amblyopia, including significant reduction in the strength and selectivity of visually-evoked responses from chronically-deprived eye (Montey and Quinlan, 2011). Systemic

delivery of the ErbB4 inhibitor in cMD mice did not affect sorting of single units into two distinct clusters based on waveform, the peak/trough ratio or the end slope of single unit waveforms from RS or FS neurons (Fig. 4-8A). Again, ErbB4 inhibition resulted in a decrease in evoked (left) and spontaneous (right) firing rates in FS neurons (spikes/s, blue; evoked, cMD 6.61±0.09, cMD+PD 4.93±0.17; spontaneous, cMD 1.85±0.06, cMD+PD 1.25±0.06, Fig. 4-8B), and a corresponding increase in evoked (left) and spontaneous (right) firing rates in RS neurons (spikes/s, green; evoked, cMD 1.62±0.09, cMD+PD 3.21±0.21; spontaneous, cMD 0.20±0.02, cMD+PD 1.09±0.08, Fig. 4-8B).

To ask if the decrease in output from FS (PV) INs and the subsequent increase in output from RS neurons reactivated sufficient ocular dominance plasticity to allow for the recovery from cMD, we did 5 days reverse deprivation following chronic MD (from P14 to P100) in wild type mice. We see no spontaneous recovery of ocular dominance (ODI) following opening of the deprived eye and closing the non-deprived eye (reverse deprivation; RD; blue cMD, red cMD+RD, Fig. 4C). However, when ErbB4 inhibition was concurrent with 5 days of RD, a significant recovery from cMD was observed (green; *$H(2)=15.37$, $p<0.001$; Kruskal-Wallis test, Fig. 4-8C). Thus inhibition of ErbB4 can be used to regulate excitability in the amblyopic visual cortex, and enables the recovery from cMD in adulthood.

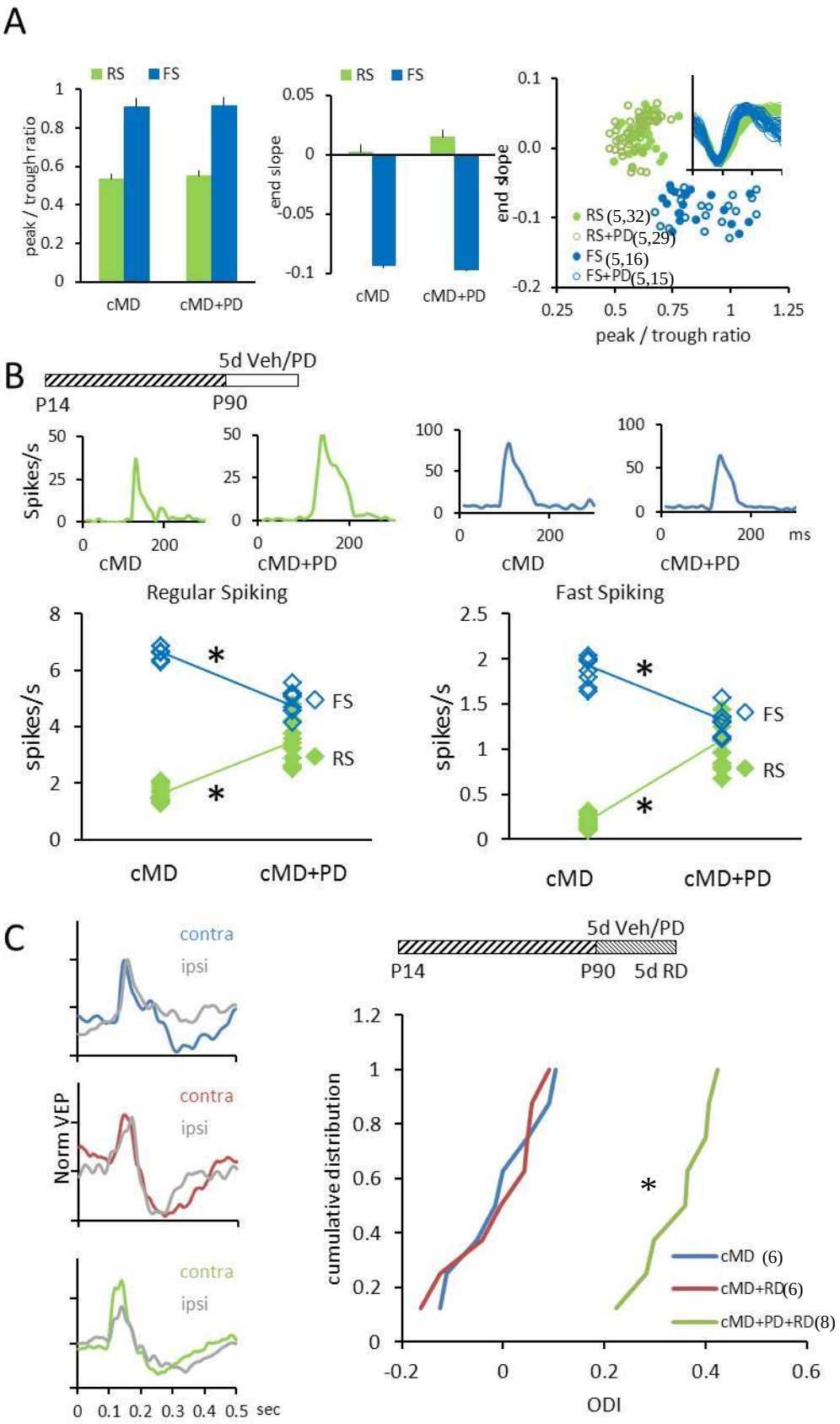
A
RS
FS
peak / trough ratio
cMD
cMD+PD
end slope
RS (5,32)
RS+PD (5,29)
FS (5,16)
FS+PD (5,15)
peak / trough ratio
B
5d Veh/PD
P14
P90
Spikes/s
Regular Spiking
Fast Spiking
ms
spikes/s
C
contra
ipsi
Norm VEP
sec
5d RD
cumulative distribution
ODI
cMD (6)
cMD+RD (6)
cMD+PD+RD (8)

Figure 4-8. Regulation of spiking output and recovery of ocular dominance in chronic MDed adult wild type mice with PD 158780. (A) PD 158780 has no effect on spiking waveform parameters of both RS and FS in chronic Mded adult wild type mice. Left, average peak / trough ratio of RS (green) and FS (blue) waveforms with or without PD 158780 treatment in chronic MDed adult wild type mice. Middle, average end slope of RS and FS waveforms with or without PD 158780 treatment in chronic MDed adult wild type mice. Right, plotting unit waveform end slope against peak / trough ratio, each spot represent one single unit, green spot represent RS, blue spot represent FS. Insert, spike waveforms normalized by amplitude from -1 to 1, green traces represent RS, blue traces represent FS. (B) PD 158780 increased evoked and spontaneous firing rates of RS (green closed diamond) and decreased evoked and spontaneous firing rates of FS (blue open diamond) in chronic MDed adult wild type mice. Upper, representative PSTH for RS and FS with or without PD 158780 treatment. Down left, evoked spiking, right, spontaneous spiking. *one-tail unpaired t-test, $p<0.05$. Lines connect averages. (C) Cumulative distribution of ocular dominance index (ODI) of VEP amplitudes recorded from chronic MDed adult wild type mice. 5 day RD increased VEP C/I only with PD 158780. *Kruskal-Wallis test, $H(2)=15.37$, $p<0.001$. Left, representative contralateral and ipsilateral VEP waveform in no RD (top), 5 day RD (middle) and PD 158780 +5 day RD (bottom) chronic MDed wild type mice.

4.4 Discussion

The critical period for ocular dominance plasticity was previously thought to be irreversible. However, here we show that ocular dominance plasticity can be reversibly, and rapidly, regulated throughout the course of postnatal development including adulthood. The neurotrophin NRG1 increases excitability in FS (PV) INs and decreases excitability in RS neurons, which can be used to inhibit ocular dominance plasticity in juveniles and DE adults. In contrast, inhibition of the NRG1 receptor tyrosine kinase (ErbB4) decreases excitability in FS (PV) INs and increases excitability in RS neurons, which can be used to engage ocular dominance plasticity in binocular and severely amblyopic adults.

This work suggests that there is a narrow range of excitability in RS neurons that permits ocular dominance plasticity. Indeed, optimal excitability can stabilize the synaptic plasticity (Bi and Poo, 1998; Fagiolini and Hensch, 2000) that is based on spike-timing-dependent (STDP) mechanism. Hyperexcitaiblity, such as seen in the visual cortex during pre-critical period, and in

NARP $^{-/-}$ mice, or hypoexcitability, such as seen in post-critical period adults, are outside the permissive range for ocular dominance plasticity. Manipulation of NRG1-ErbB4 signaling allows for drive excitability of RS neurons into the permissive range to express ocular dominance plasticity.

Importantly, stimulus selectivity was not affected by manipulations of the NRG1-ErbB4 pathway. This is consistent with our previous result that knocking out NARP does not change the orientation selectivity in the visual cortex (Gu et al., 2013), and results from other labs that optogenetic activation of FS (PV) INs only modestly affect tuning properties (Atallah et al., 2012). This result support the model that feed-forward excitation determines orientation tuning (Priebe et al., 2004). However, we didn't rule out the possibility that intracortical inhibition mediated by other types of inhibitory neurons sharpens or creates orientation tuning.

The NRG1 peptide and the ErbB4 inhibitor employed here have the potential for therapeutic treatment for amblyopia because they can cross the blood-brain barrier. The low molecular weights of PD 158780 (330.18 Da) and its high lipid solubility suggest that it may cross the blood-brain barrier without assistance (Fig. 4-6; Pardridge, 2005). The NRG1 peptide utilized here (8 kDa) is likely to be recognized by receptor-mediated transport that normally transports NRG1 across the blood-brain barrier (Kastin et al., 2004). This is in contrast to NARP, a calcium-dependent lectin that binds to the GAG side chains of proteoglycans (Tsui et al., 1996), and is therefore likely to be trapped at basement membranes of blood-brain barrier (Baeten and Akassoglou, 2011).

4.4.1 The locus for the regulation of ocular dominance plasticity

Previously, the timing of the critical period for ocular dominance plasticity was thought to be determined by the strength of perisomatic inhibition of principal neurons in the visual cortex (Hensch et al., 1998; Di Cristo et al., 2007; Rozas et al., 2001; Jiang et al., 2005). Indeed, early enzymatic removal (before critical period) of the PSA (polysialic acid) moiety of Neuronal Cell Adhesion Protein (NCAM) accelerates the maturation of perisomatic inhibition, resulting in an increase in the density of perisomatic inhibitory boutons, an increase in the frequency, not amplitude, of mIPSCs (onto layer V pyramidal neurons), and induction of a precocious critical period (Di Cristo et al., 2007). Similarly, over-expression of BDNF (during the critical period) accelerated the development of perisomatic GABAergic bouton density and increases maximal IPSC amplitudes (in layer III pyramidal neurons evoked by layer IV stimulation), and induces a precocious termination of critical period (Huang et al., 1999).

Inhibitory circuitry, especially mediated by FS (PV) INs are increasingly implicated in the regulation of synaptic plasticity (Donato et al., 2013; Kuhlman et al., 2013; Cardin et al., 2009; Gu et al., 2013). During the learning phase of Morris water maze, pharmacological inhibition of VIP neurons or activation of PV neurons induces a robust increase of PV signal in PV neurons, prevents the normal shift from high to low PV signal during training, and suppresses the behavioral performance improvement (Donato et al., 2013). Activation of excitation onto FS (PV) INs in barrel cortex by optogenetic techniques generates gamma oscillation, and rhythmically gates the synaptic input to generate synchronized responses of excitatory neurons (Cardin et al., 2009), which facilitates sensory processing and learning by amplifying signals and reducing noise in pyramidal cells (Sohal et al., 2009). This modification of sensory processing has been shown to

linearly transform the responses from PV neurons to pyramidal neurons, so it does not affect the tuning properties (Atallah et al., 2012), in agreement with our observation (Fig. 4-2).

The strength of excitation onto FS (PV) INs is also regulated by monocular deprivation. 1 day of monocular deprivation reduces the frequency of spontaneous and evoked EPSCs onto FS (PV) INs at the peak of the mouse critical period (P28; Kuhlman et al., 2013). DREADD-mediated inhibition of these synapses allows re-expression of rapid ocular dominance plasticity in older animals. However, if the excitation onto FS (PV) INs is too low, the critical period for ocular dominance plasticity cannot be initiated, perhaps because in a hyperexcitable visual cortex, visual experience cannot further decrease the excitation onto FS (PV) INs. Indeed, we have previously shown that reducing excitation onto FS (PV) INs by knocking out NARP maintains the cortex in a hyper-excitable state, which does not allow the expression of ocular dominance plasticity (Gu et al., 2013). This suggests the excitation onto FS (PV) INs should also be in an optimal range to maintain the ability to manipulate cortical excitability for the expression of ocular dominance plasticity. Interestingly, Kuhlman et al. (2013) showed 1 d MD did not reduce FS (PV) INs spiking in P45 mice, a time point at which we see robust ocular dominance plasticity. It is possible in older rodents, the time required for the reduction of FS (PV) IN spiking increases with age, such that >1 day of MD is necessary to reduce FS (PV) IN spiking at P45.

Brief MD in juvenile (P27-28) rats induces an ocular dominance shift in spiking output from both excitatory and inhibitory neurons in superficial layers of V1b, but the shift is more pronounced in inhibitory neurons in older subjects with prolonged MD (P60, Kameyama et al., 2010). However, similarly work has shown that during the critical period, the ocular dominance

shift induced by MD is delayed but still robust in inhibitory neurons compared to excitatory neurons (Gandhi et al., 2008). The inconsistence of these two observation may be explained by the fact that Kameyama et al. (2010) used VGAT-Venus mice which have normal GAD67 expression level, while Gandhi et al. (2008) used GAD67-GFP knock-in mice which have low GAD67 expression level. The low GABA content in GAD67-GFP knock-in mice could make the excitatory neurons more binocular so the response to brief MD is less robust.

4.4.2 Mechanisms of NARP and NRG1 – ErbB4 pathway to enhance excitation onto FS (PV) INs

The ability to rescue ocular dominance plasticity in the NARP $^{-/-}$ mouse, by enhancing inhibitory output with diazepam (Gu et al., 2013) or systemic administration of NRG1, suggests that NARP and NRG1-ErbB4 signaling regulate the excitability of FS (PV) INs via separate/independent pathways.

Interestingly, both NARP and NRG1 – ErbB4 interact with molecules that make up perineuronal nets (PNNs), a specialization of the extracellular matrix (ECM) that is especially dense around the cell bodies of FS (PV) INs (Balmer et al., 2009). The polysaccharide side chains on the proteoglycans that make up the extracellular matrix (and the basement membrane) are substrates for lectins, including NARP. The bacterial enzyme Chondroitinase ABC (ChABC), which degrades the glycosaminoglycan side chains of proteoglycans (Kwok et al., 2011), disrupts the integrity of perineuronal nets and reduces the expression of NARP on the surface of FS (PV) INs (Chang et al., 2010). Importantly, in vivo delivery of the ChABC degrades PNN and reactivates ocular dominance plasticity in the visual cortex of adult rats (Pizzorusso et al., 2002)

but not adult cats (Vorobyov et al., 2013). Furthermore, the maturation of ECM in rodent visual cortex occurs ~ P70 (Pizzorusso et al., 2002), plateauing at the close of the critical period for ocular dominance plasticity observed in the absence of barbiturate anesthesia (Pham et al., 2004; Huang et al., 2011). One intriguing possibility is that the maturation of dense PNN enshrouding FS (PV) INs allows for accumulation of NRG1 and NARP, resulting in a coordinated maturation of the ability to recruit inhibition from FS (PV) INs.

The precursor for NRG1 is an inactive pro-NRG1 which is membrane bound. Most NRG1 isoforms become functional following cleavage of the membrane-bound pro-NRG1 by neuropsin or BACE1, which allows the soluble ligand to bind to ErbB4 receptors (Savonenko et al., 2008; Tamura et al., 2012). Electrical stimulation onto cerebellar cultures induces ErbB phosphorylation activated by soluble NRG1, suggests that the processing and release of NRG1 is regulated in response to neuronal activity (Ozaki et al., 2004; Mei and Xiong 2008). After the cleavage, the soluble NRG1 binds to heparan sulfate proteoglycan (HSPG) of ECM, which serve as a reservoir to accumulate NRG1 for its function (Loeb et al., 1999). Furthermore, the EGF-domain of NRG1, the critical domain for the binding of NRG1 with ErbB4 that initiates the tyrosine kinase signaling pathway, directly binds to integrin, which is an adhesion protein that recognizes ECM receptors and cell surface receptors (Ieguchi et al., 2010). The integrin binding with NRG1 is critical for the NRG1–ErbB pathway, because NRG1/ErbB/integrin can form a ternary complex, and the disruption of this linkage suppresses the NRG1-ErbB4 signaling. This indicates the function of endogenous NRG1 – ErbB4 pathway requires the facilitation from ECM.

Although previous work indicates that NRG1 regulates the formation and strength of excitatory synapses onto FS (PV) INs (Ting et al., 2011; Yang et al., 2013; Abe et al., 2011), we have not yet shown the precise locus of the effects of our use of NRG1 and the ErbB4 inhibitor. It is also not known if our systemic administration of NRG1 and ErbB4 inhibitor regulate excitatory drive onto FS (PV) INs by regulating the strength of existing synapses, or regulating excitatory synapse density. To test this directly, EPSC amplitudes and connection probability from excitatory neurons to FS (PV) INs should be examined in the presence of NRG1 or ErbB4 inhibitor. However, the NRG1 rescue of ocular dominance plasticity in NARP $^{-/-}$ mice suggests that the reduction in connection probability seen in the transgenic mice does not down-regulate ErbB4 receptors in FS (PV) INs. One possibility is that since surface NARP accumulation is co-regulated with PNN development (Chang et al., 2010), knocking out NARP also suppresses the normal development of ECM, which decreases the endogenous NRG1 – ErbB4 signaling pathway. As NRG1 is released by activity from excitatory neurons (Ozaki et al., 2004; Mei and Xiong 2008), the increase in RS neuron excitability might be expected to enhance the release of NRG1 in NARP $^{-/-}$ mice. However, endogenous NRG1 is not sufficient to compensate for the loss of NARP, perhaps because, the reduction in connection probability reduces the number of excitatory synapses which release NRG1 in NARP$^{-/-}$ mice. To test this hypothesis, further experiments could compare the ErbB4 phosphorylation level in WT adult, NARP $^{-/-}$ and ChABC treated WT adult mice, to see if the phosphorylated ErbB4 density is reduced in NARP $^{-/-}$ and ChABC treated mice.

Chapter 5: Conclusions and future directions

In this thesis, I used different *in vivo* recording techniques and visual experience manipulations on rodents, to support a new model for the regulation of the critical period for ocular dominance plasticity. I showed that in the primary visual cortex, the ability to reopen the critical period with dark exposure differs over development. A refractory period, during which dark exposure is ineffective, exists towards the end of the critical period. In addition, ocular dominance plasticity is robust during the late critical period when perisomatic inhibition is mature. Enhancement of inhibition with a $GABA_AR$ modulator masks ocular dominance plasticity during the late critical period, suggesting there is sufficient perisomatic inhibition at this age to limit plasticity, but this inhibition is not fully recruited by visual experience. To examine the regulation of ocular dominance plasticity upstream of inhibitory output, I used NARP and NRG1-ErbB4 to manipulate neuronal excitability in the visual cortex. I showed that regulation of spiking in FS (PV) INs plays an important role in the regulation of the critical period. Importantly, retention of the excitability of FS and RS neurons into the permissive range can enable the expression of ocular dominance plasticity. My results also suggest that different aspects of stimulus selectivity (such as orientation tuning and ocular dominance) are regulated independently; while the excitatory synapses onto FS (PV) INs may be a good candidate for further clinical research for the treatment of amblyopia.

5.1 The recruitment of inhibition in vivo

In Chapter 2, I showed that robust ocular dominance plasticity persists after the maturation of perisomatic inhibition (P35 in rodents), but can be masked by enhancement of GABAergic inhibition with diazepam. This suggests that after P35 there is sufficient inhibition on principal

neurons to limit ocular dominance plasticity, but this inhibition is not fully recruited by visual experience at this age. This also indicates that the development of critical period may be determined "upstream" of inhibitory output onto principal neurons, which guided us to examine the regulation of excitation of FS (PV) INs in chapter 3 and 4.

My results presented in Chapter 2 disagree with some previous experiments that rapid ocular dominance plasticity is lost after the maturation of perisomatic inhibition (P35; Gordon and Stryker, 1996). It was reported that 4d MD could not induce ocular dominance shift in P35 (Gordon and Stryker, 1996) and P46 (Fagiolini and Hensch, 2000). The discrepancy may be due to the difference in the choice of anesthetics, as Gordon and Stryker (1996) and Fagiolini and Hensch (2000) used pentobarbital (a positive allosteric modulator of $GABA_A$Rs), which may mask ocular dominance plasticity after P35. Indeed, the expression of ocular dominance plasticity induced in rats with 4 day MD at P36-75 under urethane is acutely inhibited with pentobarbital (Pham et al., 2004). Throughout the thesis I used light urethane (1.4mg/kg) or isoflurane (1.5% in O_2) anesthesia to study ocular dominance plasticity. Urethane only has modest effects on GABA receptors at anesthetic dosage (Hara and Harris, 2002), and isoflurane functions as anesthetics by binding to nAchRs (Brannigan et al., 2010). Importantly, all current work in the Quinlan lab is performed in awake animals with chronically implanted electrodes.

Another discrepancy is that synaptic plasticity, especially in layer IV, is restricted much earlier in development than we observe the loss of ocular dominance plasticity over development. Using *in vitro* techniques, such as paired recordings in the mice visual cortex, it is found that white

matter → layer IV LTP and LTD lost early in development (~P20; Jiang et al., 2007). However, using *in vivo* techniques, such as VEP and single unit recordings, it is found that ocular dominance plasticity persists even after P35 in the rodent V1b (Huang et al., 2010). One possibility is that inhibition is more efficiently recruited *in vitro* by stimulated electrode implanted in white matter, than in vivo by the visual pathway. A simple test of the hypothesis that inhibition is not fully recruited by vision in juvenile wild types, despite the presence of mature perisomatic inhibition, could be performed by comparing EPSCs in FS (PV) INs in vivo evoked by visual stimulation versus stimulation in proximal layer IV or layer II/III. I predict that the maximal EPSC amplitude evoked by visual stimulation would be smaller than that generated by electrical stimulation.

5.2 The regulation of refractory period

In Chapter 2 we showed that dark exposure does not further enhance ocular dominance plasticity in rodents at P35-55. The mechanisms for the refractory period are unknown, but I will speculate on some mechanisms:

First, the refractory period reflects a time of incomplete maturation of excitation onto FS (PV) INs. The effects of DE are occluded in NARP$^{-/-}$ mice, and can be inhibited with NRG1 injection, suggesting that DE reopens the critical period by reducing the connection probability or the synaptic efficacy of excitation onto FS (PV) INs. Immature synapses are typically more plasticity, and so the reduction in excitation in response to DE may induce a compensatory increase in remaining synapses. Alternatively, immature synapses may be resistant to modifications by the pathways engaged by DE. One simple way to ask if the refractory period reflects suboptimal

excitation onto FS (PV) INs would be to enhance the excitation of FS (PV) INs with NRG1 at P45 (in the middle of the refractory period). If NRG1 inhibits ocular dominance plasticity at P45, but DE can reopen the critical period in P45 after NRG1 injection, then it suggests that a suboptimal level of excitatory drive impacts the expression of the refractory period.

The refractory period may also be due to incomplete maturation of extracellular matrix. Importantly, the ECM in the rodent visual cortex matures around P60-70 (Pizzoruso et al., 2002), which correlates with the end of the refractory period (Huang et al., 2010). It is possible that DE reactivates ocular dominance plasticity by the degradation of the ECM, but this is ineffective during a time of rapid ECM growth. Thus a decrease in PNN maturation/density would be expected in DE adults, and DE may occlude the effects of chondroitnase treatment on ocular dominance plasticity. In addition, we can enhance the development of ECM by inhibiting extracellular proteinases such as MMP9 +/- DE, which would be expected to accelerate the maturation of the ECM (Spolidoro et al., 2012). If inhibiting MMP9 suppresses ocular dominance plasticity at P45, but recovers the reactivation at this age by DE, we would conclude that the dynamics of ECM development contribute to the refractory period.

5.3 A direct rescue of the NARP $^{-/-}$ phenotype

In Chapter 3, we showed that in the absence of NARP, there is a decrease in the connection probability between pyramidal neurons and FS (PV) INs, which resulted in a hyper-excitable visual cortex that is unable to express ocular dominance plasticity. Nonetheless, diazepam can restore ocular dominance plasticity in NARP $^{-/-}$ mice, suggesting a threshold level of $GABA_A$Rs

on principal neurons. One surprising result of this work was that downstream inhibitory synapses develop normally despite the upstream deficit in excitatory drive. This suggests that the level of excitation necessary to drive the maturation of inhibitory output is lower than required to drive ocular dominance plasticity.

I used two different pharmacological treatments to rescue ocular dominance plasticity in NARP $^{-/-}$ mice, diazepam and NRG1. However, in both cases, the locus of the effect is inferred from *in vivo* electrophysiological recordings. To target excitation onto FS (PV) INs directly in adulthood, I could utilize an inducible cre-lox recombinase system to selectively express NARP in adult NARP $^{-/-}$ mice (Jaisser, 2000). I predict that after inducing the expression of NARP, it will accumulated on the surface of FS (PV) INs, resulting in an increase in connection probability between pyramidal neurons and FS (PV) INs. The increase in excitability of FS (PV) INs and decrease in excitability of RS neurons would be expected to be accompanied by a rescue of ocular dominance plasticity.

Future experiments could also attempt to rescue the NARP $^{-/-}$ phenotype using direct activation of FS (PV) INs with optogenetic techniques. To do this, cre recombinase could be expressed under a PV specific promoter, and the AAV containing floxed channelrhodopsin cDNA is delivered to V1b. With photo stimulation (470nm, 5 s per trial, 25 s inter-trial interval, approximately 30 trials) onto the visual cortex, the FS (PV) INs can be temporarily activated (Atallah et al., 2012; Lee et al., 2012). With this method, I can examine if the direct activation on FS (PV) INs will decrease the excitability of RS neurons in the NARP $^{-/-}$ mice V1b. If excitability

similar to what is observed in a critical period wild type mouse can be achieved and maintained, I could ask if various forms of plasticity, including ocular dominance plasticity, are restored.

5.4 The possible application of FS (PV) INs excitation in the clinical research for amblyopia

One aim of our research on ocular dominance plasticity is to find potential interventions to treat severe deprivation amblyopia in the clinic. At present, the most effective treatment for severe deprivation amblyopia is removal of the cataract by surgery, followed by wearing an eye patch to force the use of the deprived eye. However, these methods are more effective in juveniles, while in adults the cure rate is very low (Mitchell and MacKinnon, 2002).

Pharmacological treatments have also had mixed successes. One problem is that the blood-brain barrier may prevent the transportation of certain molecules into the brain. This can be overcome with the recent development of delivery methods using nanoparticles (Silke et al., 2013) and peptides which have active transporters, such as NRG1 (Van Dorpe et al., 2012; Kastin et al., 2004).

An additional obstacle to pharmacological approaches is specificity, which is the key step to translate animal work to clinical research. Previous models suggested that ocular dominance plasticity could be reactivated with reduced cortical inhibition. However, reducing inhibition in specific cell types (a subset of pyramidal neurons) in the visual cortex is difficult in humans. If global inhibition is reduced, the resulting hyperactivity is likely to cause seizures. To avoid these

problems, I used manipulation of the NRG1 – ErbB4 pathway to regulate FS (PV) INs excitability. This represents a potential approach for the clinical treatment for amblyopia, as ErbB4 receptors are highly enriched at excitatory synapses onto FS (PV) INs in mice (Vullhorst et al., 2009).

In summary, understanding the mechanisms for the initiation and termination of the critical period for ocular dominance plasticity may lead to insights in potential treatments for amblyopia in adults. Whether other mechanisms exist to cooperate in the regulation of the ocular dominance plasticity and whether this circuit modifies other forms of stimulus selectivity remains to be determined.

Abbreviations

Ach Acetocholine
ACSF artificial cortico-spinal fluid
AMPA α-Amino-3-hydroxy-5-methyl-4-isoxazolepropionic acid
ANOVA Analysis of variance
APV (2R)-amino-5-phosphonovaleric acid
CB cannabinoid
CBI contralateral bias index
CNQX 6-cyano-7-nitroquinoxaline-2,3-dione
DE dark exposure
DZ diazepam
ECM extracellular matrix
EPSC excitatory postsynaptic current
FS fast-spiking
GABA γ-Aminobutyric acid
GAD Glutamate decarboxylase
Glu Glutamate
IN interneuron
IPSC inhibitory postsynaptic current
LGN lateral geniculate nucleus
LM lateral-medial area
LTD long-term depression
LTP long-term potentiation
MD monocular deprivation
MMP Matrix metalloproteinase
MPA 3-mercaptopropionic acid
NARP neuronal activity related pentraxin
NMDA N-Methyl-D-aspartic acid
NRG1 neuregulin1
OSI orientation selective index
PCR polymerase chain reaction
PG proteoglycan
PNN perineuronal net
PPD pair-pulse depression
PV parvalbumin
Pyr pyramidal
RS regular-spiking
SEM standard error of the mean
TARP Transmembrane AMPAR regulatory protein
TBS theta-burst stimulation
TMS Transcranial magnetic stimulation
VEP Visually-evoked potential
VPL visual perceptual learning
V1b binocular visual cortex
WT wild type

Bibliography

Abe Y, Namba H, Kato T, Iwakura Y, Nawa H. Neuregulin-1 signals from the periphery regulate AMPA receptor sensitivity and expression in GABAergic interneurons in developing neocortex. J Neurosci. 2011 Apr 13;31(15):5699-709.

Artola A, Singer W. Long-term potentiation and NMDA receptors in rat visual cortex. Nature. 330(1987):649-52.

Ascoli GA, Alonso-Nanclares L, Anderson SA, Barrionuevo G, Benavides-Piccione R, Burkhalter A, Buzsaki G, et al. Petilla terminology: Nomenclature of features of GABAergic interneurons of the cerebral cortex. Nat Rev Neurosci. 9(2008):557-68.

Atallah BV, Bruns W, Carandini M, Scanziani M. Parvalbumin-expressing interneurons linearly transform cortical responses to visual stimuli. Neuron. 2012 Jan 12;73(1):159-70.

Baeten KM, Akassoglou K. Extracellular matrix and matrix receptors in blood-brain barrier formation and stroke. Dev Neurobiol. 2011 Nov;71(11):1018-39.

Balmer TS, Carels VM, Frisch JL, Nick TA. Modulation of perineuronal nets and parvalbumin with developmental song learning. J Neurosci. 2009 Oct 14;29(41):12878-85.

Bartos M, Alle H, Vida I. Role of microcircuit structure and input integration in hippocampal interneuron recruitment and plasticity. Neuropharmacology. 2011 Apr;60(5):730-9.

Beste C, Wascher E, Güntürkün O, Dinse HR. Improvement and impairment of visually guided behavior through LTP- and LTD-like exposure-based visual learning. Curr Biol. 21(2011):876-82.

Bi GQ, Poo MM. Synaptic modifications in cultured hippocampal neurons: dependence on spike timing, synaptic strength, and postsynaptic cell type. J Neurosci. 1998 Dec 15;18(24):10464-72.

Bjartmar L, Huberman AD, Ullian EM, Renteria RC, Liu X, Xu W, Prezioso J, Susman MW, Stellwagen D, Stokes CC, Cho R, Worley P, Malenka RC, Ball S, Peachey NS, Copenhagen D,

Chapman B, Nakamoto M, Barres BA, Perin MS. Neuronal pentraxins mediate synaptic refinement in the developing visual system. J Neurosci. 26(2006):6269-81.

Blakemore C, Tobin EA. Lateral inhibition between orientation detectors in the cat's visual cortex. Exp Brain Res. 1972;15(4):439-40.

Braddick O, Atkinson J. Development of human visual function. Vision Res. 2011 Jul 1;51(13):1588-609.

Brannigan G, LeBard DN, Hénin J, Eckenhoff RG, Klein ML. Multiple binding sites for the general anesthetic isoflurane identified in the nicotinic acetylcholine receptor transmembrane domain. Proc Natl Acad Sci U S A. 2010 Aug 10;107(32):14122-7.

Cammalleri M, Lütjens R, Berton F, King AR, Simpson C, Francesconi W, Sanna PP. Time-restricted role for dendritic activation of the mTOR-p70S6K pathway in the induction of late-phase long-term potentiation in the CA1. Proc Natl Acad Sci U S A. 2003 Nov 25;100(24):14368-73.

Cardin JA, Carlén M, Meletis K, Knoblich U, Zhang F, Deisseroth K, Tsai LH, Moore CI. Driving fast-spiking cells induces gamma rhythm and controls sensory responses. Nature. 2009 Jun 4;459(7247):663-7.

Chang MC, Park JM, Pelkey KA, Grabenstatter HL, Xu D, Linden DJ, Sutula TP, McBain CJ, Worley PF. Narp regulates homeostatic scaling of excitatory synapses on parvalbumin-expressing interneurons. Nat Neurosci. 2010 Sep;13(9):1090-7.

Chattopadhyaya B, Di Cristo G, Wu CZ, Knott G, Kuhlman S, Fu Y, Palmiter RD, Huang ZJ. GAD67-mediated GABA synthesis and signaling regulate inhibitory synaptic innervation in the visual cortex. Neuron. 2007 Jun 21;54(6):889-903.

Chevaleyre V, Takahashi KA, Castillo PE. Endocannabinoid-mediated synaptic plasticity in the CNS. Annu Rev Neurosci. 2006;29:37-76.

Chittajallu R, Isaac JT. Emergence of cortical inhibition by coordinated sensory-driven plasticity at distinct synaptic loci. Nat Neurosci. 13(2010):1240-8.

Cho KK, Khibnik L, Philpot BD, Bear MF. The ratio of NR2A/B NMDA receptor subunits determines the qualities of ocular dominance plasticity in visual cortex. Proc Natl Acad Sci U S A. 2009 Mar 31;106(13):5377-82.

Choi SY, Morales B, Lee HK, Kirkwood A. Absence of long-term depression in the visual cortex of glutamic Acid decarboxylase-65 knock-out mice. J Neurosci. 22(2002):5271-6.

Coleman JE, Law K, Bear MF. Anatomical origins of ocular dominance in mouse primary visual cortex. Neuroscience. 161(2009):561-71.

Cooke SF, Bear MF. Visual experience induces long-term potentiation in the primary visual cortex. J Neurosci. 30(2010):16304-13.

Crozier RA, Wang Y, Liu CH, Bear MF. Deprivation-induced synaptic depression by distinct mechanisms in different layers of mouse visual cortex. Proc Natl Acad Sci U S A. (2007) 104(4):1383-8.

Cynader M. Prolonged sensitivity to monocular deprivation in dark-reared cats: effects of age and visual exposure. Brain Res. (1983) 284:155-64.

Dakoji S, Tomita S, Karimzadegan S, Nicoll RA, Bredt DS. Interaction of transmembrane AMPA receptor regulatory proteins with multiple membrane associated guanylate kinases. Neuropharmacology. 2003 Nov;45(6):849-56.

Daw NW, Fox K, Sato H, Czepita D. Critical period for monocular deprivation in the cat visual cortex. J Neurophysiol. 1992 Jan;67(1):197-202.

Deans MR, Gibson JR, Sellitto C, Connors BW, Paul DL. Synchronous activity of inhibitory networks in neocortex requires electrical synapses containing connexin36. Neuron. 2001 Aug 16;31(3):477-85.

Derkach VA, Oh MC, Guire ES, Soderling TR. Regulatory mechanisms of AMPA receptors in synaptic plasticity. Nat Rev Neurosci. 2007 Feb;8(2):101-13.

Desai NS, Cudmore RH, Nelson SB, Turrigiano GG Critical periods for experience-dependent synaptic scaling in visual cortex. Nat Neurosci. 2002 Aug;5(8):783-9.

Di Cristo G, Chattopadhyaya B, Kuhlman SJ, Fu Y, Bélanger MC, Wu CZ, Rutishauser U, Maffei L, Huang ZJ. Activity-dependent PSA expression regulates inhibitory maturation and onset of critical period plasticity. Nat Neurosci. (2007) 10(12):1569-77.

Donato F, Rompani SB, Caroni P. Parvalbumin-expressing basket-cell network plasticity induced by experience regulates adult learning. Nature. 2013 Dec 12;504(7479):272-6.

Durand S, Patrizi A, Quast KB, Hachigian L, Pavlyuk R, Saxena A, Carninci P, Hensch TK, Fagiolini M. NMDA receptor regulation prevents regression of visual cortical function in the absence of Mecp2. Neuron. 2012 Dec 20;76(6):1078-90.

Fagiolini M, Fritschy JM, Löw K, Möhler H, Rudolph U, Hensch TK. Specific GABAA circuits for visual cortical plasticity. Science. 2004 Mar 12;303(5664):1681-3.

Fagiolini M, Hensch TK. Inhibitory threshold for critical-period activation in primary visual cortex. Nature. (2000) 404(6774):183-6.

Fagiolini M, Pizzorusso T, Berardi N, Domenici L, Maffei L. Functional postnatal development of the rat primary visual cortex and the role of visual experience: dark rearing and monocular deprivation. Vision Res. (1994) 34:709-20.

Falls DL. Neuregulins: functions, forms, and signaling strategies. Exp Cell Res. 2003 Mar 10;284(1):14-30.

Fischer QS, Graves A, Evans S, Lickey ME, Pham TA. Monocular deprivation in adult mice alters visual acuity and single-unit activity. Learn Mem. 2007 Apr 6;14(4):277-86.

Frenkel MY, Bear MF. How monocular deprivation shifts ocular dominance in visual cortex of young mice. Neuron. 2004 Dec 16;44(6):917-23.

Frenkel MY, Sawtell NB, Diogo AC, Yoon B, Neve RL, Bear MF. Instructive effect of visual experience in mouse visual cortex. Neuron. 51(2006):339-49.

Frischknecht R, Heine M, Perrais D, Seidenbecher CI, Choquet D, Gundelfinger ED. Brain extracellular matrix affects AMPA receptor lateral mobility and short-term synaptic plasticity. Nat Neurosci. 2009 Jul;12(7):897-904.

Gandhi SP, Yanagawa Y, Stryker MP. Delayed plasticity of inhibitory neurons in developing visual cortex. Proc Natl Acad Sci U S A. (2008) 105(43):16797-802.

Gianfranceschi L, Siciliano R, Walls J, Morales B, Kirkwood A, Huang ZJ, Tonegawa S, Maffei L. Visual cortex is rescued from the effects of dark rearing by overexpression of BDNF. Proc Natl Acad Sci U S A. 2003 Oct 14;100(21):12486-91.

Goel A, Lee HK. Persistence of experience-induced homeostatic synaptic plasticity through adulthood in superficial layers of mouse visual cortex. J Neurosci. 2007 Jun 20;27(25):6692-700.

Goldberg EM, Clark BD, Zagha E, Nahmani M, Erisir A, Rudy B. K+ channels at the axon initial segment dampen near-threshold excitability of neocortical fast-spiking GABAergic interneurons. Neuron. 2008 May 8;58(3):387-400.

Goldberg EM, Watanabe S, Chang SY, Joho RH, Huang ZJ, Leonard CS, Rudy B. Specific functions of synaptically localized potassium channels in synaptic transmission at the neocortical GABAergic fast-spiking cell synapse. J Neurosci. 2005 May 25;25(21):5230-5.

Gordon JA, Stryker MP. Experience-dependent plasticity of binocular responses in the primary visual cortex of the mouse. J Neurosci. 1996 May 15;16(10):3274-86.

Gu Y, Huang S, Chang MC, Worley P, Kirkwood A, Quinlan EM. Obligatory role for the immediate early gene NARP in critical period plasticity. Neuron. 2013 Jul 24;79(2):335-46.

Guire ES, Lickey ME, Gordon B. Critical period for the monocular deprivation effect in rats: assessment with sweep visually evoked potentials. J Neurophysiol. (1999) 81:121-8.

Gundelfinger ED, Frischknecht R, Choquet D, Heine M. Converting juvenile into adult plasticity: a role for the brain's extracellular matrix. Eur J Neurosci. 2010 Jun;31(12):2156-65.

Hanover JL, Huang ZJ, Tonegawa S, Stryker MP. Brain-derived neurotrophic factor overexpression induces precocious critical period in mouse visual cortex. J Neurosci. 1999 Nov 15;19(22):RC40.

Hara K, Harris RA. The anesthetic mechanism of urethane: the effects on neurotransmitter-gated ion channels. Anesth Analg. 2002 Feb;94(2):313-8

Harauzov A, Spolidoro M, DiCristo G, De Pasquale R, Cancedda L, Pizzorusso T, Viegi A, Berardi N, Maffei L. Reducing intracortical inhibition in the adult visual cortex promotes ocular dominance plasticity. J Neurosci. 2010 Jan 6;30(1):361-71.

Haylock-Jacobs S, Keough MB, Lau L, Yong VW. Chondroitin sulphate proteoglycans: extracellular matrix proteins that regulate immunity of the central nervous system. Autoimmun Rev. 2011 Oct;10(12):766-72.

He HY, Hodos W, Quinlan EM. Visual deprivation reactivates rapid ocular dominance plasticity in adult visual cortex. J Neurosci. (2006) 26(11):2951-5.

He HY, Ray B, Dennis K, Quinlan EM. Experience-dependent recovery of vision following chronic deprivation amblyopia. Nat Neurosci. (2007) 10(9):1134-6.

Heimel JA, Hartman RJ, Hermans JM, Levelt CN. Screening mouse vision with intrinsic signal optical imaging. Eur J Neurosci. 25(2007):795-804.

Hensch TK, Fagiolini M, Mataga N, Stryker MP, Baekkeskov S, Kash SF. Local GABA circuit control of experience-dependent plasticity in developing visual cortex. Science. 1998 Nov 20;282(5393):1504-8.

Hensch TK, Fagiolini M. Excitatory-inhibitory balance and critical period plasticity in developing visual cortex. Prog Brain Res. 2005;147:115-24.

Heynen AJ, Yoon BJ, Liu CH, Chung HJ, Huganir RL, Bear MF. Molecular mechanism for loss of visual cortical responsiveness following brief monocular deprivation. Nat Neurosci. 2003 Aug;6(8):854-62.

Holmes JM, Repka MX, Kraker RT, Clarke MP. The treatment of amblyopia. Strabismus. 2006 Mar;14(1):37-42.

Huang S, Gu Y, Quinlan EM, Kirkwood A. A refractory period for rejuvenating GABAergic synaptic transmission and ocular dominance plasticity with dark exposure. J Neurosci. 2010 Dec 8;30(49):16636-42.

Huang ZJ, Kirkwood A, Pizzorusso T, Porciatti V, Morales B, Bear MF, Maffei L, Tonegawa S. BDNF regulates the maturation of inhibition and the critical period of plasticity in mouse visual cortex. Cell. 1999 Sep 17;98(6):739-55.

Huang ZJ. Activity-dependent development of inhibitory synapses and innervation pattern: role of GABA signalling and beyond. J Physiol. (2009) 587:1881-8.

Hubel DH, Wiesel TN, LeVay S. Plasticity of ocular dominance columns in monkey striate cortex. Philos Trans R Soc Lond B Biol Sci. 1977 Apr 26;278(961):377-409.

HUBEL DH, WIESEL TN. EFFECTS OF VISUAL DEPRIVATION ON MORPHOLOGY AND PHYSIOLOGY OF CELLS IN THE CATS LATERAL GENICULATE BODY. J Neurophysiol. 1963 Nov;26:978-93.

HUBEL DH, WIESEL TN. Receptive fields of single neurones in the cat's striate cortex. J Physiol. 1959 Oct;148:574-91.

HUBEL DH, WIESEL TN. Receptive fields, binocular interaction and functional architecture in the cat's visual cortex. J Physiol. 1962 Jan;160:106-54.

Ieguchi K, Fujita M, Ma Z, Davari P, Taniguchi Y, Sekiguchi K, Wang B, Takada YK, Takada Y. Direct binding of the EGF-like domain of neuregulin-1 to integrins ({alpha}v{beta}3 and {alpha}6{beta}4) is involved in neuregulin-1/ErbB signaling. J Biol Chem. 2010 Oct 8;285(41):31388-98.

Issa NP, Trachtenberg JT, Chapman B, Zahs KR, Stryker MP. The critical period for ocular dominance plasticity in the Ferret's visual cortex. J Neurosci. 1999 Aug 15;19(16):6965-78.

Jaisser F. Inducible gene expression and gene modification in transgenic mice. J Am Soc Nephrol. 2000 Nov;11 Suppl 16:S95-S100.

Jang HJ, Cho KH, Kim HS, Hahn SJ, Kim MS, Rhie DJ. Age-dependent decline in supragranular long-term synaptic plasticity by increased inhibition during the critical period in the rat primary visual cortex. J Neurophysiol. (2009) 101:269-75.

Jiang B, Huang S, de Pasquale R, Millman D, Song L, Lee HK, Tsumoto T, Kirkwood A. The maturation of GABAergic transmission in visual cortex requires endocannabinoid-mediated LTD of inhibitory inputs during a critical period. Neuron. 66(2010):248-59.

Jiang B, Huang ZJ, Morales B, Kirkwood A. Maturation of GABAergic transmission and the timing of plasticity in visual cortex. Brain Res Brain Res Rev. (2005) 50(1):126-33.

Jiang B, Treviño M, Kirkwood A. Sequential development of long-term potentiation and depression in different layers of the mouse visual cortex. J Neurosci. (2007) 27(36):9648-52.

Kameyama K, Sohya K, Ebina T, Fukuda A, Yanagawa Y, Tsumoto T. Difference in binocularity and ocular dominance plasticity between GABAergic and excitatory cortical neurons. J Neurosci. 2010 30(4):1551-9.

Kaneko M, Stellwagen D, Malenka RC, Stryker MP. Tumor necrosis factor-alpha mediates one component of competitive, experience-dependent plasticity in developing visual cortex. Neuron. 2008 Jun 12;58(5):673-80.

Kastin AJ, Akerstrom V, Pan W. Neuregulin-1-beta1 enters brain and spinal cord by receptor-mediated transport. J Neurochem. 2004 Feb;88(4):965-70.

Katzner S, Nauhaus I, Benucci A, Bonin V, Ringach DL, Carandini M. Local origin of field potentials in visual cortex. Neuron. 61(2009):35-41.

Kawaguchi Y, Kubota Y. GABAergic cell subtypes and their synaptic connections in rat frontal cortex. Cereb Cortex. 7(1997):476-86.

Kirkwood A, Bear MF. Hebbian synapses in visual cortex. J Neurosci. 14(1994):1634-45.

Klausberger T, Roberts JD, Somogyi P. Cell type- and input-specific differences in the number and subtypes of synaptic GABA(A) receptors in the hippocampus. J Neurosci. 2002 Apr 1;22(7):2513-21.

Koch SM, Ullian EM. Neuronal pentraxins mediate silent synapse conversion in the developing visual system. J Neurosci. 2010 Apr 14;30(15):5404-14.

Kreczko A, Goel A, Song L, Lee HK. Visual deprivation decreases somatic GAD65 puncta number on layer 2/3 pyramidal neurons in mouse visual cortex. Neural Plast. 2009:415135.

Kuhlman SJ, Lu J, Lazarus MS, Huang ZJ. Maturation of GABAergic inhibition promotes strengthening of temporally coherent inputs among convergent pathways. PLoS Comput Biol. 2010 Jun 3;6(6):e1000797.

Kuhlman SJ, Olivas ND, Tring E, Ikrar T, Xu X, Trachtenberg JT. A disinhibitory microcircuit initiates critical-period plasticity in the visual cortex. Nature. 2013 Sep 26;501(7468):543-6.

Kuhlman SJ, Tring E, Trachtenberg JT. Fast-spiking interneurons have an initial orientation bias that is lost with vision. Nat Neurosci. 14(2011):1121-3.

Kwok JC, Dick G, Wang D, Fawcett JW. Extracellular matrix and perineuronal nets in CNS repair. Dev Neurobiol. 2011 Nov;71(11):1073-89.

Lai C, Lemke G. An extended family of protein-tyrosine kinase genes differentially expressed in the vertebrate nervous system. Neuron. 1991 May;6(5):691-704.

Lambo ME, Turrigiano GG. Synaptic and intrinsic homeostatic mechanisms cooperate to increase L2/3 pyramidal neuron excitability during a late phase of critical period plasticity. J Neurosci. 2013 May 15;33(20):8810-9.

Law AJ, Wang Y, Sei Y, O'Donnell P, Piantadosi P, Papaleo F, Straub RE, Huang W, Thomas CJ, Vakkalanka R, Besterman AD, Lipska BK, Hyde TM, Harrison PJ, Kleinman JE, Weinberger DR. Neuregulin 1-ErbB4-PI3K signaling in schizophrenia and phosphoinositide 3-kinase-p110δ inhibition as a potential therapeutic strategy. Proc Natl Acad Sci U S A. 2012 Jul 24;109(30):12165-70.

Lee HK, Takamiya K, Han JS, Man H, Kim CH, Rumbaugh G, Yu S, Ding L, He C, Petralia RS, Wenthold RJ, Gallagher M, Huganir RL. Phosphorylation of the AMPA receptor GluR1 subunit is required for synaptic plasticity and retention of spatial memory. Cell. 2003 Mar 7;112(5):631-43.

Lee SH, Kwan AC, Zhang S, Phoumthipphavong V, Flannery JG, Masmanidis SC, Taniguchi H, Huang ZJ, Zhang F, Boyden ES, Deisseroth K, Dan Y. Activation of specific interneurons improves V1 feature selectivity and visual perception. Nature. 2012 Aug 16;488(7411):379-83.

Lehmann K, Löwel S. Age-dependent ocular dominance plasticity in adult mice. PLoS One. 2008 Sep 1;3(9):e3120.

Li KX, Lu YM, Xu ZH, Zhang J, Zhu JM, Zhang JM, Cao SX, Chen XJ, Chen Z, Luo JH, Duan S, Li XM. Neuregulin 1 regulates excitability of fast-spiking neurons through Kv1.1 and acts in epilepsy. Nat Neurosci. 2011 Dec 11;15(2):267-73.

Li L, Bender KJ, Drew PJ, Jadhav SP, Sylwestrak E, Feldman DE. Endocannabinoid signaling is required for development and critical period plasticity of the whisker map in somatosensory cortex. Neuron. 2009 Nov 25;64(4):537-49.

Liu CH, Heynen AJ, Shuler MG, Bear MF. Cannabinoid receptor blockade reveals parallel plasticity mechanisms in different layers of mouse visual cortex. Neuron. (2008) 58(3):340-5.

Liu Y, Tao YM, Woo RS, Xiong WC, Mei L. Stimulated ErbB4 internalization is necessary for neuregulin signaling in neurons. Biochem Biophys Res Commun. 2007 Mar 9;354(2):505-10.

Loeb JA, Khurana TS, Robbins JT, Yee AG, Fischbach GD. Expression patterns of transmembrane and released forms of neuregulin during spinal cord and neuromuscular synapse development. Development. 1999 Feb;126(4):781-91.

Maffei A, Lambo ME, Turrigiano GG. Critical period for inhibitory plasticity in rodent binocular V1. J Neurosci. 2010 Mar 3;30(9):3304-9.

Maffei A, Nataraj K, Nelson SB, Turrigiano GG. Potentiation of cortical inhibition by visual deprivation. Nature. 443(2006):81-4.

McBain CJ, Kauer JA. Presynaptic plasticity: targeted control of inhibitory networks. Curr Opin Neurobiol. 2009 Jun;19(3):254-62. Epub 2009 Jul 4.

McCurry CL, Shepherd JD, Tropea D, Wang KH, Bear MF, Sur M. Loss of Arc renders the visual cortex impervious to the effects of sensory experience or deprivation. Nat Neurosci. 13(2010):450-7.

McGee AW, Yang Y, Fischer QS, Daw NW, Strittmatter SM. Experience-driven plasticity of visual cortex limited by myelin and Nogo receptor. Science. 2005 Sep 30;309(5744):2222-6.

McKeon RJ, Höke A, Silver J. Injury-induced proteoglycans inhibit the potential for laminin-mediated axon growth on astrocytic scars. Exp Neurol. 1995 Nov;136(1):32-43.

McMahon SA, Díaz E. Mechanisms of excitatory synapse maturation by trans-synaptic organizing complexes. Curr Opin Neurobiol. 2011 Apr;21(2):221-7.

Mei L, Xiong WC. Neuregulin 1 in neural development, synaptic plasticity and schizophrenia. Nat Rev Neurosci. 2008 Jun;9(6):437-52.

Michaluk P, Mikasova L, Groc L, Frischknecht R, Choquet D, Kaczmarek L. Matrix metalloproteinase-9 controls NMDA receptor surface diffusion through integrin beta1 signaling. J Neurosci. 2009 May 6;29(18):6007-12.

Mitchell DE, MacKinnon S. The present and potential impact of research on animal models for clinical treatment of stimulus deprivation amblyopia. Clin Exp Optom. 2002 Jan;85(1):5-18.

Miyata S, Komatsu Y, Yoshimura Y, Taya C, Kitagawa H. Persistent cortical plasticity by upregulation of chondroitin 6-sulfation. Nat Neurosci. 2012 Jan 15;15(3):414-22.

Morales B, Choi SY, Kirkwood A. Dark rearing alters the development of GABAergic transmission in visual cortex. J Neurosci. (2002) 22(18):8084-90

Morishita H, Miwa JM, Heintz N, Hensch TK. Lynx1, a cholinergic brake, limits plasticity in adult visual cortex. Science. 2010 Nov 26;330(6008):1238-40.

Mower GD, Christen WG. Role of visual experience in activating critical period in cat visual cortex.J Neurophysiol. 1985 53:572-89.

Mower GD, Guo Y. Comparison of the expression of two forms of glutamic acid decarboxylase (GAD67 and GAD65) in the visual cortex of normal and dark-reared cats. Brain Res Dev Brain Res. 2001 Jan 31;126(1):65-74.

Mrsic-Flogel TD, Hofer SB, Ohki K, Reid RC, Bonhoeffer T, Hübener M. Homeostatic regulation of eye-specific responses in visual cortex during ocular dominance plasticity. Neuron. 2007 Jun 21;54(6):961-72.

Niell CM, Stryker MP. Highly selective receptive fields in mouse visual cortex. J Neurosci. 2008 Jul 23;28(30):7520-36.

Niell CM, Stryker MP. Modulation of visual responses by behavioral state in mouse visual cortex. Neuron. 2010 Feb 25;65(4):472-9.

O'Brien RJ, Xu D, Petralia RS, Steward O, Huganir RL, Worley P. Synaptic clustering of AMPA receptors by the extracellular immediate-early gene product Narp. Neuron. 1999 Jun;23(2):309-23.

Ozaki M, Itoh K, Miyakawa Y, Kishida H, Hashikawa T. Protein processing and releases of neuregulin-1 are regulated in an activity-dependent manner. J Neurochem. 2004 Oct;91(1):176-88.

Pardridge WM. The blood-brain barrier: bottleneck in brain drug development. NeuroRx. 2005 Jan;2(1):3-14.

Pham TA, Graham SJ, Suzuki S, Barco A, Kandel ER, Gordon B, Lickey ME. A semi-persistent adult ocular dominance plasticity in visual cortex is stabilized by activated CREB. Learn Mem. 2004 Nov-Dec;11(6):738-47.

Pitcher GM, Kalia LV, Ng D, Goodfellow NM, Yee KT, Lambe EK, Salter MW. Schizophrenia susceptibility pathway neuregulin 1-ErbB4 suppresses Src upregulation of NMDA receptors. Nat Med. 2011 Apr;17(4):470-8.

Pizzorusso T, Medini P, Berardi N, Chierzi S, Fawcett JW, Maffei L. Reactivation of ocular dominance plasticity in the adult visual cortex. Science. 2002 Nov 8;298(5596):1248-51.

Pizzorusso T, Medini P, Landi S, Baldini S, Berardi N, Maffei L. Structural and functional recovery from early monocular deprivation in adult rats. Proc Natl Acad Sci U S A. 2006 May 30;103(22):8517-22.

Polat U, Ma-Naim T, Belkin M, Sagi D. Improving vision in adult amblyopia by perceptual learning. Proc Natl Acad Sci U S A. 2004 Apr 27;101(17):6692-7.

Porciatti V, Pizzorusso T, Maffei L. The visual physiology of the wild type mouse determined with pattern VEPs. Vision Res. 1999 Sep;39(18):3071-81.

Pouille F, Scanziani M. Enforcement of temporal fidelity in pyramidal cells by somatic feed-forward inhibition. Science. 2001 Aug 10;293(5532):1159-63.

Priebe NJ, Mechler F, Carandini M, Ferster D. The contribution of spike threshold to the dichotomy of cortical simple and complex cells. Nat Neurosci. 2004 Oct;7(10):1113-22.

Prusky GT, Douglas RM. Characterization of mouse cortical spatial vision. Vision Res. 44(2004):3411-8.

Prusky GT, Douglas RM. Developmental plasticity of mouse visual acuity. Eur J Neurosci. 2003 Jan;17(1):167-73.

Qin Y, Zhu Y, Baumgart JP, Stornetta RL, Seidenman K, Mack V, van Aelst L, Zhu JJ. State-dependent Ras signaling and AMPA receptor trafficking. Genes Dev. 2005 Sep 1;19(17):2000-15.

Quinlan EM, Olstein DH, Bear MF. Bidirectional, experience-dependent regulation of N-methyl-D-aspartate receptor subunit composition in the rat visual cortex during postnatal development. Proc Natl Acad Sci U S A. 1999 Oct 26;96(22):12876-80.

Ranson A, Cheetham CE, Fox K, Sengpiel F. Homeostatic plasticity mechanisms are required for juvenile, but not adult, ocular dominance plasticity. Proc Natl Acad Sci U S A. 109(2012):1311-6.

Ross RM, McNair NA, Fairhall SL, Clapp WC, Hamm JP, Teyler TJ, Kirk IJ. Induction of orientation-specific LTP-like changes in human visual evoked potentials by rapid sensory stimulation. Brain Res Bull. 76(2008):97-101.

Rossi FM, Pizzorusso T, Porciatti V, Marubio LM, Maffei L, Changeux JP. Requirement of the nicotinic acetylcholine receptor beta 2 subunit for the anatomical and functional development of the visual system. Proc Natl Acad Sci U S A. 2001 May 22;98(11):6453-8.

Rozas C, Frank H, Heynen AJ, Morales B, Bear MF, Kirkwood A. Developmental inhibitory gate controls the relay of activity to the superficial layers of the visual cortex. J Neurosci. (2001) 21(17):6791-801.

Sale A, Maya Vetencourt JF, Medini P, Cenni MC, Baroncelli L, De Pasquale R, Maffei L. Environmental enrichment in adulthood promotes amblyopia recovery through a reduction of intracortical inhibition. Nat Neurosci. 2007 Jun;10(6):679-81.

Sato M, Stryker MP. Distinctive features of adult ocular dominance plasticity. J Neurosci. 2008 Oct 8;28(41):10278-86.

Savonenko AV, Melnikova T, Laird FM, Stewart KA, Price DL, Wong PC. Alteration of BACE1-dependent NRG1/ErbB4 signaling and schizophrenia-like phenotypes in BACE1-null mice. Proc Natl Acad Sci U S A. 2008 Apr 8;105(14):5585-90.

Sawtell NB, Frenkel MY, Philpot BD, Nakazawa K, Tonegawa S, Bear MF. NMDA receptor-dependent ocular dominance plasticity in adult visual cortex. Neuron. 38(2003):977-85.

Scheuss V, Neher E. Estimating synaptic parameters from mean, variance, and covariance in trains of synaptic responses. Biophys J. 81(2001):1970-89.

Shatz CJ, Stryker MP. Ocular dominance in layer IV of the cat's visual cortex and the effects of monocular deprivation. J Physiol. 1978 Aug;281:267-83.

Sia GM, Béïque JC, Rumbaugh G, Cho R, Worley PF, Huganir RL. Interaction of the N-terminal domain of the AMPA receptor GluR4 subunit with the neuronal pentraxin NP1 mediates GluR4 synaptic recruitment. Neuron. 2007 Jul 5;55(1):87-102.

Sieghart W. Structure and pharmacology of gamma-aminobutyric acidA receptor subtypes. Pharmacol Rev. 47(1995):181-234.Smith GB, Heynen AJ, Bear MF. Bidirectional synaptic mechanisms of ocular dominance plasticity in visual cortex. Philos Trans R Soc Lond B Biol Sci. 364(2009):357-67.

Smith GB, Bear MF. Bidirectional ocular dominance plasticity of inhibitory networks: recent advances and unresolved questions. Front Cell Neurosci. 2010 Jun 17;4:21.

Smith SL, Trachtenberg JT. Experience-dependent binocular competition in the visual cortex begins at eye opening. Nat Neurosci. 10(2007):370-5.

Spolidoro M, Baroncelli L, Putignano E, Maya-Vetencourt JF, Viegi A, Maffei L. Food restriction enhances visual cortex plasticity in adulthood. Nat Commun. 2011;2:320.

Spolidoro M, Putignano E, Munafò C, Maffei L, Pizzorusso T. Inhibition of matrix metalloproteinases prevents the potentiation of nondeprived-eye responses after monocular deprivation in juvenile rats. Cereb Cortex. 2012 Mar;22(3):725-34.

Stellwagen D, Malenka RC. Synaptic scaling mediated by glial TNF-alpha. Nature. 2006 Apr 20;440(7087):1054-9.

Sugiyama S, Di Nardo AA, Aizawa S, Matsuo I, Volovitch M, Prochiantz A, Hensch TK. Experience-dependent transfer of Otx2 homeoprotein into the visual cortex activates postnatal plasticity. Cell. 134(2008):508-20.

Tagawa Y, Kanold PO, Majdan M, Shatz CJ. Multiple periods of functional ocular dominance plasticity in mouse visual cortex. Nat Neurosci. 2005 Mar;8(3):380-8.

Tamura H, Kawata M, Hamaguchi S, Ishikawa Y, Shiosaka S. Processing of neuregulin-1 by neuropsin regulates GABAergic neuron to control neural plasticity of the mouse hippocampus. J Neurosci. 2012 Sep 12;32(37):12657-72.

Tan GH, Liu YY, Hu XL, Yin DM, Mei L, Xiong ZQ. Neuregulin 1 represses limbic epileptogenesis through ErbB4 in parvalbumin-expressing interneurons. Nat Neurosci. 2011 Dec 11;15(2):258-66.

Ting AK, Chen Y, Wen L, Yin DM, Shen C, Tao Y, Liu X, Xiong WC, Mei L. Neuregulin 1 promotes excitatory synapse development and function in GABAergic interneurons. J Neurosci. 2011 Jan 5;31(1):15-25.

Toyoizumi T, Miller KD. Equalization of ocular dominance columns induced by an activity-dependent learning rule and the maturation of inhibition. J Neurosci. 29(2009):6514-25.

Trachtenberg JT, Trepel C, Stryker MP. Rapid extragranular plasticity in the absence of thalamocortical plasticity in the developing primary visual cortex. Science. 2000 Mar 17;287(5460):2029-32.

Tsui CC, Copeland NG, Gilbert DJ, Jenkins NA, Barnes C, Worley PF. Narp, a novel member of the pentraxin family, promotes neurite outgrowth and is dynamically regulated by neuronal activity. J Neurosci. 16(1996):2463-78.

Van Dorpe S, Bronselaer A, Nielandt J, Stalmans S, Wynendaele E, Audenaert K, Van De Wiele C, Burvenich C, Peremans K, Hsuchou H, De Tré G, De Spiegeleer B. Brainpeps: the blood-brain barrier peptide database. Brain Struct Funct. 2012 Jul;217(3):687-718.

Vida I, Bartos M, Jonas P. Shunting inhibition improves robustness of gamma oscillations in hippocampal interneuron networks by homogenizing firing rates. Neuron. 2006 Jan 5;49(1):107-17.

Vorobyov V, Kwok JC, Fawcett JW, Sengpiel F. Effects of digesting chondroitin sulfate proteoglycans on plasticity in cat primary visual cortex. J Neurosci. 2013 Jan 2;33(1):234-43.

Vullhorst D, Neddens J, Karavanova I, Tricoire L, Petralia RS, McBain CJ, Buonanno A. Selective expression of ErbB4 in interneurons, but not pyramidal cells, of the rodent hippocampus. J Neurosci. 2009 Sep 30;29(39):12255-64.

Waddingham PE1, Butler TK, Cobb SV, Moody AD, Comaish IF, Haworth SM, Gregson RM, Ash IM, Brown SM, Eastgate RM, Griffiths GD. Preliminary results from the use of the novel Interactive binocular treatment (I-BiT) system, in the treatment of strabismic and anisometropic amblyopia. Eye (Lond). 2006 Mar;20(3):375-8.

Wan X, Mathers DA, Puil E. Pentobarbital modulates intrinsic and GABA-receptor conductances in thalamocortical inhibition. Neuroscience. 2003;121(4):947-58.

Wang XB, Bozdagi O, Nikitczuk JS, Zhai ZW, Zhou Q, Huntley GW. Extracellular proteolysis by matrix metalloproteinase-9 drives dendritic spine enlargement and long-term potentiation coordinately. Proc Natl Acad Sci U S A. 2008 Dec 9;105(49):19520-5.

Webber AL, Wood J. Amblyopia: prevalence, natural history, functional effects and treatment. Clin Exp Optom. 2005 Nov;88(6):365-75.

Wen L, Lu YS, Zhu XH, Li XM, Woo RS, Chen YJ, Yin DM, Lai C, Terry AV Jr, Vazdarjanova A, Xiong WC, Mei L. Neuregulin 1 regulates pyramidal neuron activity via ErbB4 in parvalbumin-positive interneurons. Proc Natl Acad Sci U S A. 2010 Jan 19;107(3):1211-6.

Williams C, Northstone K, Harrad RA, Sparrow JM, Harvey I; ALSPAC Study Team. Amblyopia treatment outcomes after screening before or at age 3 years: follow up from randomised trial. BMJ. 2002 Jun 29;324(7353):1549.

Woo RS, Li XM, Tao Y, Carpenter-Hyland E, Huang YZ, Weber J, Neiswender H, Dong XP, Wu J, Gassmann M, Lai C, Xiong WC, Gao TM, Mei L. Neuregulin-1 enhances depolarization-induced GABA release. Neuron. 2007 May 24;54(4):599-610.

Xu D, Hopf C, Reddy R, Cho RW, Guo L, Lanahan A, Petralia RS, Wenthold RJ, O'Brien RJ, Worley P. Narp and NP1 form heterocomplexes that function in developmental and activity-dependent synaptic plasticity. Neuron. 2003 Jul 31;39(3):513-28.

Xu X, Roby KD, Callaway EM. Immunochemical characterization of inhibitory mouse cortical neurons: three chemically distinct classes of inhibitory cells. J Comp Neurol. 2010 Feb 1;518(3):389-404.

Yang JM, Zhang J, Chen XJ, Geng HY, Ye M, Spitzer NC, Luo JH, Duan SM, Li XM. Development of GABA circuitry of fast-spiking basket interneurons in the medial prefrontal cortex of erbb4-mutant mice. J Neurosci. 2013 Dec 11;33(50):19724-33.

Yau HJ, Wang HF, Lai C, Liu FC. Neural development of the neuregulin receptor ErbB4 in the cerebral cortex and the hippocampus: preferential expression by interneurons tangentially migrating from the ganglionic eminences. Cereb Cortex. 2003 Mar;13(3):252-64.

Yazaki-Sugiyama Y, Kang S, Câteau H, Fukai T, Hensch TK. Bidirectional plasticity in fast-spiking GABA circuits by visual experience. Nature. 2009 462(7270):218-21.

Yoon BJ, Smith GB, Heynen AJ, Neve RL, Bear MF. Essential role for a long-term depression mechanism in ocular dominance plasticity. Proc Natl Acad Sci U S A. 2009 Jun 16;106(24):9860-5. Epub 2009 May 22.